ADDIS ABABA UNIVERSITY
ADDIS ABABA INSTITUTE OF TECHNOLOGY (AAiT)
SCHOOL OF ELECTRICAL & COMPUTER ENGINEERING
DEPARTMENT OF ELECTRICAL ENGINEERING

STUDY OF DOUBLY FED INDUCTION GENERATOR CONTROL UNDER GRID FAULT CONDITIONS

A thesis submitted to Addis Ababa Institute of Technology, School of Graduate Studies, Addis Ababa University in partial fulfillment of the requirement for the Degree of Master of Science in Control Engineering

By

Teshale Tadesse

Advisor: Dr. Mengesha Mamo

ADDIS ABABA, ETHIOPIA

June, 2016

ADDIS ABABA UNIVERSITY
ADDIS ABABA INSTITUTE OF TECHNOLOGY (AAiT)
SCHOOL OF ELECTRICAL & COMPUTER ENGINEERING
DEPARTMENT OF ELECTRICAL ENGINEERING

STUDY OF DOUBLY FED INDUCTION GENERATOR CONTROL UNDER GRID FAULT CONDITIONS

By:-TESHALE TADESSE

APPROVED BY BOARD OF EXAMINERS

_____	_____
Chairman, Department of Graduate Committee	Signature
Dr. Mengesha Mamo	_____
Advisor	Signature
Dr. Getachewu Biru	_____
Internal Examiner	Signature
Prof. N.P. Singh	_____
External Examiner	Signature

Declaration

I, the undersigned, declare that this thesis work is my original work, has not been presented for a degree in this or any other universities, and all sources of materials used for the thesis work have been fully acknowledged.

Teshale Tadesse _____
Name Signature

Place: Addis Ababa Institute of Technology, Addis Ababa University, Addis Ababa

Date of Submission: May, 2016

This thesis has been submitted for examination with my approval as a university advisor.

Dr. Mengesha Mamo _____
Advisor's Name Signature

Acknowledgement

Primarily, I would like to give glory to God and the Virgin Mary without which the completion of this thesis would have been unthinkable. Next, I would like to express my deepest gratitude to my advisor, Dr. Mengesha Mamo for his expertise guidance, constructive comments, suggestions and encouragement. He has been a constant source of inspiration throughout this work. I am also grateful to thank Mr. Andinet Negash for his kind help , advices and materials support. Last but not least, I would like to thank my family, classmate Amdail Shefaw, friends who stood always by my side.

Abstract

Wind power is growing rapidly around the world as a means of dealing with the world energy shortage and associated environmental problems. A wind electrical generation system is the most cost effective of all the environmentally clean and safe renewable energy sources in world.

In this thesis, double fed induction generator and grid system are modeled under normal conditions of the grid system and under grid faulty conditions. Any abnormalities associates with grid are going to affect the system performance. Taking this into account, the performance of double fed induction generator (DFIG) variable speed wind turbine under network faults is studied using simulation developed in MATLAB/SIMULINK results show the fault behavior of the double fed induction generator when a sudden short circuit and voltage dip on the grid side. After the clearance the short circuit fault and voltage dip the proportional integral controller manages to restore the wind turbine's normal operation.

The three-phase fault model is done by giving a fault equivalent resistance value of 0.01Ω and voltage dip at grid side with the value of 0.45p.u. At this time, the current, voltage, active power and reactive power value of DFIG is fluctuating between 0.2p.u and 1.36p.u, 0.7p.u and 1.12p.u, 0 and 6MW, 0.75 and 0.42MVAr, respectively. But in order to operate at normal operation the DFIG current and voltage value is at 1p.u. The maximum active power that generated from DFIG is 9MW. To stabilize the system the proportional integral controller compare the reference voltage and current with generated and minimize the error between voltage and current. The proportional integral controller minimizes the error by decreasing the rising time and makes the value of current and voltage to 1p.u. The detailed results of steady state and faulty or three-phase short circuit on grid system has been noted and analyzed with proper justification. In order to increase the fault ride through capabilities of the system, crowbar protection and series dynamic resistor could be added to the system.

This thesis done by modeling and simulating of the controller using Matlab/Simulink in wind turbine system integrated with grid system. Finally, we observed and interpreted the result with Matlab/Simulink simulation software.

Keywords:- , doubly fed induction generator; wind turbine; proportional integral controller; MATLAB/SIMULINK;

Contents

List of Figures

List of Tables

List of Abbreviations

AC	Alternating Current
CDFIG	Cascaded Doubly Fed Induction generator
DC	Direct Current
DFIG	Doubly-Fed Induction Generator
DOIG	Double Output Induction Generator
EMF	Electromotive force
FOC	Field Orientated Control
GSC	Grid Side Converter
HAWT	Horizontal-axis Wind Turbine
IGBT	Insulated-Gate Bipolar Transistors
IM	Induction Motor/ Machine
LQR	Linear Quadratic Regulator
LVRT	Low Voltage Ride Through
MATLAB	MATrix LABoratory
PAC	Pitch Angle Control
PCC	Point of Common Coupling
PI	Proportional Integrator controller
PID	Proportional Integral Derivative controller
PMSG	Permanent Magnet Synchronous Generator
RSC	Rotor Side Converter
VAWT	Vertical-axis Wind Turbine
VSC	Voltage Source Converters
WECS	Wind Energy Conversion Systems
WRIG	Wound Rotor Induction Generator
WTG	Wind Turbine Generators

1. Chapter One: Introduction

1.1. Background

Electrical power is the most widely used source of energy for our homes, work places and industries. Population and industrial growth have led to significant increases in power consumption over the past three decades. Natural resources like coal, petroleum and gas that have driven our power plants, industries and vehicles for many decades are becoming depleted at a very fast rate. This serious issue has motivated nations across the world to think about alternative forms of energy which utilize inexhaustible natural resources [1].

The combustion of conventional fossil fuel across the globe has caused increased level of environmental pollution. Several international conventions and forums have been set up to address and resolve the issue of climate change. These forums have motivated countries to form national energy policies dedicated to pollution control, energy conservation, and energy efficiency, development of alternative and clean sources of energy. The "Kyoto Protocol to the Convention on Climate Change" has enforced international environmental regulations which are more stringent than the 1992 earth summit regulations.

Renewable energy like solar, wind, and tidal currents of oceans is sustainable, inexhaustible and environmentally friendly clean energy. Due to all these factors, wind power generation has attracted great interest in recent years. Undoubtedly, wind power is today's most rapidly growing renewable energy source. Even though the wind industry is young from a power systems point of view, significant strides have been made in the past 20 years. Wind turbine capacity has grown from 1.3 kW to machines producing 1.5 MW and more. Increasing reliability has contributed to the cost decline, with availability of modern machines reaching 97- 99%. Wind plants have benefited from steady advances in technology made over past 15 years. Much of the advancement has been made in the components dealing with grid integration, the electrical machine, power converters, and control capability. We are now able to control the real and reactive power of the machine, limit power output and control voltage and speed. There is lot of research going on around the world in this area and technology is being developed that offers great deal of capability. It requires an understanding of power systems, machines and applications of power electronic converters and control schemes put together on a common platform [2].

Typically wind generation equipment is categorized in three general classifications: (1) Utility scale- Corresponds to large turbines (900kW-3.5MW) used to generate bulk power for energy markets. (2) Industrial Scale- Corresponds to medium sized turbines (50kW-250kW) mainly used by industries for remote grid production to meet local power requirement. (3) Residential Scale- Corresponds to small sized turbines (400 watts-50kW) mainly utilized for battery charging. Most of the commercially available utility-scale wind turbines are based on the "Danish concept" turbine configuration. This configuration has a horizontal axis, three-bladed rotor, an upwind orientation, and an active yaw system to keep the blades always oriented in the direction of wind flow. The drive train consists of a low-speed shaft connecting the rotor to the gearbox, speed increasing gearbox, a high speed shaft connecting gearbox to the generator. The generators from established manufacturers typically operate at 550-690V (AC).

Unlike a conventional power plant that uses synchronous generators, a wind turbine can operate as fixed-speed or variable-speed. In a fixed-speed wind turbine, the stator of the generator is directly connected to the grid. However, in a variable-speed wind turbine, the machine is controlled and connected to the power grid through a power electronic converter. There are various reasons for using a variable-speed wind turbine. (1) Variable-speed wind turbines offer a higher energy yield in comparison to constant speed turbines. (2) The reduction of mechanical loads and simple pitch control can be achieved by variable speed operation. (3) Variable-speed wind turbines offer acoustic noise reduction and extensive controllability of both active and reactive power. (4) Variable-speed wind turbines show less fluctuation in the output power. The permanent magnet synchronous generator (PMSG) and doubly-fed induction generator (DFIG) are the two machines on which the variable-speed wind turbines are based [3].

The doubly-fed induction generator (DFIG) is a 'special' variable speed induction machine and is widely use as modern large wind turbine generators. It is a standard, wound rotor induction machine with its stator windings directly connected to the grid and its rotor windings connected to the grid through an AC/DC/AC pulse width modulated (PWM) converter. The AC/DC/AC converter normally consists of a rotor side converter (RSC) and a grid-side converter (GSC). By means of the bi-directional converter in the rotor circuit, the DFIG is able to work as a generator in both sub-synchronous (positive slip $s > 0$) and super-synchronous (negative slip $s<0$) operating area [4]. Depending on the operating condition of the drive, the power is fed in or out of the rotor. If ($P_{rotor}<0$): it is flowing from the grid via the converter to the rotor in sub-synchronous mode or vice versa ($P_{rotor}>0$) in super-synchronous mode. In case (sub-synchronous and

super-synchronous) the stator is feeding energy to the grid (P_{stator}> 0).For variable speed systems with limited variable-speed range, e.g. ±30% of synchronous speed, the DFIG is reported to be an interesting solution. The back-to-back converter consists of two converters, i.e., rotor-side converter (RSC) and grid-side converter (GSC) connected back-to-back. Between the two converters a DC-link capacitor is placed. With the RSC it is possible to control the torque or the speed of the DFIG. Doubly fed induction machines can be operated as a generator as well as a motor in both sub-synchronous and super-synchronous speeds using the RSC control. Only the two generating modes at sub-synchronous and super synchronous speeds are of interest for wind power generation.

DFIG wind turbine has many advantages, like, its capability for better reactive power management, it needs only low power converter-inverter circuits, and no sudden variation in torque with variation in speed and hence the output power will be smooth, it is that the converter needed to control the machine is moved to the rotor, and the rotor can be made to handle significantly less power than the stator but still be able to control the power through the stator. The DFIG is an adjustable-speed induction machine which is widely used in modern wind power industry. Compared to a direct-driven synchronous generator system, one major advantage of DFIG is that the power electronic converters have to handle only a fraction (20-30%) of the total system power. This means that power losses in power electronic converters of a DFIG are much lesser than the direct connected synchronous generator which has to handle the total system power.

DFIG offers several advantages when compared with fixed speed generators including speed control. These merits are primarily achieved via control of the RSC. Many works have been proposed for studying the behavior of DFIG based wind turbine system connected to the grid. Most existing models widely use vector control DFIG. The stator is directly connected to the grid and the rotor is fed to magnetize the machine. But, its drawback is very sensitive to grid disturbances.

Unlike a conventional fixed-speed induction machine, a DFIG delivers power to the grid from both the stator and rotor paths. The DFIG frequency converter can be a potential cause of concern for effective control of a DFIG system. From a different point of view, although d-q vector control technique regulates DFIG speed, it also changes the basic parameters of the DFIG such as torque, stator real/reactive power, rotor real/reactive power and the effectiveness of PWM converter modulation. This demands an integrative approach for investigation and evaluation of the DFIG characteristics.

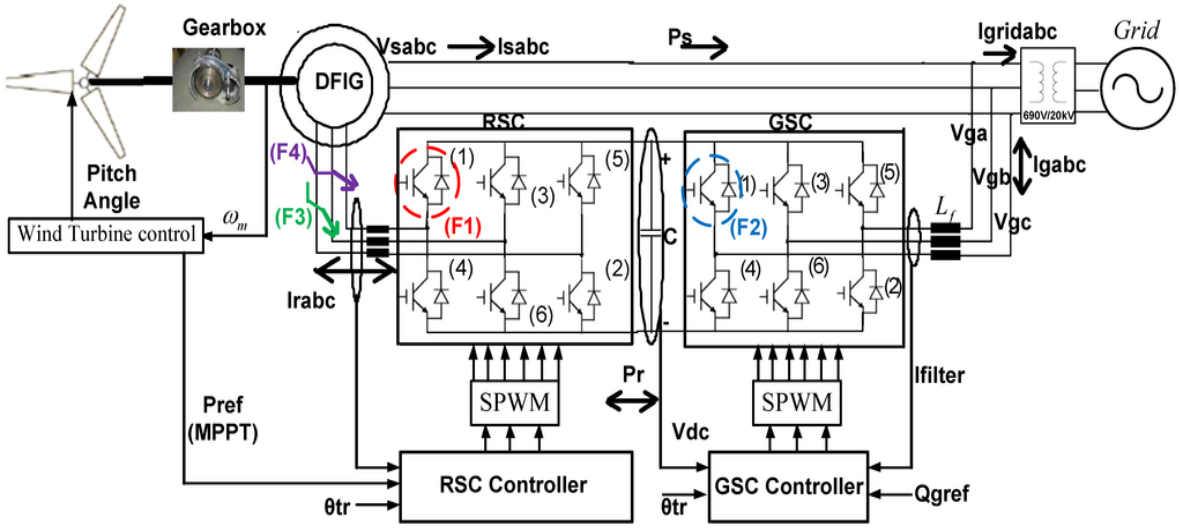

Figure 1.1 DFIG wind turbine integrated with grid system

Further, the effectiveness of DFIG controller in extracting maximum energy from the wind by decoupled d-q voltage control is extremely important in analyzing its design and performance. The energy captured and converted from the wind by a DFIG depends not only on the induction machine but also on the integrated aerodynamic and electrical systems of the wind turbine. Also their control technique under variable wind conditions has to be analyzed to assess the overall performance of a DFIG. In order to better design and manage a DFIG control system under variable wind conditions, it is important to understand how the electrical characteristics of the generator and the aerodynamic characteristics of the turbine blades affect the energy extraction and speed control of a DFIG system. Traditionally, DFIG electrical and aerodynamic characteristics are usually inspected in separate environments. Few efforts have been made to study DFIG behavior by combining the two characteristics together in one integrative environment. Unlike a conventional fixed-speed induction machine, a DFIG has sophisticated controls at both wind turbine and generator levels, and the extracted power by a DFIG relies not only on the aerodynamic properties of the turbine blades but also on the coordination of the mechanical, electrical and power converter systems under variable wind conditions. Those issues must be considered collectively in DFIG system study and controller designs so as to enhance the overall system performance, efficiency and transient stability. The main features of this research are (1) a study of generator converted power characteristics using DFIG d-q steady-state model and faulty state model, (2) an investigation of extracted power characteristics versus generator, slip, and (3) grid faulty conditions with extracted power characteristics of the turbine blades for DFIG speed control study.

Proportional-Integral(PI) controllers is a combination of proportional and an integral controller the output (also called the actuating signal) is equal to the summation of proportional and integral of the error signal. As we know in a proportional and integral controller output is directly proportional to the summation of proportional of error and integration of the error signal [5]. The proportional-Integral (PI) controller is used to calculate the error value as the difference between a measured process variable and a desired set point. The PI controller attempts to minimize the error. It helps in reducing the steady state error, thus makes the system more stable. Slow response of the over damped system can be made faster with the help of these controller. Due to their unique ability they can return the controlled variable back to the exact set point following a disturbance that's why these are known as reset controllers. Its drawbacks are increasing the maximum overshoot of the system, tends to make the system unstable because it responds slowly towards the produced error. After designing a controller for the DFIG for maximum energy extraction, the main issue and overall goal is to obtain effective control of the faulty conditions of the grid. A suitable control system has to be designed to achieve successful control of grid fault conditions.

1.2. Statement of the Problem

Doubly Fed Induction Generator (DFIG) is widely used for wind turbine electricity generation. A typical system of wind turbine contains a DFIG along with a back-to-back, DC-link converter and WTG. The rotor side converter (RSC) is used to control the machine speed and reactive power. The stator side converter is used to maintain the DC-bus voltage constant. During grid voltage dips or sag and short circuit on grid side consequently rotor current rises. This leads to damage to DFIG, converter switches, DC-link capacitors and electromagnetic torque fluctuations which cause mechanical stress on the drive-train system of wind turbine. To overcome those problems, we can use a controller that can control the speed of the rotor and the slip of the generator with following the natural curve of the DFIG. At a time of grid fault, the wind turbine or DFIG will wait until the fault is extracted otherwise, it will interrupt themselves from the system and generate the power to the nearby bus.

1.3. Objective of Thesis

1.3.1. General Objective

The main objective of this thesis is study of DFIG under grid fault condition in wind power generation systems.

1.3.2. Specific Objectives

- Model the controller speed of the rotor using a proportional integral controller, in order to stabilize rotor speed and slip of the generator.
- Evaluate the performance of DFIG during voltage sag or dip and three-phase short-circuit condition on grid side.
- Evaluate the active power and reactive power at a time of grid fault.
- Conduct power flow control during normal condition of grid, during grid faulty condition and after clearances of grid fault of wind turbine.
- Conduct the faulty system with MATLAB/SIMULINK.

1.4. Literature Review

Around this thesis idea, several methods for DFIG power flow control under grid fault conditions in wind turbine were proposed and analyzed.

In [6], a technique is described which the objective to keep the generator has connected to the grid in case of a grid failure so that it can resume power generation after clearance of the fault in the grid. The key of the technique is to limit the high currents and to provide a bypass for it in the rotor circuit via a set of resistors that are connected to the rotor windings without disconnecting the converter from the grid. The wind turbine can resume normal operation within a few hundred milliseconds after the fault has been cleared.

In [7], wind turbines can either operate at fixed speed or variable speed. For a fixed speed wind turbine the generator is directly connected to the electrical grid. For variable speed wind turbine the generator is controlled by power electronic equipment. There are several reasons for using variable-speed operation of wind turbines; among those are possibilities to reduce stresses of the mechanical structure, acoustic noise reduction and the possibility to control active and reactive power. Most of the major

wind turbine manufactures are developing new larger wind turbines in the 3MW to 5MW range. These large wind turbines are all based on variable-speed operation with pitch control using a direct driven synchronous generator (without gearbox) or DFIG. Fixed-speed induction generators with stall control are regarded as unfeasible for these large wind turbines. DFIGs are commonly used by the wind turbine industry for larger wind turbines. Under this paper, it didn't consider the fault condition. It only studies at variable speed of wind.

In [8], Describes the dynamic behavior of a typical fixed speed wind turbine connected to the grid; the model is developed in the simulation tool MATLAB/SIMULINK and created as a modular structure. The pitch control system is used for stabilization of the wind turbine at grid faults. In this way, voltage stability of the system with grid-connected wind turbines can be improved by using blade angle control for a temporary reduction of the wind turbine power during a short-circuit fault in the grid.

In [9], Control strategy for a DFIG feeding an unbalanced grid or stand-alone load. Explain a new methodology to compensate the stator voltage unbalance of DFIG has been proposed. The effects of voltage unbalances in DFIG have been discussed, equivalent circuits and small-signal models, appropriate to design the current control loops, have been proposed. Experimental results have been presented to validate the proposed control methodology. For stand-alone and grid-connected applications the performance of the control system has been tested considering variable-speed operation, fixed-speed operation and step connection of unbalanced loads.

In [10], Transient stability simulation of a fixed speed wind turbine by Matlab/Simulink is explains the detailed overview of fixed speed wind turbine. Describes the dynamic behavior of a typical fixed speed wind turbine connected to the grid; the model is developed in the simulation tool Matlab/Simulink and created as a modular structure. The pitch control system is used for stabilization of the wind turbine at grid faults. In this way, voltage stability of the system with grid connected wind turbines can be improved by using blade angle control for a temporary reduction of the wind turbine power during a short-circuit fault in the grid.

In [11], Decoupled of active and reactive power control of a DFIG is explaining detailed explanation for the active and reactive power in wind turbine systems. It provides decoupled regulation of the primary side active and reactive power and it is suitable for both electric energy generation and drive applications. The

mathematical model of the machine written in an appropriate d-q reference frame is established to investigate simulations. In order to control the power flowing between the stator of the DFIG and the network or grid, a decoupled control of active power and reactive power is synthesized using PI controllers. Their respective performances are in terms of stator currents references tracking.

Recently,[12], the DFIG became the popular configuration in variable speed wind energy applications. The development and use of the DFIG machines was dictated by the need for wide operational range as well as the necessity to allow flexible power flow control, grid integration as well as economic reasons. The use of the DFIG machines, however, increased the long term cost and complexity of the wind energy generation.

1.5. Motivation for this Thesis

Wind is intermittent or stopping and starting at irregular intervals. Many time the voltage dip and three-phase short circuit will happen on grid sides. Grid voltage dip cause many problems for induction generators; torque pulsations, reactive power pulsations and unbalanced currents in grid system.

In double fed induction wind generators, three-phase short circuit and voltage dip on grid side cause a number of problems, such as over-current, unbalanced currents, reactive power pulsations, unbalanced voltage on grid system and stress or damage on the mechanical components from torque pulsation. Therefore, beyond a certain amount of unbalance, double fed induction wind generators are switched out of the network or grid system. This can further weaken the grid. DFIGs, control of the rotor speed allows for adjustable currents operation and reactive power control.

1.6. Contribution of the Thesis

In this work, the gaps between theory and practical simulation are completely filled with clear explanations. The simulations are proven with provided models. The undertaking in this thesis aims to extend this treatment to a DFIG wind turbine system. It is the intention of the author to quickly get the reader familiar with the mathematical constructs, the basic physics of the machines and the control theory necessary to construct a working model or MATLAB/SIMULINK model. Provided along with the theory is a working simulation model in the Simulink environment. Every chapter is geared towards understanding the system for simulation purposes.

1.7. Thesis Outline

Chapter -2 deals with induction machine with basic dynamic d-q model, axes transformation, double fed induction generator, deals with detail modeling of wind turbine coupled with DFIG and also modeling of wind turbine in brief. Chapter-3 deals with, power flow control in wind turbine, power balance and also mode of operation of DFIG,.Chapter-4 deals with control design, design of inner control loop and design of outer control loop. Chapter-5 deals with simulation results in normal operation of the grid, faulty conditions and after fault clearance conditions. Chapter- 6 deals with the conclusions, recommendations and future work in details.

2. Chapter Two: Theoretical Background

2.1. Introductions

An induction generator or asynchronous generator is a type of alternating current (AC) electrical generator that uses the principles of induction motors to produce power. Induction generators operate by mechanically turning their rotors faster than synchronous speed. A regular AC asynchronous motor usually can be used as a generator, without any internal modifications. Induction generators are useful in applications such as mini hydro power plants, wind turbines, or in reducing high-pressure gas streams to lower pressure, because they can recover energy with relatively simple controls. An induction generator usually draws its excitation power from an electrical grid; sometimes, however, they are self-excited by using phase-correcting capacitors. Because of this, induction generators cannot usually "black start" a de-energized distribution system.

Like other electrical machines, induction machines can be operated as either generators or motors. They are cheap to manufacture, reliable and find their way in most possible applications. Variable speed drives require inexpensive power electronics and computer hardware, and allowed induction machines to become more versatile. In particular, vector or field-oriented control allows induction motors to replace DC motors in many applications.

The Induction motors (IM) for many years have been regarded as the workhorse in industry. Recently, the induction motors were evolved from being a constant speed motors to a variable speed. In addition, the most famous method for controlling induction motor is by varying the stator voltage or frequency. To use this method, the ratio of the motor voltage and frequency should be approximately constant. With the invention of Field Orientated Control, the complex induction motor can be modeled as a DC motor by performing simple transformations. In a similar manner to a dc machine, in induction motor the armature winding is also on the rotor, while the field is generated by currents in the stator winding. However the rotor current is not directly derived from an external source but results from the emf induced in the winding as a result of the relative motion of the rotor conductors with respect to the stator field [13].

The concept of the steady state torque control of an induction motor is extended to transient states of operation in the high performance, vector control ac drive system based on the field operation principle (FOP). The FOP defines condition for decoupling the field control from the torque control. A field oriented

induction motor emulates a separately exited dc motor in two aspects: i)Both the magnetic field and torque developed in the motor can be controlled independently. ii) Optimal condition for the torque production, resulting in the maximum torque per unit ampere, occurs in the motor both in steady state and in transient condition of operation.

2.2. Dynamic d-q Model

It has been found that some of the induction machine inductances are functions of the rotor speed, whereupon the coefficients of the differential equations (voltage equations) that describe the behavior of these machines are time varying except when the rotor is stalled. A change of variables is often used to reduce the complexity of these differential equations. The general transformation refers machine variables to a reference that rotates at an arbitrary angular velocity. All known real transformations are obtained from axis transformation by simply assigning the speed of the rotation of reference frame.

In the late 1920s, [14] **R.H. Park** formulated a change of variables which, in effect, replaced the variables (voltages, current and flux linkages) associated with the stator windings of a synchronous machine with variables associated with fictitious windings rotating with the rotor. In other words, he transformed or referred, the stator variables to a frame of reference fixed in the rotor. He referred stator variables to the rotor that choosing an appropriate frame of reference can simplify machine equations immensely. The reason is an electric machine is basically comprised of electric circuits in relative motion linked by mutual inductances. The inductances vary with rotor position through time, however if the frame of reference is rotated at the proper speed the inductances will appear constant and the machine is simplified. Park's transformation, which revolutionized electric machine analysis, has the unique property of eliminating all time-varying inductances from the voltage equations of the synchronous machine which occur due to: (1) Electric circuits in relative motion and (2) Electric circuits with varying magnetic reluctance.

H.C. Stanley, [15], in late 1930's proposed a model for induction machine with respect to stationary reference frame. He showed that the time-varying inductances in the voltage equations of an induction machine due to electric circuits in relative motion could be eliminated by transforming the variables associated with the rotor windings to variables associated with fictitious stationary windings. In this case the rotor variables are transformed to a frame reference fixed in the stator.

Later **G. Bryon's**, proposed a transformation of both stator and rotor variables to a synchronously rotating reference frame that moves with the rotating magnetic field. Lastly **Krause** and **Thomas** proposed a model for induction machine with respect to stationary reference frame [15].

2.2.1. Axes Transformation

Consider a three-phase induction machine with stationary stator winding axes a_s-b_s-c_s with voltages v_{as}, v_{bs}, v_{cs} and with respect to the stationary reference frame (d^s-q^s), the voltages are referred as v^s_{ds}, v^s_{qs}. Assume that the d^s-q^s–axes are oriented at an angle θ. The voltages v^s_{ds}- v^s_{qs} can be resolved into a_s-b_s-c_s components.

$$\begin{pmatrix} V_{as} \\ V_{bs} \\ V_{cs} \end{pmatrix} = \begin{bmatrix} \cos\theta & \sin\theta & 1 \\ \cos(\theta-120°) & \sin(\theta-120°) & 1 \\ \cos(\theta+120°) & \sin(\theta+120°) & 1 \end{bmatrix} \begin{pmatrix} V_{ds} \\ V_{qs} \\ V_{0s} \end{pmatrix} \quad (2.1)$$

The corrosponding inverse releation of the above equation is:

$$\begin{pmatrix} V_{ds} \\ V_{qs} \\ V_{0s} \end{pmatrix} = \begin{bmatrix} \cos\theta & \cos(\theta-120°) & \cos(\theta+120°) \\ \sin\theta & \sin(\theta-120°) & \sin(\theta+120°) \\ 1/2 & 1/2 & 1/2 \end{bmatrix} \begin{pmatrix} V_{as} \\ V_{bs} \\ V_{cs} \end{pmatrix} \quad (2.2)$$

The voltages on the d^s-q^s can be converted into d^e-q^e reference frame (synchronously rotating frame). To find the synchronously rotating reference frame, we use a triagonometric relation.

$$V^e_{qs} = V^s_{qs}\cos\theta_e - V^s_{ds}\sin\theta_e \quad (2.3)$$

$$V^e_{ds} = V^s_{qs}\sin\theta_e - V^s_{ds}\cos\theta_e \quad (2.4)$$

Resolving the rotating frame parameter into stationary reference frame:

$$V^s_{qs} = V_{qs}\cos\theta_e + V_{ds}\sin\theta_e \quad (2.5)$$

$$V^s_{ds} = -V_{qs}\sin\theta_e + V_{ds}\cos\theta_e \quad (2.6)$$

Let, $V_{as} = V_m\cos(\omega_e t + \emptyset)$ (2.7)

$$V_{bs} = V_m\cos(\omega_e t - 2\pi/3 + \emptyset) \quad (2.8)$$

$$V_{cs}=V_m\cos(\omega_e t+2\pi/3+\emptyset) \quad (2.9)$$

From equations 2.5-2.9, we get the reference frame:

$$V^s_{qs}=V_m\cos(\omega_e t+\emptyset) \quad (2.10)$$

$$V^s_{ds}=-V_m\sin(\omega_e t+\emptyset) \quad (2.11)$$

From equation: - $V_{qs}=V_m\cos\emptyset$ (2.12)

$$V_{ds}=-V_m\sin\emptyset \quad (2.13)$$

This shows that the sinusoidal variables in a stationary frame appear as DC quantity.

$$|V|=V_m \quad (2.14)$$

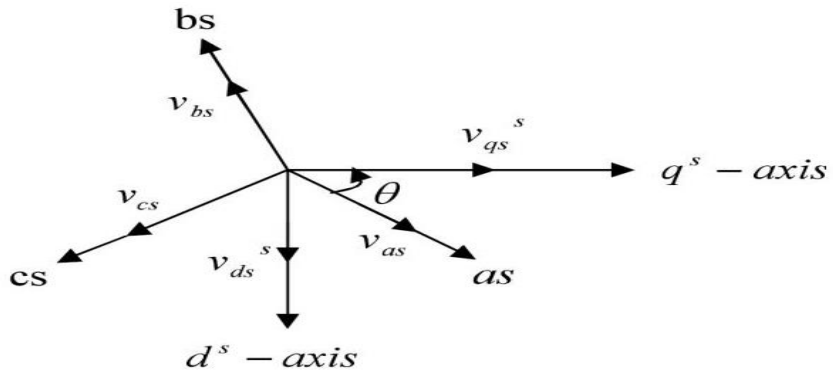

Figure 2.1 Stationary frame a-b-c to d-q axes transformation

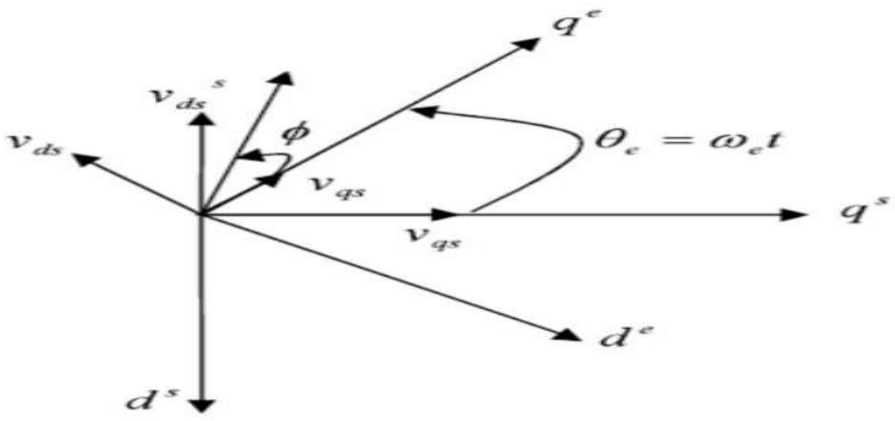

Figure 2.2 Stationary frame d-q to synchronous rotating frame d-q

2.2.2. Synchronously Rotating Reference Frame-Dynamic Model (Kron's equation)

The stator circuit equations are [16]:

$$V^s_{qs}=R_s i^s_{qs}+\frac{d}{dt}\psi^s_{qs} \quad (2.15)$$

$$V^s_{ds}=R_s i^s_{ds}+\frac{d}{dt}\psi^s_{ds} \quad (2.16)$$

Where, ψ^s_{qs} and ψ^s_{ds}, q-axis and d-axis flux linkage respectively.

$$V_{qs}=R_s i_{qs}+\frac{d}{dt}\psi^s_{qs}+\omega_e\psi_{ds} \quad (2.17)$$

$$V_{ds}=R_s i_{ds}+\frac{d}{dt}\psi^s_{ds}-\omega_e\psi_{ds} \quad (2.18)$$

If the rotor is not rotating, the rotor equations will be written as:

$$V_{qr}=R_r i_{qr}+\frac{d}{dt}\psi^s_{qr}+\omega_e\psi_{dr} \quad (2.19)$$

$$V_{dr}=R_r i_{dr}+\frac{d}{dt}\psi^s_{dr}+\omega_e\psi_{qr} \quad (2.20)$$

Where, ω_e is the reference frame speed that interprets stationary circuit variables referred to the synchronously rotating reference frame and ω_r is the reference frame speed that interprets stationary circuit variables referred to a reference frame fixed in the rotor.

2.2.3. The Equivalent Circuit of a DFIG

The steady state equivalent circuit of an induction machine is a widely known topic cover thoroughly by many authors. Figure 2.3 and 2.4 shows the standard model for a caged machine [17]. The modification for a DFIG operation is simply to include the rotor voltage V_r, see Figure 2.3 and 2.4. Note that, it is necessary to divide it by the slip to bring the frequency of the rotor to that of the stator. Furthermore, notice that all rotor parameters are referred in magnitude to the stator by an equivalent turns ratio.

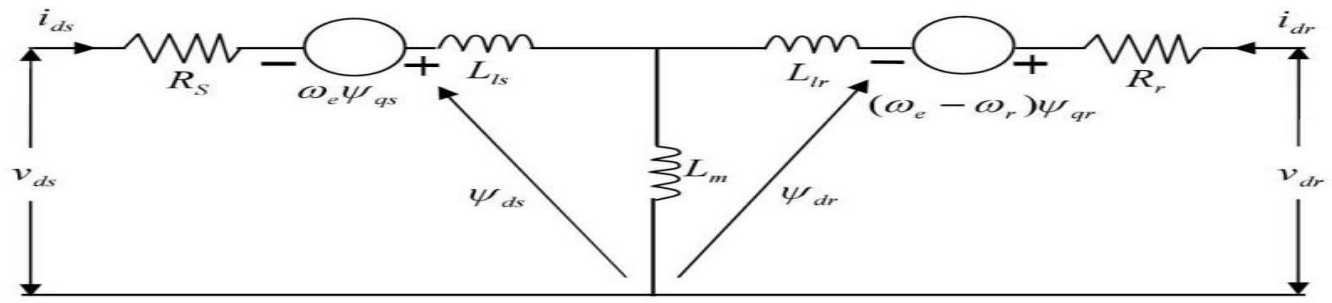

Figure 2.3 The equivalent circuit of d-axis

If rotor rotates, then the equation will be:

$$V_{qr}=R_r i_{qr}+\frac{d}{dt}\psi^s_{qr}+(\omega_e-\omega_r)\psi_{dr} \quad (2.21)$$

$$V_{dr}=R_r i_{dr}+\frac{d}{dt}\psi^s_{dr}+(\omega_e-\omega_r)\psi_{dr} \quad (2.22)$$

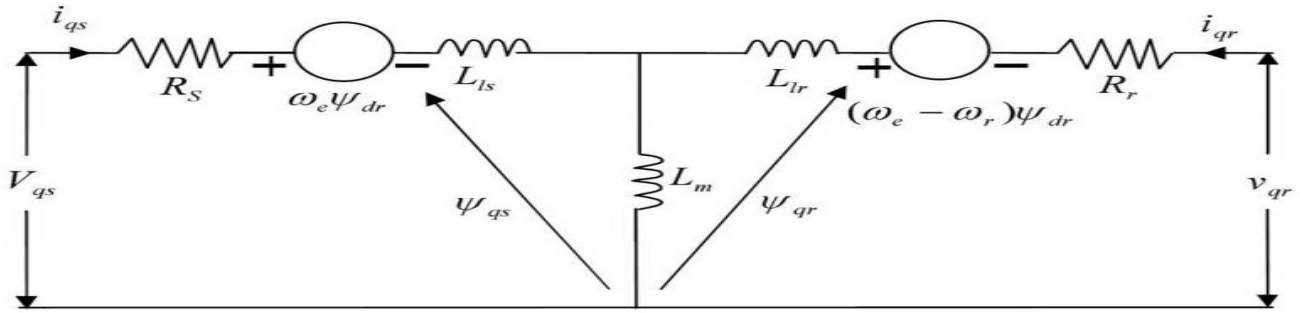

Figure 2.4 The equivalent circuit of q-axis

The flux linkage expressions in terms of the circuit currents are:

$$\Psi_{qs}=L_{ls}i_{qs}+L_m(i_{qs}+i_{qr}) \quad (2.23)$$

$$\Psi_{qr}=L_{lr}i_{qr}+L_m(i_{qs}+i_{qr}) \quad (2.24)$$

$$\Psi_{ds}=L_{ls}i_{ds}+L_m(i_{ds}+i_{dr}) \quad (2.25)$$

$$\Psi_{dr}=L_{lr}i_{dr}+L_m(i_{ds}+i_{dr}) \quad (2.26)$$

$$\Psi_{qm}=L_m(i_{qs}+i_{qr}) \quad (2.27)$$

$$\Psi_{dm}=L_m(i_{ds}+i_{dr}) \quad (2.28)$$

We can write the above equations using matrix form as follows:

$$\begin{bmatrix} V_{qs} \\ V_{ds} \\ V_{qr} \\ V_{dr} \end{bmatrix} = \begin{bmatrix} R_s + SL_s & \omega_e L_s & SL_m & \omega_e L_m \\ -\omega_e L_s & R_s + SL_s & -\omega_e L_m & SL_m \\ SL_s & (\omega_e - \omega_r)L_m & R_r + SL_r & (\omega_e - \omega_r)L_r \\ -(\omega_e - \omega_r)L_m & SL_m & -(\omega_e - \omega_r)L_m & R_r + SL_r \end{bmatrix} \begin{bmatrix} i_{qs} \\ i_{ds} \\ i_{qr} \\ i_{qr} \end{bmatrix} \quad (2.29)$$

2.2.4. The Equivalent Circuit of a DFIG under Fault Conditions

As the fault process has a very small time constant compared to that of the system, the slip does not vary during the fault. Because of this, the DFIG may be considered to behave like a synchronous machine. In other word, synchronous machine parameters may be applied to a DFIG fault simulator. To argue for this possibility being valid, one must be familiar with the function of the synchronous generator [18].

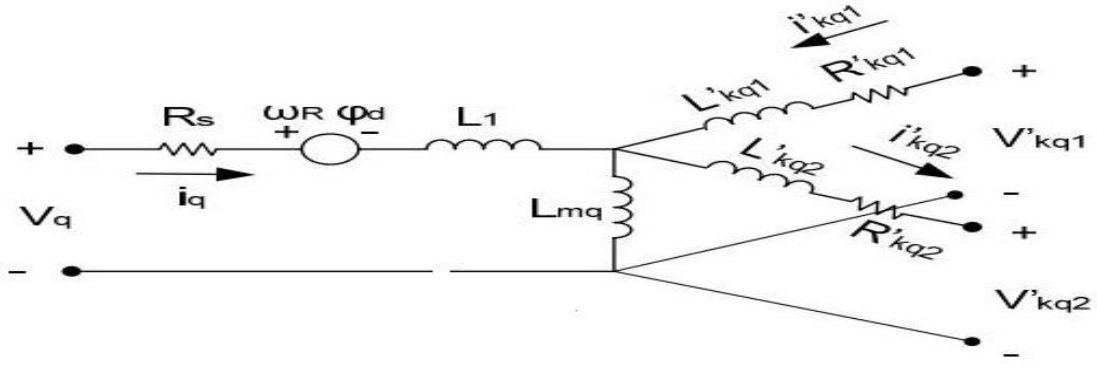

Figure 2.5 The equivalent circuits of q-axis under fault conditions

A synchronous machine is fed from a three-phase voltage source in the stator exactly like the induction machine. The difference is in the rotor, where the synchronous machine has a constant magnetic field generator. The source may be either permanent magnets or windings fed with DC voltage [19]. The three-phase stator voltages produce a rotating field which interacts with the constant field of the rotor. Unlike the case of the induction machine, the synchronous machine has no slip (the rotor field leads the stator field in a generator)

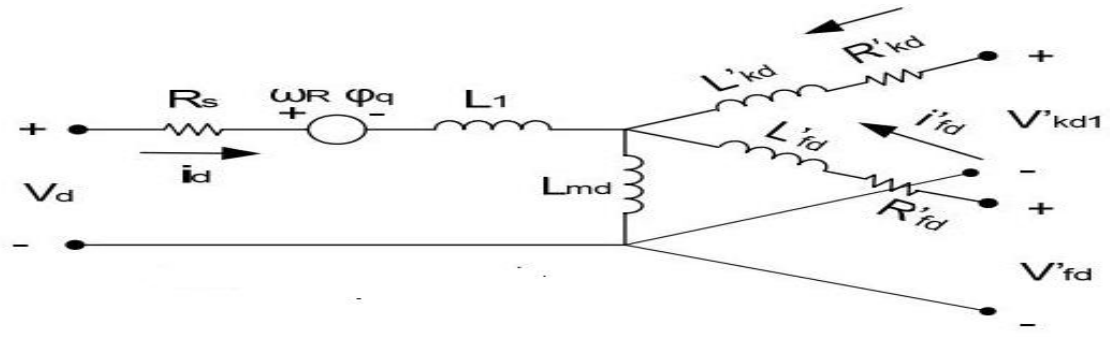

Figure 2.6 The equivalent circuits of d-axis under fault conditions

In Figures 2.5 and 2.6, the subscript kq, kd stands for amortization circuits and subscript, fd for the field winding, respectively.

Starting the synchronous machine working as a generator (wanting to connect to the consumer) or a motor requires special attention. To start the machine, a stronger field is needed because the windings are not magnetized and the mechanical inertia which tends to keep the rotor in stand still state. The starting field cannot be obtained by the stator and rotor alone [19]. As a consequence, the machine will start in an asynchronous manner. A synchronization procedure is needed. For this, power electronics are used to control the field. To assist at start up by creating a surplus field, an amortizations winding is used. After the machine had started, the amortization circuit is taken out as the machine is fully magnetized.

Stator voltage equation:

$$V_q=R_s i_q+\frac{d}{dt}\phi_q-\omega_R\phi_d \tag{2.30}$$

$$V_d=R_s i_d+\frac{d}{dt}\phi_d-\omega_R\phi_q \tag{2.31}$$

Where, V_q—q-axis voltage, V_d—d-axis voltage, R_s—stator resistance, i_q—q-axis current, i_d—d-axis current, ϕ_q—q-axis flux, ϕ_d—d-axis flux, and ω_R—rotor speed.

The flux equations show a dependency of inductances and currents:

$$\phi_q=L_q i_q+L_{mq} i'_{kq} \tag{2.32}$$

$$\phi_d=L_d i_d+L_{md}(i'_{fd}+i'_{kd}) \tag{2.33}$$

where, L_q, L_d—leakage inductance, L_{mq}, L_{md}—magnetization inductance, i_{fd}—field circuit current in d-axis, i'_{kq}—field circuit current in q-axis and $i'_{kd(q)}$—amortization circuit current in d-q- axis. The prime indicates that to differentiate source current from field circuit and amortization circuit current.

Flux equations are presented as:

$$\phi'_{fd}=L'_{fd}i'_{fd}+L_{md}(i'_{d}+i'_{kd}) \quad (2.34)$$

$$\phi'_{kd}=L'_{kd}i'_{kd}+L_{md}(i'_{d}+i'_{fd}) \quad (2.35)$$

$$\phi'_{kq1}=L'_{kq}i'_{kq1}+L_{mq}i_{q} \quad (2.36)$$

$$\phi'_{kq2}= L'_{kq2}i'_{kq2}+L_{mq}i'_{q} \quad (2.37)$$

Field circuit voltage equation from Figure 2.6:

$$V'_{fd}=R'_{fd}i'_{fd}+\frac{d}{dt}\phi'_{fd} \quad (2.38)$$

Amortization circuit voltage equations:

$$V'_{kd}=R'_{kd}i'_{kd}+\frac{d}{dt}\phi'_{kd} \quad (2.39)$$

Where, R'_{kd}—is the resistance of the amortization circuit.

For Figure 2.5 the amortization q-voltage is:

$$V'_{kq1}=R'_{kd1}i'_{kq1}+\frac{d}{dt}\phi'_{kq1} \quad (2.40)$$

For diagram present in Figure 2.5:

$$V'_{kq2}=R'_{kd2}i'_{kq2}+\frac{d}{dt}\phi'_{kq2} \quad (2.41)$$

2.3. Wind Turbine and Wind Energy Conversion System

2.3.1. Wind Turbine

Wind turbines are mechanical devices specifically designed to convert part of the kinetic energy of the wind into mechanical energy. The wind turbine captures the wind's kinetic energy of air mass by a rotor consisting of two or more blades which is mechanically coupled to an electrical generator. Most of the time the turbine is mounted on a tall tower to enhance the wind energy capture. The sites with steady high wind produce more energy over the year. Wind turbines convert aerodynamic power into electrical energy. In a wind turbine two conversion processes take place. The aerodynamic power (available in the wind) is first converted into mechanical power. Next, that mechanical power is converted into electrical power. Those power conversations are shown on Figure 2.7 below.

A modern wind turbine comprises of the principal components such as the tower, the yaw, the rotor and the nacelle, which houses the gear box and the generator. The tower holds the main part of the wind turbine and keeps the rotating blades at a height to capture sufficient wind power. The yaw mechanism is used to turn the wind turbine rotor blades in direction of the wind. The gearbox transforms the slower rotational speeds of the wind turbine to higher rotational speeds on the electrical generator side. Electrical generator will generate electricity when its shaft is driven by the wind turbine, whose output is maintained as per specifications, by employing suitable control and supervising techniques. The block diagram of a typical wind energy conversion system is shown in Figure 2.7 below.

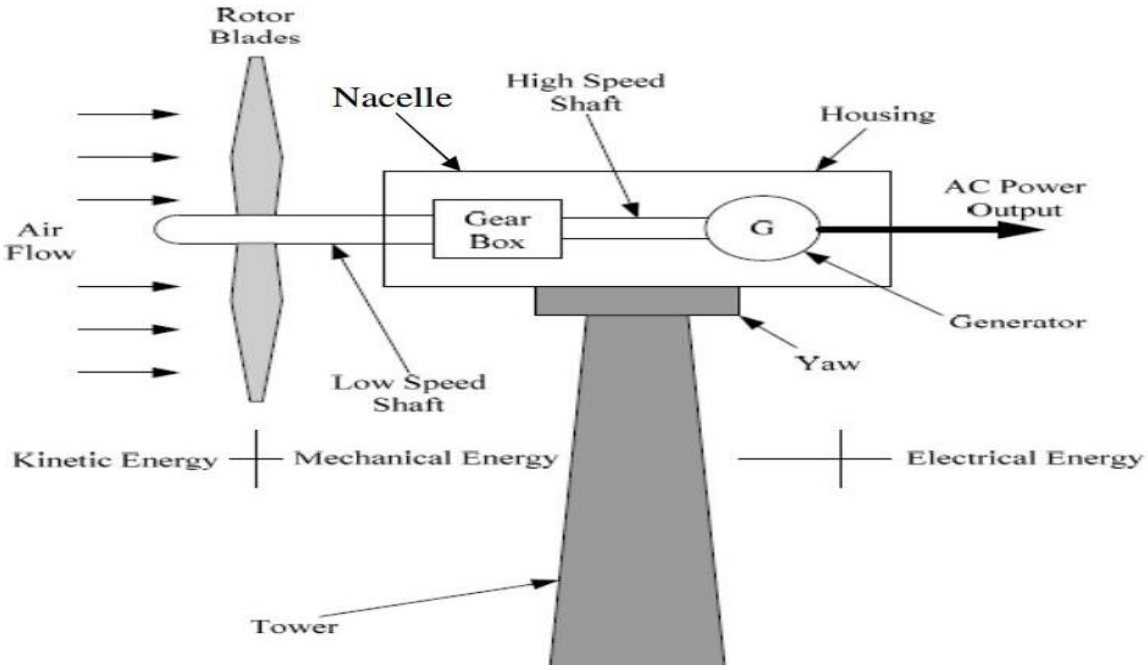

Figure 2.7 Block diagram of wind energy conversion system

The **tip speed ratio** (λ) is defined as the ratio of the speed of the extremities of a wind turbine rotor to the speed of the free wind speed. Modern wind turbines are also classified as high rotation speed ones and low rotation speed ones. This ratio can be taken as a metric in comparing the different characteristics of the wind turbines.

Solidity (σ) is other parameter, which is used to distinguish wind turbines. It is usually defined as the percentage of the area of the rotor, which contains material rather than air.

Classification of wind turbine rotors

Wind turbines are usually classified into two categories, according to the orientation of the axis of rotation rotor with respect to the direction of wind [20]. Those are :(1) Vertical-axis turbines and (2) Horizontal-axis turbines**.**

Vertical-axis Wind Turbine (VAWT)

The axis of rotation of vertical axis wind turbine (VAWT) is vertical to the ground and almost perpendicular to the wind direction. The VAWT can receive wind from any direction. Hence complicated yaw devices can

be eliminated. Vertical axis machines have very good aerodynamic efficiency and have low manufacture cost and simple control systems. The generator and the gearbox of such systems can be housed at the ground level, which makes the tower design simple and more economical. Moreover, the maintenance of these turbines can be done at the ground level. Advantages of the VAWT are; Easy maintenance for ground mounted generator and gearbox, receive wind from any direction (no yaw control required), and simple blade design and low cost of fabrication.

For vertical axis machines the solidity of turbine is defined as:

$$\sigma=\frac{z.c}{r} \tag{2.42}$$

Where parameter σ is the solidity of the turbine, z is the number of the blades, r is the radius of the rotor and c is the chord (width) of the blade.

Disadvantages of a vertical-axis wind turbine are; not self-starting (require generator to run in motor mode at start), lower efficiency (the blades lose energy as they turn out of the wind), limited options for speed regulations in high wind speed, difficulty in controlling blade over-speed, and oscillatory component in the aerodynamic torque is high.

The first windmills were built based on the vertical-axis structure. This type has only been incorporated in small-scale installations. Typical VAWTs include the Darrius rotor, after the French engineer who invented it in 1920s [20]. VAWTs contain vertical rotor, often slightly curved symmetrical airfoils. The largest VAWT was installed in Canada, the electricity generating capacity of 4200KW. Since the end of the 1980s, however, the research and development of VAWT has almost stopped world-wide.

Horizontal-axis Wind turbines (HAWT)

The axis of rotation of horizontal axis wind turbines (HAWT) is horizontal to the ground and almost parallel to the wind stream. They can operate with the blades in front of the wind (up-wind) or behind the wind (down-wind). They have one, two, three or a large number of blades and they cover approximately 90% of the installed wind turbines around the world. Most of today's commercial wind machines are three blades HAWTs due to their aerodynamic stability. The most common design of modern turbines is based on the horizontal-axis structure [20]. HAWT are mounted on towers. The tower's role is to raise the wind turbine above the ground to intercept stronger winds in order to harness more energy. Higher efficiency, low cut-in

wind speed, easy furling or ability to turn the blades, lower cost to power ration and high power coefficient are the distinct advantages of horizontal axis machines.

Disadvantages of the horizontal-axis; generator and gearbox should be mounted on a tower (thus restricting maintenance servicing), more complex design required due to the need for yaw or tail drive.

For horizontal axis machines the solidity of the turbine is defined as:

$$\sigma = \frac{z.c.r^2}{\pi r} \tag{2.43}$$

Where, parameter σ is the solidity of the turbine, z is the number of the blades, ris the radius of the rotor and c is the chord (width) of the blade. In this section basic properties of wind are described which are very important for power controller design of a DFIG.

2.3.2. Annual Wind Distribution

The annual wind distribution is an extremely important factor for the power output of a wind turbine. The wind speed is never same throughout the year and keeps changing with different weather conditions. Considering this factor the average wind speed for a short period of time depends not only on the annual wind speed but also on the wind distribution. It has been found that annual wind distribution can be described by statistical concept of **Weibull probability density function** [21]. This Weibull probability density function is given by:

$$f(\omega) = \frac{k}{c}\left(\frac{\omega}{c}\right)^{k-1} e^{-(k/c)^k} \tag{2.44}$$

Where, k-is a shape parameter, c-is a scale parameter and ω-is the wind speed. Therefore, the average wind speed can be obtained as:

$$\omega_{avg} = \int_0^{\infty} \omega f(\omega) d\omega \tag{2.45}$$

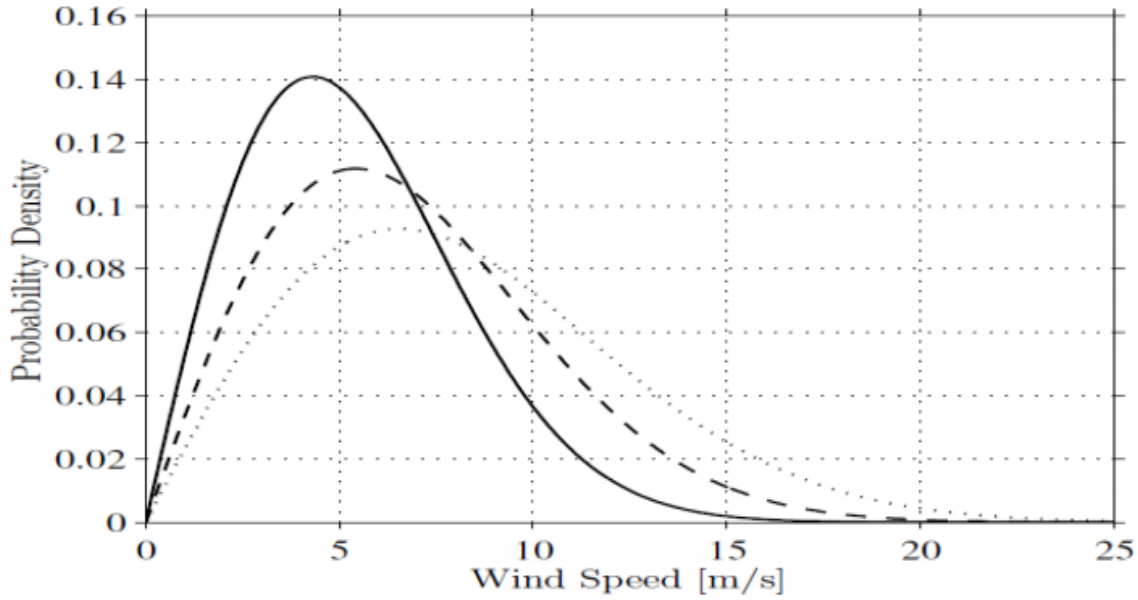

Figure 2.8 Weibull distributions for wind speeds: 5.4m/s, 6.8m/s and 8.2m/s

2.3.3. Power Extracted from the Wind

Wind is the movement of air in response to pressure differences within the atmosphere. Pressure differences exert a force which causes air masses to move from a region of high pressure to one of low pressure. Such pressure differences are caused primarily by differential heating effects of the sun on the surface of the earth. Thus wind energy can be considered to be a form of solar energy [22].

The mechanical power produced by a wind turbine is proportional to the cube of the wind speed. The rotational speed of the wind turbine for which maximum power is obtained is different for different wind speeds. Therefore, variable speed operation is necessary to maximize the energy yield. Variable speed turbines are connected to the grid via an electronic converter that decouples the rotational speed of the wind turbine from the grid frequency, enabling variable speed operation.

The derivation of power extraction from wind:

1. Wind velocity:

$$V=\frac{\Delta X}{\Delta t} \tag{2.46}$$

Where, V-is the speed of wind, ΔX-is the displecement of wind moving during a Δt (change of time)

2. Air mass flowing:

$$\Delta m=\rho A\Delta X \tag{2.47}$$

Where, m –is air mass flowing in atmosphere, ρ- is air density and A-is swept area.

3. Mass flow rate at swept area:

$$Q_t=\frac{\Delta m}{\Delta t}=\rho\frac{A_t\Delta X}{\Delta t}=\rho A_t V_t \tag{2.48}$$

4a. Kinetic energy change:

$$\Delta KE=\frac{1}{2}m(V^2{}_1-V^2{}_2) \tag{2.49}$$

Where ΔKE- is change of kinetic energy,

4b. Force on turbine blades:

$$F=ma=m\frac{\Delta V}{\Delta t}=Q_t(V_1-V_2) \tag{2.50}$$

Where, F-is the force of turbine blades.

5a. Power extracted:

$$P=\frac{\Delta KE}{\Delta t}=\frac{1}{2}\frac{m}{\Delta t}=\frac{1}{2}Q_t(V^2{}_1-V^2{}_2) \tag{2.51}$$

Where, P- is the power that extracted from wind.

5b. Power extracted:

$$P=FV_t=Q_tV_t(V_1-V_2) \tag{2.52}$$

6a. Substitute equation (3) into (5a):

$$P=(\frac{1}{2})\rho A_tV_t(V^2{}_1-V^2{}_2) \tag{2.53}$$

6b. Substitute equation (3) into (5b):

$$P=\rho A_tV^2{}_t(V_1-V_2) \tag{2.54}$$

7. Equate equation 6a and 6b:

$$\Rightarrow\left(\frac{1}{2}\right)V_t(\mathrm{V^2}_2\text{-}\,\mathrm{V^2}_1)=\mathrm{V^2}_t(V_2-V_1)\Rightarrow\left(\frac{1}{2}\right)V_t(V_1-V_2)(V_1+V_2)=\mathrm{V^2}_t(V_1-V_2)\Rightarrow\left(\frac{1}{2}\right)(V_1+V_2)=V_t \quad (2.55)$$

8. Substitute (7) into (6b):

$$P=\rho A_t(\left(\frac{1}{2}\right)(V_1+V_2))^2{}_t(V_1-V_2)=\frac{\rho A_t}{4}(\mathrm{V^2}_1\text{-}\,\mathrm{V^2}_2)(V_1+V_2) \quad (2.56)$$

9. Factor out v_1^3:

$$P=\rho A_t\mathrm{V^3}_t(1-\left((\frac{V_2}{V_1})^2\right)*(1+\frac{V_2}{V_1}) \quad (2.57)$$

10. Define wind stream speed ratio, *a*: This ratio is fixed for a given turbine & control condition**.**

$$a=\frac{V_2}{V_1} \quad (2.58)$$

11. Substitute into power expression of (9):

$$P=\rho\frac{A_t\mathrm{V^3}_1}{4}(1-a^2)(1+a) \quad (2.59)$$

12. Differentiate and find *a*, which maximizes function:

$$\frac{\partial P}{\partial a}=\rho\frac{A_t\mathrm{V^3}_1}{4}[-2a(a+1)+(1-a^2)]=0\Rightarrow -2a^2-2a+1-a^2=-3a^2-2a+1=0\Rightarrow(-3a+1)(a+1)=0\Rightarrow a=\frac{1}{3},\ a=-1 \quad (2.60)$$

13. Find the maximum power by substituting a=1/3 into (11):

$$P=\rho\frac{A_t\mathrm{V^3}_1}{4}(1-\frac{1}{9})(\frac{4}{3})=\rho\frac{A_t\mathrm{V^3}_1}{4}\frac{8}{9}\frac{4}{3}=\frac{8\rho A_t\mathrm{V^3}_1}{27} \quad (2.61)$$

14. Define C_p, the power (or performance) coefficient, which gives the ratio of the power extracted by the converter, P, to the power of the air stream, P_{in}.

Power extracted by the converter:-

$$P=\rho\frac{A_t\mathrm{V^3}_1}{4}(1-a^2)(1+a) \quad (2.62)$$

Power of the air stream:-

$$P_{in}=\frac{\Delta KE}{\Delta t}=\frac{1}{2}\frac{m}{\Delta t}(\mathrm{V^2}_1-0)=\frac{1}{2}Q_t\mathrm{V^2}_1=\frac{1}{2}\rho A_tV_1\mathrm{V^2}_1=\frac{1}{2}\rho A_t\mathrm{V^3}_1 \quad (2.63)$$

$$C_p = \frac{P}{P_{in}} = \frac{\frac{\rho A_t V^3{}_1 (1-a^2)(1+a)}{4}}{\frac{1}{2}\rho A_t V^3{}_1} = \frac{1}{2}(1-a^2)(1+a) \quad (2.64)$$

The total power is the mechanical power extracted by a wind turbine from the wind is expressed by the **cube law** [11].

$$P = C_p P_{in} = \frac{1}{2} C_p \rho A_t V^3{}_1 \quad (2.65)$$

Where, ρ-is the air density [kg/m^3], A_t-is the area covered by the rotor blades in [m^2], C_p-is the turbine performance coefficient [dimensionless], V_t-is the wind speed [m/s],

$$\lambda = R\frac{\omega}{V} \quad (2.66)$$

Where, R- is the radius of the rotor blades, ω- is the angular speed of the blades and λ-is the tip-speed-ratio.

The air density (ρ) depends on factors, such as plane altitude and air temperature and may vary between 1.07 kg/m^3 in hot and high altitude region to 1.395 kg/m^3 in a cold and low lying region. The performance coefficient $C_p$is a function of the tip-speed-ratio **λ** and the pitch angle of the rotor blades β. It depends on the aerodynamic principles governing the wind turbine and may change from one wind turbine to another.

The performance coefficient $C_p$can be found by two ways: One way to get $C_p$is by using lookup table from the manufacturer data sheets. Another way is by approximating C_p by using a non-linear function. The second method is used in this thesis because it gives more accurate results and is faster simulation.

$$C_p(\beta,\lambda) = c_1\left(\frac{c_2}{\lambda_i} - c_3\beta - c_4\right)e^{-\frac{c_5}{\lambda_i}} + c_6\lambda \quad (2.67)$$

Where, c_1=0.22, c_2=116, c_3=0.4, c_4=5, c_5=12.5 and c_6=0

$$\frac{1}{\lambda} = \frac{1}{\lambda+0.08\beta} - \frac{0.035}{\beta^3+1} \quad (2.68)$$

The mathematical representation of C_p is obtained through the expression given below where a_{ij} coefficients are given in [12]. The curve has been obtained for values of λ between 2 and 13.

$$c_p(\beta,\lambda) = \sum_{i=0}^{4}\sum_{j=0}^{4} a_{ij}\beta^i\,\lambda^j \quad (2.69)$$

This implies that higher values of wind generates power more than the rated capacity of the generator and low speed wind generates small power or sometimes may not be sufficient to turn the turbine rotor. For each

pitch angle of the rotor blades, there is an optimum tip-speed-ratio$\lambda_{opt}$for which $C_p$takes a maximum value. This is to say, maximum power extraction from wind for that particular pitch angle. Hence, at low speeds of wind, the angular speed of the rotor blades is regulated to an optimum valueω_{m_opt}through DFIG controls at the rotor blades.

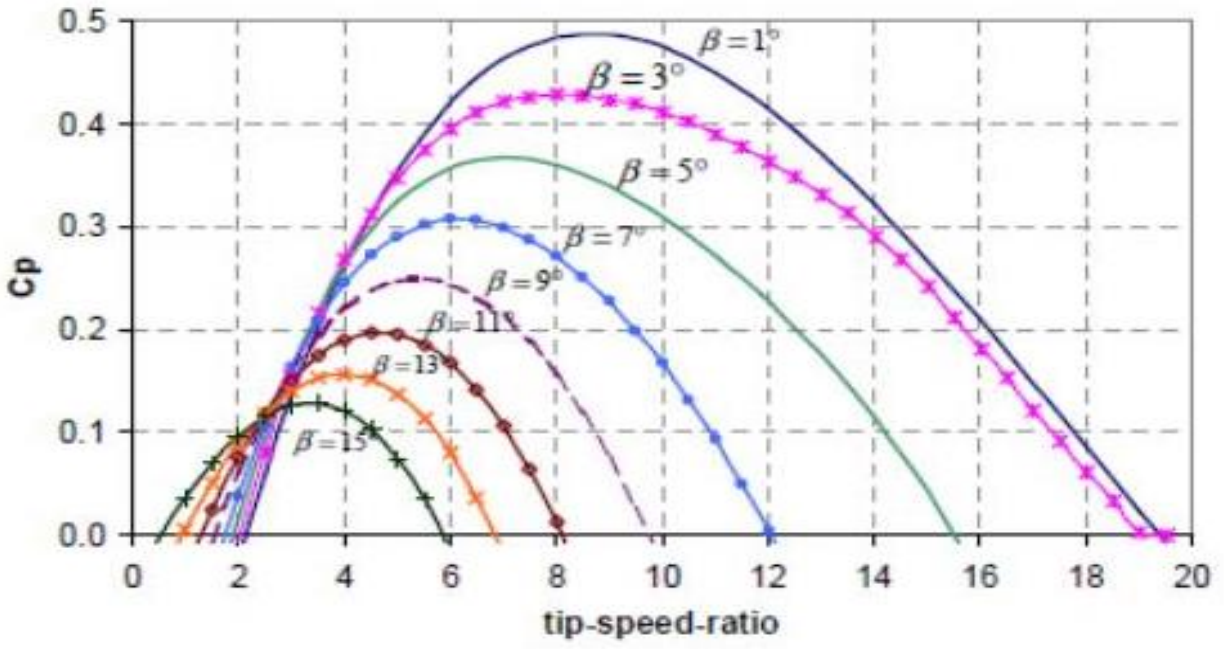

Figure 2.9 A 1.5MW wind turbine curves

15. The maximum value of $C_p$occurs when its numerator is maximum, i.e., when a=1/3**:**

$$C_p = \frac{P}{P_{in}} = \frac{1}{2}\left(\frac{8}{9}\right)\left(\frac{4}{3}\right) = \frac{16}{27} = 0.5926 \qquad (2.70)$$

This fraction is described by the power coefficient of the turbine, which is a function of the blade pitch angle (β) and the tip-speed ratio (λ). It can be found that the maximum power from a wind system is 59.3% of the total wind power. This is called **the Betz limit** for maximum power extraction from the wind system.

2.4. Doubly Fed Induction Generator

Among the various renewable sources, wind energy has gained much attraction in the past few years because of its availability and eco-friendly nature. Large sized wind turbines (WT) are of two types: fixed speed wind turbine generators and variable speed wind turbine generators.

2.4.1. Fixed Speed Wind Turbine Generators

Fixed speed wind turbine generator has the following properties: simple and robust, cannot operate to efficiently capture the energy in the wind, can operate at one speed and the wind speed is variable, for each wind speed there is a certain turbine shaft speed that produces maximum power, and can only operate at maximum aerodynamic efficiency for one particular wind speed. As the wind varies from this speed the efficiency of the wind turbine is reduced.

2.4.2. Variable Speed Wind Turbine Generators

To solve those all problems mentioned under 2.4.1, I recommend to use the best wind turbine generator is the variable speed wind turbine generators. We must use a variable speed wind turbine generators. The wind turbine must be made to operate at variable speeds and to follow the curve of maximum power extraction. Therefore, variable speed wind turbine utilizes the available wind resource more efficiently than fixed speed wind turbine. In Figure 2.10, a variable speed wind turbine capable of tracking the maximum power curve will extract more power than a fixed speed turbine for every wind speed except at point (B = B') in the diagram below.

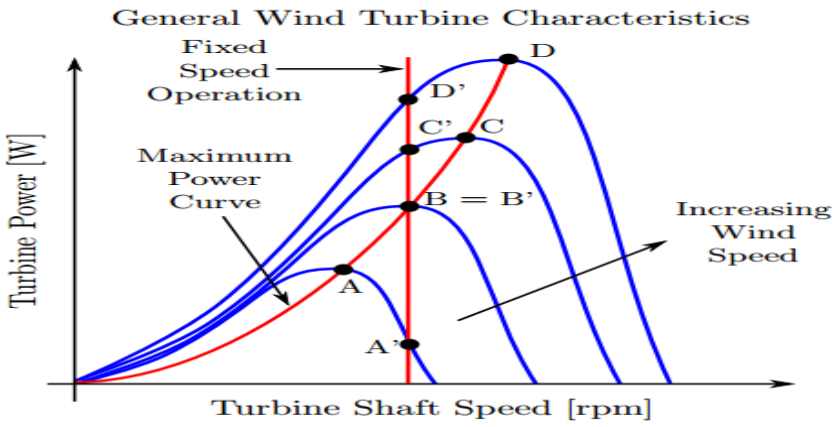

Figure 2.10 General wind turbine characteristics curve

2.4.3. The Advantage of a DFIG Configuration

Doubly fed induction generator (DFIG) is a popular variable speed wind turbine system [23]. The advantages of using DFIG in wind turbine systems are: its capability for better reactive power management, it needs only low power converter-inverter circuits, and no sudden variation in torque with variation in speed and hence the output power will be smooth.

The main advantage of a DFIG is that the converter needed to control the machine is moved to the rotor, and the rotor can be made to handle significantly less power than the stator but still be able to control the power through the stator. The power handled by the rotor is roughly proportional to the slip or relative speed difference from synchronous speed.

But, wind power system based on the DFIG is very sensitive to grid disturbances. A sudden dip in the grid voltage would cause over-currents and over-voltages in the rotor windings and if this exceeds the limit it will destroy the converter if no protection elements are installed. In the conventional protection methods, the DFIG will be disconnected from the grid during the fault. The ability of WT to stay connected to the grid during voltage sags or dip is termed as the low voltage ride through (LVRT) capability. To achieve the LVRT requirement for DFIG WTs, the over-current that can occur in rotor and stator circuits and the DC-link over-voltage during grid fault should be considered properly.

A doubly fed induction machine (DFIM**)** is wound rotor induction machine with its stator windings directly connected to the grid and its rotor windings connected to the grid through a converter. By means of a bi-directional converter in the rotor circuit the DFIG is able to work as generator in both sub-synchronous and super-synchronous modes. DFIG is connected with back-to-back converters.

In this thesis, the grid side converter itself compensates for the reactive power rather than providing an additional compensating device. Additional power is also extracted from the rotor side. The machine side converter controls the rotor speed by using the voltage frequency control technique while the grid side converter controls the DC-link voltage and ensures the operation by making the reactive power drawn by the system from the utility to zero by using the voltage oriented control technique. The grid side current is controlled by using reference current generation in d-q theory.

Wound rotor induction generators (WRIG**s**) are provided with three-phase windings on the rotor and on the stator. They may be supplied with energy at both rotor and stator terminals. Hence, they are called DFIG or double output induction generators (DOIGs) in the generator mode. Both motoring and generating operation modes are feasible, provided the power electronic converters that supply the rotor circuit via slip rings and brushes are capable of handling power in both directions.

The AC/DC/AC Converter is divided in to two components the rotor side converter (RSC) and the grid side converter (GSC). These converters are voltage sourced converters that use force commutated power electronic devices to synthesize an AC voltage from a DC source. A capacitor connected on the DC side acts as the DC voltage source. A coupling inductor is used to connect the grid side converter to the grid.

2.5. Classification of Wind Turbine based on Generation Technologies

According to differences in generation technology, wind turbines have been classified into four basic types [24]:

a) Type 1: Fixed-speed wind turbines,

b) Type 2: Variable-slip wind turbines,

c) Type 3: Doubly-fed induction generator (DFIG) winds turbines and

d) Type 4: Full-converter wind turbines.

2.5.1. Type 1: Fixed-Speed Wind Turbines

Fixed-speed wind turbines (popularly known as the "Danish concept") are the most basic utility scale wind turbines in operation. External reactive power support is necessary to compensate for the reactive power consumed by the induction machine. Because of the limited speed range in which these turbines operate, they are prone to torque spikes that may damage the mechanical subsystems within a turbine and cause transients in the electrical circuitry. These turbines may employ stall regulation, active stall regulation or blade pitch regulation to regulate power at high wind speeds. Despite being relatively robust and reliable, there are significant disadvantages of this technology, namely that energy capture from the wind is suboptimal and reactive power compensation is required. An example of a popular fixed-speed wind turbine is the NEG Micon NM64/1500 turbine, rated at 1.5MW. A schematic for a fixed-speed wind turbine is shown in Figure 2.11 [24].

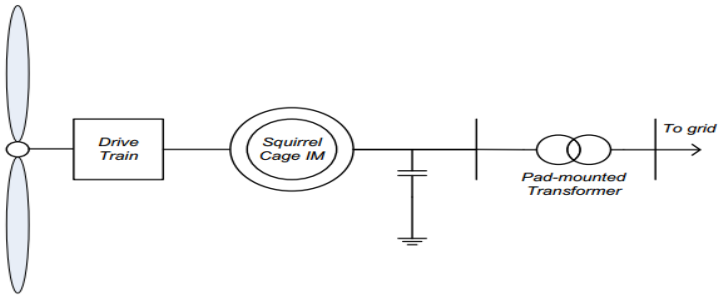

Figure 2.11 Fixed-speed wind turbine schematics

2.5.2. Type 2: Variable-Slip Wind Turbines

Variable-slip wind turbines are designed to operate at a wide range of rotor speeds. These turbines usually employ blade pitching for power regulation. Speed and power controls allow these turbines to extract more energy from a given wind regime than fixed-speed turbines can. Variable-slip turbines employ wound-rotor induction machines that allow access to both the stator and the rotor of the machine. The rotor circuit of the machine is connected to an alternating current (AC)/direct current (DC) converter and a fixed resistance.

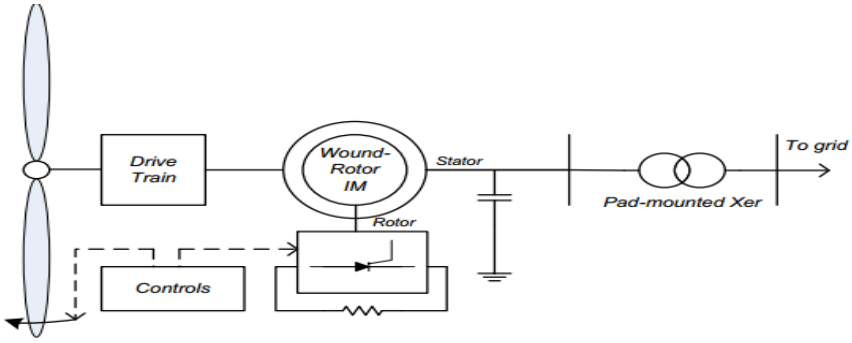

Figure 2.12 Variable-slip wind turbine schematics

The converter is switched to control the effective resistance in the rotor circuit of the machine to allow a wide range of operating slip (speed) variation (up to 10%). However, power is lost as heat in the external rotor circuit resistance. A controller may be employed to vary the effective external rotor resistance for optimal power extraction. Reactive power compensation is still required. Vestas OptiSlip turbines, such as the Vestas V66 (1.65MW), were the most successful turbines to employ this technology. A schematic for this technology is shown in Figure 2.12 [24].

2.5.3. Type 3: Doubly-Fed Induction Generator (DFIG) Wind Turbines

DFIG turbines remedy the problem of power loss in the rotor circuit by employing a back-to-back AC/DC/AC converter in the rotor circuit to recover the slip power. Flux vector control of rotor currents allows decoupled real and reactive output power as well as maximized wind power extraction and lowered mechanical stresses. Also, these turbines usually employ blade pitching for power regulation. Because the converter handles only the power in the rotor circuit, it does not need to be rated at the machine's full output power.

The disadvantages of this technology namely, higher cost and complexity are offset by the ability to extract more energy from a given wind regime than the preceding technologies. The General Electric 1.5MW wind turbine is an example of a successful DFIG implementation; more than 15,000 have been installed in different country. A schematic for this technology is shown in Figure 2.13.

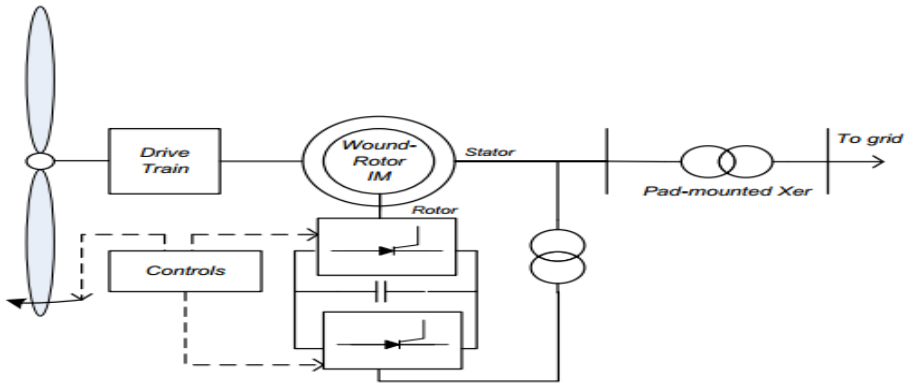

Figure 2.13 DFIG wind turbine schematics

2.5.4. Type 4: Full-Converter Wind Turbines

In full-converter turbines, a back-to-back AC/DC/AC converter is the only power flow path from a wind turbine to the grid. Thus, there is no direct connection to the grid, and the converter has to be rated to handle the entire output power. These turbines usually employ high pole count, permanent magnet, synchronous generators to allow low-speed operation, thus allowing the elimination of the gearbox to increase reliability. Nonetheless, using induction generators is also possible. Also, full-converter turbines offer independent real and reactive power control, and they typically employ blade pitching for power regulation. Although these turbines are relatively expensive, the increased reliability and simplicity of the control scheme vis-à-vis DFIG turbines are attractive features, especially in offshore installations where maintenance is costly. Enercon manufactures turbines based on this technology, such as the popular E82 2MW turbine .A schematic for this technology is shown in Figure 2.14.

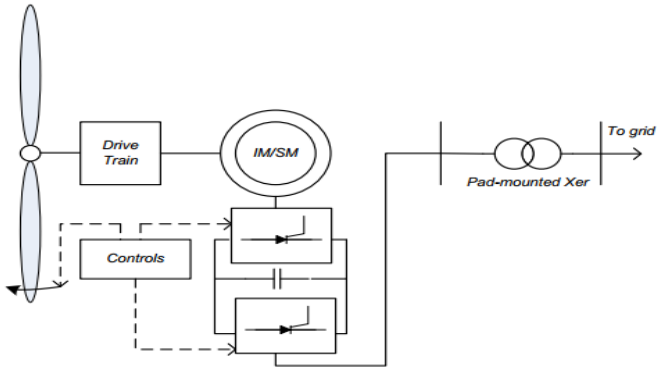

Figure 2.14 Full-converter wind turbine schematics

From those four types of wind turbine, we can detail explain about a Type 3. DFIG turbine model has also been developed using the MATLAB SimPowerSystems toolbox. This model is a phasor model [7]; it treats the power system as a balanced three-phase fixed-frequency network in which each phase voltage is identical in magnitude but out of phase by 120 degrees. Phasor simulation replaces the differential equations representing the network with a set of algebraic equations at a fixed frequency. Phasor simulation facilitates transient stability studies of systems with multiple machines. Phasor simulations, also known as positive sequence simulations, cannot be used to study unbalanced events. This model is better adapted to simulate the low-frequency electromechanical oscillations within seconds to minutes. Another technique available to simulate a generator is to use a three-phase representation, in which an unbalanced simulation can be performed. The unbalanced conditions may come from the grid unbalanced voltage (faults, dips, or other transients) or unbalanced grid impedance.

2.6. Operating Principle of DFIG

The mainstream high-power wind-energy conversion systems (WECSs) are based on doubly-fed induction generators (DFIGs). The stator windings of DFIGs are directly connected to the grids, and rotor windings are connected to the grids through back-to-back power electronic converters. The back-to-back converter consists of two converters, i.e., rotor side converter (RSC) and grid side converter (GS**C**). Between the two converters a DC-link capacitor is placed, as energy storage, in order to keep the voltage variations in the DC-link voltage small. Control of the DFIG is more complicated than the control of a standard induction machine. In order to control the DFIG the rotor current is controlled by a power electronic converter. Wind turbines use a DFIG consisting of a Wound rotor induction generator (WRIG) and an AC/DC/AC power electronic converter.

The stator winding is connected directly to a three-phase, frequency of 50Hz grid while the rotor is fed at variable frequency through theca/DC/AC converter via slip-rings to allow DFIG to operate at variable speeds in response to changing wind speeds. A typical application, for DFIG is wind turbines, since they operate in a limited speed range of approximately 20-25%.

The total system is that the machine-side converter controls the speed, while the grid-side converter controls the DC-link voltage and ensures the operation at unity power factor (i.e. zero reactive power). By means of a bi-directional converter in the rotor circuit the DFIG is able to work as a generator in both sub-synchronous and super-synchronous modes. Depending upon the operating condition, power is fed in to or

out of the rotor (which is the case of super synchronous mode), then it flows from the rotor via the converter to the grid.

2.6.1. DFIG Capability Curves and the Coordinated Reactive Power Controller

2.6.1.1. Two- Mass Model

In stability analysis, when the system response to heavy disturbances is analyzed the drive-train system must be approximated at least a two-mass spring and damper model. It includes generator inertia (J_G), turbine friction damping (D_T) and generator friction damping (D_G).

$$T_T=K_{sh}(\theta_T-\theta_G)-D_T\omega_T=J_T\frac{d\omega r}{dt} \quad (2.71)$$

Where, T_T-is turbine torques and K_{Sh}- is shaft stiffness (Nms/rad)

$$K_{sh}(\theta_T-\theta_G)-T_G-\omega_T D_G=J_G\frac{d\omega e}{dt} \quad (2.72)$$

$$T_{sh}=K_{sh}(\theta_T-\theta_G) \quad (2.73)$$

Where, T_{sh}-is shaft torques (Nm), D_T- turbine friction damping and θ_T, θ_G-turbine and generator angular position (rad).

The idea of using a two-mass mechanical model is to get more accurate response from the generator and the power converter during grid faults and to have a more accurate prediction of the impact on the power systems. A two-mass model (i.e. turbine, drive-shaft and generator inertia) has been used for the DFIG while the drive-train system was represented with finite shaft stiffness. The RSC and GSC reactive power controllers comprise of two control schemes: a slow controller and fast current controller. In terms of the GSC an additional droop is implemented within the slow controller, since both controllers control the reactive power at the point of common coupling (PCC).

2.6.1.2. DFIG Reactive Power Capability Characteristics

The reactive power capability curve of the DFIG can be accredited to both the RSC and GSC. The reactive power capability charts were derived considering the limiting factors and the methodology outlined for the GE 1.5MW DFIG.

Doubly Fed Induction Machine is an induction machine which has four mode of operation where it can work as a generator and as a motor in both positive slip and negative slip region. Both stator and rotor of DFIG are connected with the grid where stator winding is directly connected while, rotor winding is also connected with grid via a back-to-back three-phase voltage source converters. A capacitor of high rating (C_{dc}) connects these two converters and power is flowing through these winding depends upon torque and flux developed machine [25].

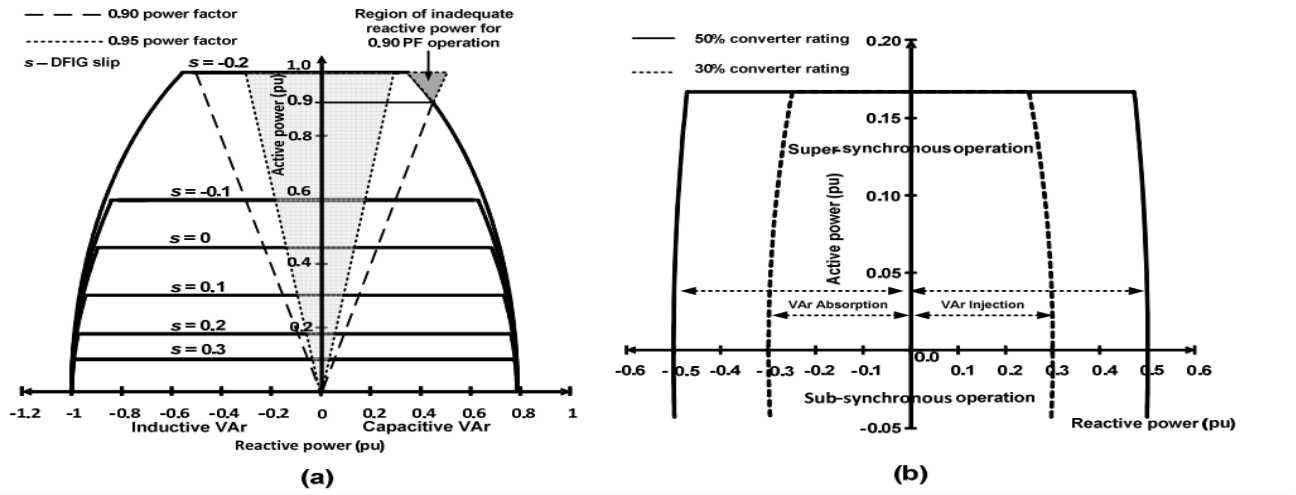

Figure 2.15 DFIG capability curve; a) RSC and b) GSC

The RSC reactive power capability is mainly constrained by the stator current, rotor current and rotor voltage limits [25]. These limiting factors further depend on the operating slip of the machine, and hence individual capability curves were produced for several values of slip. The RSC is capable of operating between +0.95 to -0.95 power factor across the full active power range of the DFIG without additional reactive power support from the GSC. However, 0.90 lagging power factor operation reactive power capability is limited to 0.90 p.u active power output, hence additional reactive power must be provided by the GSC during such conditions.

The GSC reactive power capability is mainly limited by the DC-link and the back-to-back converter ratings, which was derived based on the method outlined in [25]. The GSC capability chart indicates ±0.28 p.u. average reactive power capability for a 30% converter rating across its full operating range while for a 50% converter rating the average reactive power capability increases to ±0.48 p.u. Therefore, a 50% converter

rating indicates a combined reactive power capability of 1.28 p.u during zero active power production. However, during full active power production this reduces to 0.83 p.u.

2.7. Double Fed Induction Generator under Fault

2.7.1. Introduction

There can be many causes for a voltage dip, short circuits somewhere in the grid, switching operations associated with a temporary disconnection of a supply, the flow of the heavy currents that are caused by the start of large motor loads, or large currents drawn by transformer saturation.

Voltage dips due to short-circuit faults cause the majority of equipment trip. Faults are either symmetrical (three-phase or three-phase-to-ground faults) or non-symmetrical (single-phase (1ϕ) or double-phase (2ϕ) or double-phase-to ground faults). Depending on the type of fault, the magnitudes of the voltage dips of each phase might be equal (symmetrical fault) or unequal (non-symmetrical faults). The magnitude of a voltage dip or sag at a certain point in the system depends mainly on the type of the fault, the distance to the fault, the system configuration, and the fault impedance.

The dynamics of the DFIG have two poorly damped poles in the transfer function of the machine, with an oscillation frequency close to the line or grid frequency. These poles will cause oscillations in the flux if the doubly-fed induction machine is exposed to a grid disturbance. After such a disturbance, an increased rotor voltage will be needed to control the rotor currents. When this required voltage exceeds the voltage limit of the converter, it is not possible any longer to control the current as desired. This implies that a voltage dip can cause high induced voltages or currents in the rotor circuit. The high currents on the rotor might destroy the converter of DFIG wind turbine system, if nothing is done to protect it. The rotor currents of the machine are shown for a voltage dip of 85%, implying, that only 15% of the grid voltage remains.

2.7.2. DFIG Wind Turbine under Grid Fault Condition

Consider DFIG in which, immediately after a three-phase fault occurs, the stator voltage and flux reduces toward zero. The voltage drop depends on the location of the fault. The rotor current then increases to attempt to maintain the flux linkage within the rotor windings constant. However, for a DFIG the increase in

the rotor current immediately after a fault will be determined by two factors. The first is the change in the stator flux and the second is the change in the rotor injected voltage.

Grid side converter controls reactive power flow during the fault condition and maintains the voltage of DC link capacitor during normal operating condition. Hence, GSC acts as a rectifier during normal operating condition and as an inverter during fault condition. Rotor side converter control active power and reactive power flowing DFIG by application of vector control method. As grid frequency depends upon active power flow and grid voltage depends upon reactive power flow. By controlling active and reactive power flow we can control the frequency and voltage of gird. To study the control of three-phase current one method is applied in which three-phase grid currents i_a, i_b, i_c are converted into direct axis current i_d and quadeture-axis current i_q [26].

2.7.3. DFIG Wind Turbine Behavior Immediately after the Fault

In the fault instant, the voltage at the DFIG generator terminal drops and it leads to a corresponding decrease of the stator and rotor flux in the generator. This results in a reduction of the electromagnetic torque, reactive power and active power. As the stator flux decreases, the magnetization that has been stored in the magnetic field has to be released. The generator starts its demagnetization over the stator, which is illustrated by the reactive power peak in the moment of the fault.

In the fault moment, as the stator voltage decreases significantly, high current transients appear in the stator and rotor windings. In order to compensate for the increasing rotor current, the rotor side converter increases the rotor voltage reference, which implies a rush of power from the rotor terminals through the converter. On the other side, as the grid voltage has dropped immediately after the fault, the grid side converter is not able to transfer the whole power from the rotor through the converter further to the grid. The grid side converter's control of the DC-voltage reaches thus quickly its limitation. As a result, the additional energy goes into charging the DC-bus capacitor and the DC-voltage rises rapidly.

2.7.4. DFIG Wind Turbine Behavior at Fault Clearance Time

During the fault, the stator voltage and rotor flux have been reduced, the injected rotor voltage has been changed and the rotor speed has been increased. Immediately the fault is cleared the stator voltage is restored, and the demagnetized stator and rotor oppose this change in flux thus leading to an increase in the rotor and stator currents.

2.8. DFIG Protection Schemes during Grid Faults

For wind power generation systems, the doubly-fed induction generator (DFIG) currently dominates with its variable wind speed tracking ability and relatively low cost compared to full-rated converter systems, e.g. permanent magnet synchronous generator (PMSG**)**.

Significant disadvantage of the DFIG is its vulnerability to grid disturbances because the stator windings are connected to the grid through a transformer and switchgear with only the rotor-side buffered from the grid via a partially rated converter. Therefore, to protect the wind farm from interruptions due to onshore grid faults and wind farm faults, a crowbar protects the induction generator and associated power electronic devices. This protection system is widely used in industrial applications.

2.8.1. Crowbar Protection

A crowbar is a set of resistors that are connected in parallel with the rotor winding on occurrence of an interruption, bypassing the RSC. The active crowbar control scheme connects the crowbar resistance when necessary and disables it to resume DFIG control. For active crowbar control schemes, the control signals are activated by the RSC devices [which are usually insulated-gate bipolar transistors (IGBTs)]. These have voltage and current limits that must not be exceeded. Therefore, the RSC voltages and currents are the critical regulation references. The DC-link bus voltage can increase rapidly under these conditions, so it is also used as a monitored variable for crowbar triggering [27].

A major disadvantage of crowbar protection is that the RSC has to be disabled when the crowbar is active and therefore the generator consumes reactive power leading to further deterioration of grid voltage.

2.8.2. DC-Chopper

A braking resistor (DC-chopper) is connected in parallel with the DC-link capacitor to limit the overcharge during low grid voltage. This protects the IGBT from over-voltage and can dissipate energy, but this has no effect on the rotor current.

2.8.3. Series Dynamic Resistor

In a similar way to the series dynamic braking, which has been used in the stator side of generators, a dynamic resistor is proposed to be switched in series with the rotor (series dynamic resistor) and this limits the rotor over-current. Being controlled by a power electronic switch, in normal operation, the switch is on

and the resistor is bypassed; during fault conditions, the switch is off and the resistor is connected in series to the rotor winding [28].

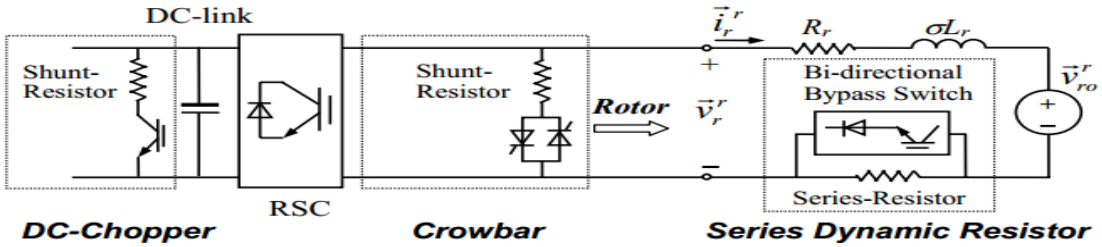

Figure 2.16 DFIG rotor equivalent circuits with all protection schemes

The difference between the series dynamic resistor and the crowbar or DC-link braking resistor is its topology. The latter are shunt-connected and control the voltage while the series dynamic resistor has the distinct advantage of controlling the current magnitude directly. Moreover, with the series dynamic resistor, the high voltage will be shared by the resistance because of the series topology; therefore, the induced overvoltage may not lead to the loss of converter control. Hence, it not only controls the rotor overvoltage which could cause the RSC to lose control, but also limits the high rotor current. In addition, limiting the current reduces the charging current of the DC-link capacitor, which helps avoid DC-link overvoltage. Therefore, with the series dynamic resistor, the RSC does not need to be inhibited during the fault.

The crowbar is adequate for protection of the wind turbine system during grid faults in onshore developments. The adverse impact of temporarily losing RSC of a DFIG in a small-scale wind farm can be tolerated since it only involves a small amount of reactive power consumption; which is not presently the case for large-scale offshore wind farms.

3. Chapter Three: Power Flow Control in Wind Turbine

The phase sequence of the AC voltage generated by the RSC is positive for sub-synchronous speed and negative for super-synchronous speed. The frequency of this voltage is equal to the product of the grid frequency and the absolute value of the slip. The RSC and the GSC have the capability of generating or absorbing reactive power and could be used to control the reactive power or the voltage at the grid terminals. The RSC is used to control the wind turbine output power and the voltage (reactive power) measured at the grid terminals. The GSC is used to regulate the voltage of the DC bus capacitor [28].

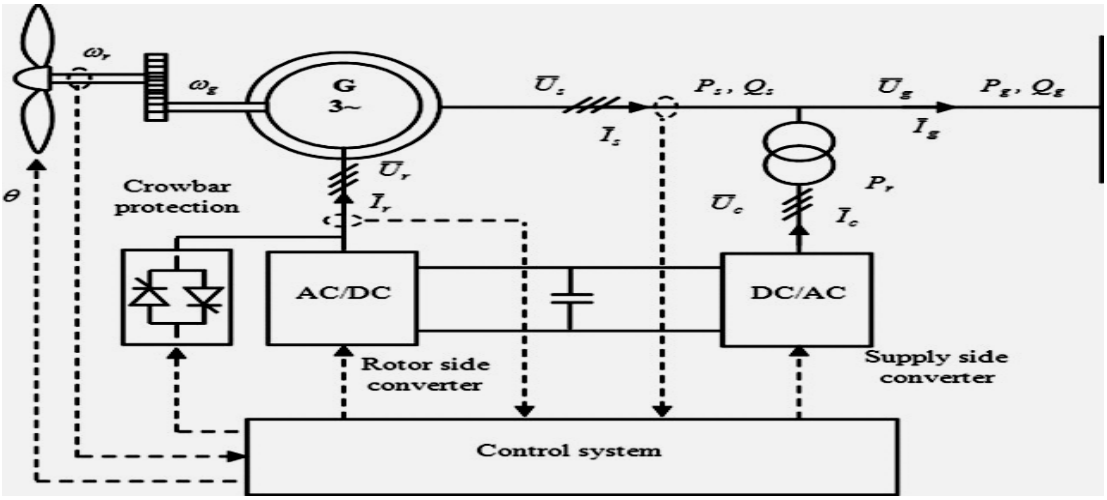

Figure 3.1 DFIG power flow control

3.1. Overall Power Flow in DFIG Wind Turbine System during Grid Fault

The overall energy flow diagram of wind power generation is illustrated in Figure 3.2. The input energy is the kinetic energy stored in the wind. The wind drives the mechanical linkage that converts wind energy into mechanical energy and the electrical linkage converts mechanical energy into useful electrical power from a wind power plant to the energy consumers via transmission and distribution lines.

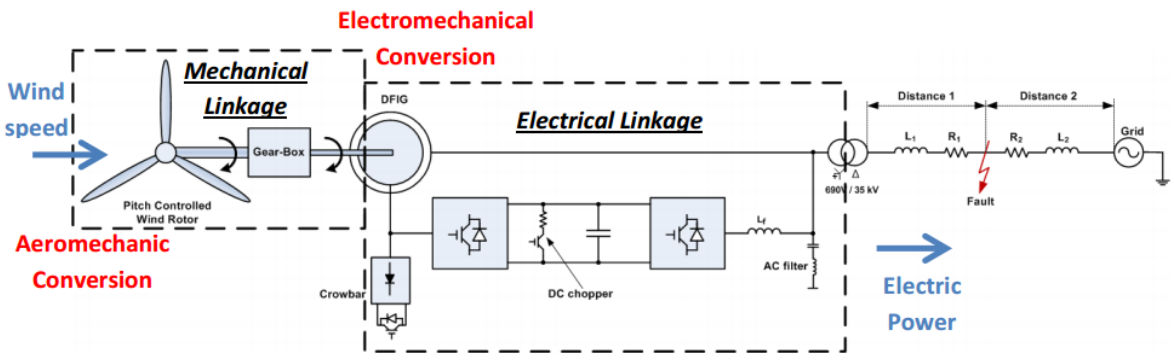

Figure 3.2 Overall energy flows in grid systems

3.1.1. Mechanical Linkage

The mechanical linkage consists of different components, like, shaft, blades, gearbox etc. The input is an aerodynamic input and the output is the electrical output. The source of mechanical stresses (mechanical loads) are diverse.

3.1.1.1. Aerodynamic Input

The aerodynamic input consists of the average wind speed and additional turbulent wind speed. The turbulence is the higher frequency components, caused by wind obstruction (ridges, trees, other turbines) that creates mini swirls of wind imposed on individual blades. In addition, one turbine may experience different wind turbulence from other turbines within a wind power plant. Generally speaking, wind turbulence may excite the mechanical components within the mechanical linkage and may be detrimental to the mechanical component when it hits its frequency modes.

3.1.1.2. Mechanical Output

The mechanical output is the torque that drives the generator. In Type 1 and Type 2 turbines, this torque is a function of the rotational speed. In Type 3 and Type 4 turbines, this torque is controllable by the power converter. The mechanical output converted from the aerodynamic power is affected by the aerodynamic and mechanical controls.

3.1.1.3. Inherent Short-Term Storage and Damping

The inherent short-term storage that exists within the mechanical linkage includes the blade aero-elasticity, the kinetic energy in and out of the rotating mass (shaft, gearbox, generator, blades) and potential energy within the shaft and gearbox stiffness. Short-term storage also includes the inherent damping in the blade-air interaction, the gear-to-gear in the oil bath of the gearbox, the wind age from the air-cooled generator, and/or liquid friction losses in the water- or oil-cooled generator. All of these actually provide some kind of buffer to smooth out the energy spikes presented to the turbines by the presence of turbulence or other sources.

3.1.1.4. Aerodynamic and Mechanical Control

The aerodynamic control of a wind turbine is provided by stalling a wind turbine (self-limiting aerodynamic control). However, the stalled-control wind turbine has not been adapted in the newer turbines. Most of the new turbines use pitch control to adjust the aerodynamic input. Another type of control used in a wind turbine affecting the aerodynamic input is the yaw drive. Mechanical brakes (electromagnetic or hydraulic) are also common in WTGs to avoid a possible runaway event when a wind turbine loses its connection to the grid, and to stop the turbine during parking or repair/maintenance.

3.1.2. Electrical Linkage

The electrical linkage consists of different components (generator, power converter, capacitor, inductor, controllers, etc.). The input is a mechanical torque at the generator shaft input and the output is the electrical power. The sources of electrical stresses (voltage and current) in a wind turbine are diverse.

3.1.2.1. Grid Side Transmission Lines

Many events may occur at the grid as results of natural causes (lightning; short circuits caused by falling trees or animals; shorted, sagging lines caused by high winds, etc.) or man-made events(capacitor switching, loss of lines during fault clearing, loss of generators, loss of loads, etc.).These events may create overload currents, overvoltage and under voltages, or normal/unbalanced voltages. However, before being cleared, the abnormal event may be severe enough that it creates irreversible damage on the turbine components (the gearbox, generator, power converters, etc.), especially if the event creates torque or voltage spikes. These events may not cause instant fatal effects; however, if left uncorrected, the torque pulsations and unequal heating in the generator stator windings may lead to catastrophic failures.

3.1.2.2. Point of Interconnection to Substation

The point of interconnection of a transformer is often chosen to be the high side of the substation transformer, where the metering is installed and the revenue is accounted. At the substation, protections (circuit breakers, transient voltage suppressors, fuses, etc.) are in place to keep the transformer, switchgear, and generators from experiencing abnormal conditions (short-circuit currents, over-voltages, etc.). If the various protections installed at the substation malfunction (e.g., because of aging, improper maintenance, damage, or the wrong coordination of relay protection), the abnormal events can be transmitted to the generators and power converters connected to a power line.

3.1.2.3. Generators and Power Converters

Generators and power converters are connected to the grid. In Type 1, 2, and 3 WTGs, the generator stator windings are connected to a power grid; hence, any voltages and frequency disturbances may affect wind turbine components instantly and directly. In Type 4 WTGs, a power converter connects the grid to the stator winding of the generator; thus, there is less direct impact of line disturbance on WTGs.

3.1.2.4. Power Converters

The power converters for Type 3 and Type 4 WTGs are connected to the grid; thus, anything that occurs on the grid can be passed to a generator directly (for Type 1, 2, and 3 WTGs) or indirectly(for Type 4 WTGs). The power converter and generators are very susceptible to abnormal events occurring on transmission lines. Subsequently, because of abnormal events on the grid, the generated torque may impact the wind turbine mechanical components. Further, the extreme ramping rates and turbulence coming to the wind power plant may affect the power system to which it is connected.

3.2. Power Balance Relations

The equivalent circuit in Figure 2.3-2.6 completely neglects any mechanical power losses and the electrical core losses. This model has been chosen to match up with the complexity of the dynamic model required for control. It is still more than detailed enough to describe the basic power balance and flow through the machine. The purpose of this section is to give an idea how power flows in the four different modes.

3.2.1. Active Power Balance

First of all there are three places active power can be injected or removed from the machine; the stator terminals, the rotor terminals and the rotor shaft. Additionally some active power is dissipated as heat from

the stator and rotor winding resistances. Both stator and rotor currents are assumed to be entering the machine, that is they are in motoring convention. This means that a positive P_s or P_r implies the machine is consuming power from the respective terminals and negative P_s and P_r implies the machine is supplying power from the respective terminals.

$$P_s = 3Re\{V_s * I_s^*\} \quad (3.1)$$

$$P_r = 3Re\{V_r * I_r^*\} \quad (3.2)$$

In the motoring convention, P_{mech} is chosen positive for motoring power; that is $P_{mech}>0$, i.e. the machine is producing mechanical torque. $P_{mech}<0$ implies that the machine requires mechanical power from an outside source, the prime mover. The mechanical power modelled by the resistor $R_r(\frac{1-s}{s})$is:

$$P_{mech,Rr} = 3|I_r|^2 R_r(\frac{1-s}{s}) \quad (3.3)$$

When $\mathbf{P_{mech,Rr}}$ is positive and it represents dissipation of electrical power, which matches the definition of P_{mech} where electrical power is converted to mechanical for positive values. Note that a negative value of slip will make $P_{mech,Rr}$ negative, which means it is supplying electrical power. The mechanical power modelled by the voltage source V_r $(\frac{1-s}{s})$is:

$$P_{mech,Vr} = 3(\frac{1-s}{s})Re\{V_r I_r^*\} \quad (3.4)$$

Notice the voltage is in source convention; the current is leaving the positive terminal. This is in opposition to the definition of P_{mech} since a positive value of $P_{mech,Vr}$ means electrical power is injected into the circuit. The reason for choosing this polarity for V_r $(\frac{1-s}{s})$ was to match with the polarity of V_r when separating V_r/s into V_r and V_r $(\frac{1-s}{s})$. Now the full expression for mechanicalpower can be written:

$$P_{mech} = P_{mech,Rr} - P_{mech,Vr} \quad (3.5)$$

$$P_{mech} = 3|I_r|^2 R_r(\frac{1-s}{s}) - 3(\frac{1-s}{s})Re\{V_r * I_r^*\} \quad (3.6)$$

Finally, the power dissipation from the stator and rotor winding resistances are given as:

$$P_{cu,s}= 3|I_s|^2R_s \quad (3.7)$$

$$P_{cu,r} = 3|I_r|^2R_r \quad (3.8)$$

The power in the stator and rotor pass to each other through the air gap. For motoring convention, positive power at the air gap implies power flowing from the stator to the rotor. On the stator side,

$$P_{ag}= P_s - P_{cu,s} \quad (3.9)$$

On the rotor side,

$$- P_{ag}= P_r - P_{cu,r}- P_{mech} \quad (3.10)$$

Therefore, the power balance of the entire machine is,

$$P_s+ P_r= P_{cu,r}+ P_{cu,s}+ P_{mech} \quad (3.11)$$

Where, P_{ag}, P_s, $P_{cu,s}$, $P_{cu,r,}$ P_r and P_{mech}, air-gap power, stator power, power dissipation from the stator and rotor winding resistances, stator power and mechanical power, respectively.

All power on the stator side is electrical in nature while the rotor is host to both mechanical and electrical power. Electrical power in the rotor is sometimes referred to as slip power [29], because its magnitude is proportional to slip.

$$P_{slip}= P_{cu,r}- P_r \quad (3.12)$$

$$= 3|I_r|^2R_r - 3Re\{V_r*I_r^*\} \quad (3.13)$$

Therefore, the total power passing through rotor is:

$$-P_{ag}= 3|I_r|^2R_r/s- 3Re\{V_r*I_r^*\}1/s \quad (3.14)$$

Now it is apparent to see, $P_{slip}= sP_{ag}$ (3.15)

$$P_{mech}= (1 - s)P_{ag} \quad (3.16)$$

3.2.2. Reactive Power Balance

Reactive power is necessary to magnetize the machine windings. Unlike a conventional induction machine that must draw reactive power from its stator, the DFIG can inject reactive power through the rotor to better utilize the copper in its windings. That is the reactive power load of the machine, which constitutes an increase in current can be shared by both windings [30].The leakage and magnetizing inductances L_s ,L_r and L_m consume reactive power denoted by Q_{Ls}, Q_{Lr} and Q_{Lm} respectively. The stator and rotor terminals are ports that can exchange (either consume or supply) the reactive power Q_s and Q_r. Additionally, there is a voltage source V_r $(\frac{1-s}{s})$ which can exchange the reactive power Q_{vir}. By analyzing the model in a completely mathematical sense, the reactive power balance is:

$$Q_{Ls}+ Q_{Lr}+ Q_{Lm}= Q_s+ Q_r+ Q_{vir} \quad (3.17)$$

Where;

$$Q_s= 3\mathrm{Im}\ \{V_s*I_s^*\} \quad (3.18)$$

$$Q_r= 3\mathrm{Im}\ \{V_r*I_r^*\} \quad (3.19)$$

$$Q_{Ls}= 3|I_s|^2\omega_s*L_s \quad (3.20)$$

$$Q_{Lr}= 3|I_r|^2\omega_s*L_r \quad (3.21)$$

$$Q_{Lm} = 3|I_s+ I_r|^2\omega_s*L_m \quad (3.22)$$

$$Q_{vir}= 3\mathrm{Im}\{\ (\frac{1-s}{s})V_r*I_r^*\} \quad (3.23)$$

Note that Q_{Ls}, Q_{Lr}, Q_{Lm}, Q_s and Q_r have physical meaning, whereas Q_{vir} is more obscure. According to [31] the term Q_{vir} which arises from the voltage source $V_r(\frac{1-s}{s})$is a virtual effect of the external circuit and is necessary to include when the circuit manipulations to reduce the rotor to the stator are applied. The reactive power introduced to the circuit from this modeling element actually comes from the external circuit (the power converter).

3.3. Modes of Operation of DFIG

All machines are capable of working in the four quadrant operation depicted, provided they are connected to a capable drive. A wound rotor induction machine is able to operate in modes that a caged induction machine cannot because of the added flexibility provided by the access to the rotor terminals. It is able to achieve a full four quadrant operation for a uni-directional shaft rotation. This is different from the usual definition of four quadrant operation. That is they can motor and generate in the forward and reverse directions. The ability to reverse direction is unnecessary in wind turbine applications; the turbine blades will always spin the shaft in the same direction.

Induction machines are designed to operate around their synchronous speed. When the shaft spins slower than synchronous speed it is known as sub-synchronous operation and the machine can only motor. When the shaft spins faster than synchronous speed it is known as super-synchronous operation and the machine can only generate. This is because the direction of the induced torque in an induction machine depends on the speed. A wound rotor machine can be made to generate or motor above or below synchronous speed and thus achieves this sort of four quadrant operation.

3.3.1. Characteristics of the DFIG Wind Turbine System

The exchange of power through the terminals of a wound rotor machine can be explained here in this section. It will be seen that the intrinsic nature of the flow is well suited for variable speed generation. For this discussion, the dissipated power in the stator and rotor resistances will be neglected to simplify the explanation and make the fundamental points clear. As a renewable resource, wind has several important characteristics including that it is hard to predict and that its direction and speed vary quickly and randomly. These features complicate the process of converting energy from wind to electricity.

The negative value of the slip implies running the machine above synchronous speed in the direction of the rotating field. As the torque direction is simultaneously reversed (opposite to the direction of the rotating field), the machine has to be driven by a source of mechanical power to counteract the opposing torque. In the process the machine acts as a generator feeding power to the source. For s>1, the machine runs in a direction opposite to that of the rotating field and the internal torque. In order to sustain this condition, the machine should also be driven by a mechanical power source. This mode of operating the induction machine is known as plugging and is equivalent to an electrical braking method.

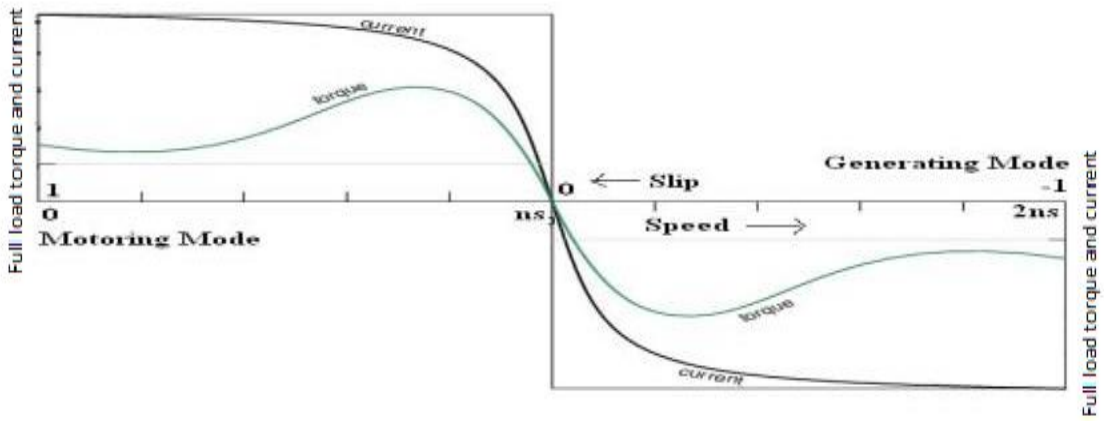

Figure 3.3 Natural curve of slip for the DFIG (full load torque and current)

As the rotor speed spins slower or faster than synchronous, the slip begins to increase. The power flowing stays proportional to this slip and everything keeps working if the proper frequency alternating currents are injected into the rotor. Now by limiting the speed ranges around synchronous, the power flow through the rotor is limited as well. If the speed range was extended all of the way to zero, or all of the way to twice synchronous, then the rotor would have to handle full power and the advantage would be lost. Fortunately, to cover the normal range of wind speeds that exist in nature, it has been found that the slip range only needs to extend about 30% above or below synchronous, so the power converter can be reduced to 30% as well [31].

3.3.1.1. Sub-synchronous Motoring

This mode is characterized by $P_{mech}>0$, that is mechanical power is available at the shaft, and a slip in the range of $0 < s < 1$.See figure 3.3.

$$P_{ag}=\frac{Pmech}{1-s} \Rightarrow P_{ag}>0 \; and \; |P_{ag}| > |P_{mech}| \tag{3.24}$$

$$\therefore P_{slip}= sP_{ag} \Rightarrow P_{slip}>0 \tag{3.25}$$

Therefore, the power flows across the air gap from stator to rotor side. There is more power at the air-gap than available at the shaft, and the extra power is present at the rotor terminals.

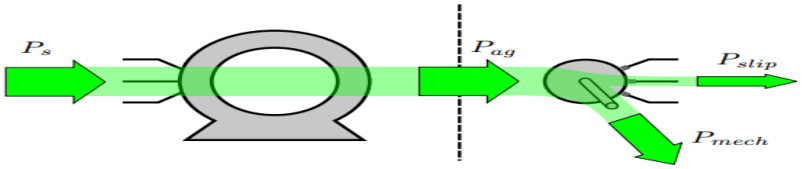

Figure 3.4 Power flow in sub-synchronous motoring mode

3.3.1.2. Super-synchronous Motoring

This mode is characterized by $P_{mech}>0$, and a slip in the range of $-1< s <0$.

$$P_{ag}=\frac{Pmech}{1-s} \Rightarrow P_{ag}>0 \; and \; |P_{ag}| < |P_{mech}| \tag{3.26}$$

$$\therefore P_{slip}= sP_{ag} \Rightarrow P_{slip}<0 \tag{3.27}$$

As with sub-synchronous motoring, P_{ag} is still positive, it flows across the air-gap from the stator to the rotor. This time it is less than P_{mech} and the power required to sustain motoring must be input to the rotor; this is seen by P_{slip} becoming negative.

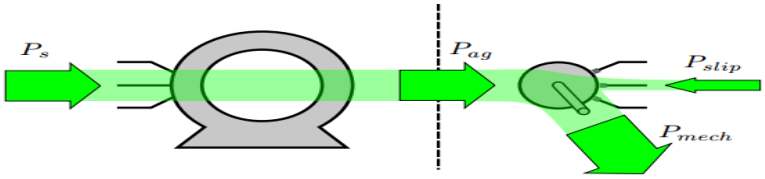

Figure 3.5 Power flow in the super-synchronous motoring mode

3.3.1.3. Super-synchronous Generating

This mode is characterized by $P_{mech}<0$, that is mechanical power is needs to be input to the shaft, and a slip in the range of $-1< s <0$.

$$P_{ag}=\frac{Pmech}{1-s} \Rightarrow P_{ag}<0 \; and \; |P_{ag}| < |P_{mech}| \tag{3.28}$$

$$\therefore P_{slip}= sP_{ag} \Rightarrow P_{slip}>0 \tag{3.29}$$

The main input to the system is in the rotor now, reversing the direction of P_{ag} to transfer power to the stator. The input mechanical power is greater than the air-gap power and the extra power is available from the rotor terminals.

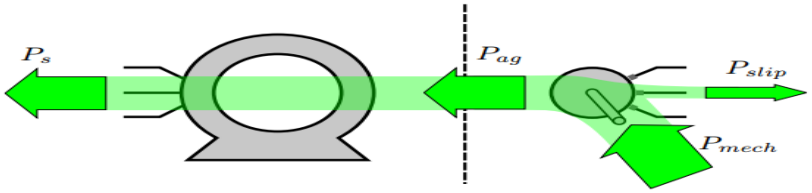

Figure 3.6 Power flow in the super-synchronous generating mode

3.3.1.4. Sub-synchronous Generating

This mode is characterized by $P_{mech}<0$ and a slip in the range of $0 < s <1$.

$$P_{ag}=\frac{Pmech}{1-s} \Rightarrow P_{ag}<0 \text{ and } |P_{ag}| > |P_{mech}| \quad (3.30)$$

$$\therefore P_{slip}= sP_{ag} \Rightarrow P_{slip}<0 \quad (3.31)$$

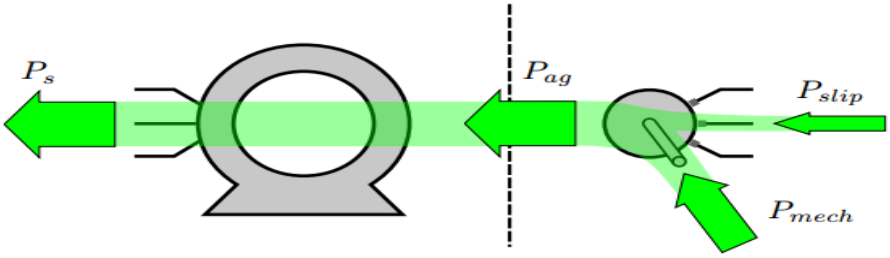

Figure 3.7 Power flow in sub-synchronous generating mode

As with super-synchronous generation $P_{ag}<0$ and power is transferred from the rotor to the stator. This time the mechanical power is less than the air-gap power and extra power must be injected into the rotor to sustain the generating mode. Electrical power in the rotor is sometimes referred to as slip power.

4. Chapter Four: Controller Design

4.1. Introduction

Proportional plus Integral (PI) controller is used to calculate the error value as the difference between a measured process variable and a desired set point. The controller attempts to minimize the error. The combination of proportional and integral terms is important to increase the speed of the response and also to eliminate the steady state error. The PID (Proportional-Integral-Derivative) controller block is reduced to P (Proportional) and I (Integral) in Matlab/Simulink blocks.

4.2. Parameter Selection of the controller

Proportional plus Integral (PI) control

A proportional-integral controller is a control loop feedback mechanism commonly used in industrial control systems. PI controller continuously calculates an error value as the difference between a desired set point and measured process variable. The controller attempts to minimize the error over time by adjustment of a control variable, such as the position of a control valve, a damper or the power supplied to a heating element. Including a term that is a function of the integral of the error can, with the type of plant shown in Figure 4.1 below, eliminate steady-state errors.

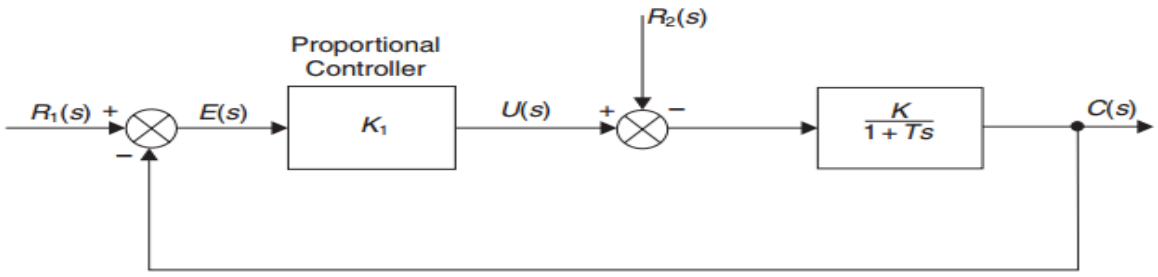

Figure 4.1 Proportional control of a first-order plant

Consider a control law of the form:

$$u(t)=K_1e(t)+ K_2\int edt \qquad (4.1)$$

Taking Laplace transforms:

$$U(s) = (K_1+K_2/s)\, E(s)$$

$$=K_1\ (1+K_2/K_1s)\ E(s)$$
$$=K_1\ (1+1/T_is)\ E(s) \quad (4.2)$$

In above equation, T_i is called the integral action time and formally defined as, the time interval in which the part of the control signal due to integral action increases by an amount equal to part of the control signal due to proportional action when error is unchanging [31]. Inserting the PI-control law gives in above equation (4.2) into the first-order plant transfer function shown below: The plant transfer function is:

$$(U(s)-R_2(s))(\frac{K}{1+T_s}) = C(s) \quad (4.3)$$

And the proportional control law, from the equation:

$$u(t) = K_1e(t) \text{ it becomes },U(s) = K_1(R_1(s)-C(s)) \quad (4.4)$$

Inserting the above equation (4.4) into equation (4.3) gives:

$$C(s) = \frac{\{K_1(R_1(s)-C(s))-R_2(s)\}K}{(1+T_s)} \quad (4.5)$$

This can be written as:

$$\{(1+K_1K) +T_s\}C(s) =K_1KR_1(s)-KR_2(s) \quad (4.6)$$

Re-arranging above equation (4.6) gives

$$C(s)=\frac{(\frac{K_1K}{1+K_1K})R_1(s)-(\frac{K}{1+K_1K})R_1(s)}{\{1+(\frac{T}{1+K_1K})s\}} \quad (4.7)$$

When $r_1(t)$ is a unit step and $r_2(t)$ is zero, the Final Value Theorem:

$$f(\infty)=\lim_{t\to\infty} f(t)^1 = \lim_{s\to\infty}(sF(s))^1 \quad (4.8)$$

Gives the steady-state response:

$$c(t)=(\frac{K_1K}{1+K_1K}) \quad \text{as } t \Rightarrow\infty \quad (4.9)$$

Hence, for the system to have zero steady-state error, the terms in equation (4.7) should be

$$\frac{K_1K}{1+K_1K}=1, \qquad \frac{K}{1+K_1K}=0 \tag{4.10}$$

This can only happen if the open-loop gains constant K_1K is infinite. In practice this is not possible and therefore the proportional control system will always produce steady-state errors. These can be keeping the open-loop gain constant K_1K as high as possible. Since the close-loop time-constant form above equation (4.7) is:

$$T_c= \left(\frac{T}{1+K_1K}\right) \tag{4.11}$$

Then maintaining K_1K at a high value will reduce the close-loop time constant and therefore improve the system transient response. Inserting the PI-control law given in above equation (4.2) into first-order plant transfer function in equation (4.3) gives:

$$C(s) =\frac{(K_1(1+\frac{1}{Tis})(R_1(s)-C(s)-R_2(s))K}{(1+T_s)} \tag{4.12}$$

This can be written as:

$$\{T_iT_s^2+T_i(1+K_1K)s+K_1K\}C(s) = K_1K\ (1+T_is)\ R_1(s)-K_1KT_isR_2(s) \tag{4.13}$$

Re-arranging gives:

$$C(s) = \frac{(1+T_{is})R_1(s)-T_{is}R_2(s)}{\left(\frac{T_iT}{K_1K}\right)s^2+T_{is}\left(1+\frac{1}{K_1K}\right)s+1} \tag{4.14}$$

4.3. Proportional-Integral Controller

The traditional proportional integral (PI) controller is usually adopted with either stator voltage orientation (SVO) or stator flux orientation. In this PI controller, perfect regulation is only achievable for the DC components, steady state error is zero and a lot of derivatives can be obtained at high frequency terms. There are typically two control strategies for the variable-speed wind turbine. In low wind speed below rated value; the speed controller can continually adjust the speed of the rotor to maintain the speed at a level, which gives the maximum power coefficient. Then the efficiency of the turbine will increase. Pitch angle regulation is required in conditions above the rated wind speed when the rotational speed is kept constant.

Small change in pitch angle can affect the power output of the wind turbine system. Based on the general description, PI controller is adopted in the rotor circuit of DFIG.**P** accounts for present values of the error. For example, if the error is large and positive, the control output will also be large and positive. **I** accounts for past values of the error. For example, if the current output is not sufficiently strong, error will accumulate over time, and the controller will respond by applying a stronger action.

The purpose of the control can be summarized in three aims as follows:

1. Optimizing the power output when a wind speed is less than rated wind speed
2. Keeping the rotor power at design limits when the wind speed is above rated wind speed
3. Minimize the fatigue loads of the turbine mechanical components.

Why I choose the PI controller?

In an active Proportion-Integral-Derivative (**PID**) pitch controller, the sensitivity of aerodynamic power to the rotor collective blade pitch angle is negative. With positive control gains, the derivative term will increase the effective inertia of the drive-train. Because of the above reasons I recommend using a proportion integral (PI) controller.

However, Bouthezzar suggest using only a proportional pitch controller based on the test results that show a more complex controller (PI & PID) will make the pitch control more turbulent without a significant improvement of the power regulation performance. Moreover, it is shown that using an advanced control strategy such as LQR(Linear Quadratic Regulator)control design technique ensures a better power tracking than the PID controller, but this turns out to be still insufficient to meet all the control objectives (Eisenhut et al. 2007).

Theoretical method to calculate PI-controller Gain

Change in the pitch angle is:

$$\dot{\beta}= (\beta_d-\beta)/\tau_\beta \tag{4.15}$$

$$\beta/\beta_d=\frac{1}{\tau\beta+1} \tag{4.16}$$

This is the transfer function for the actuator. Where τ_β-is a time constant depends on the pitch actuator.

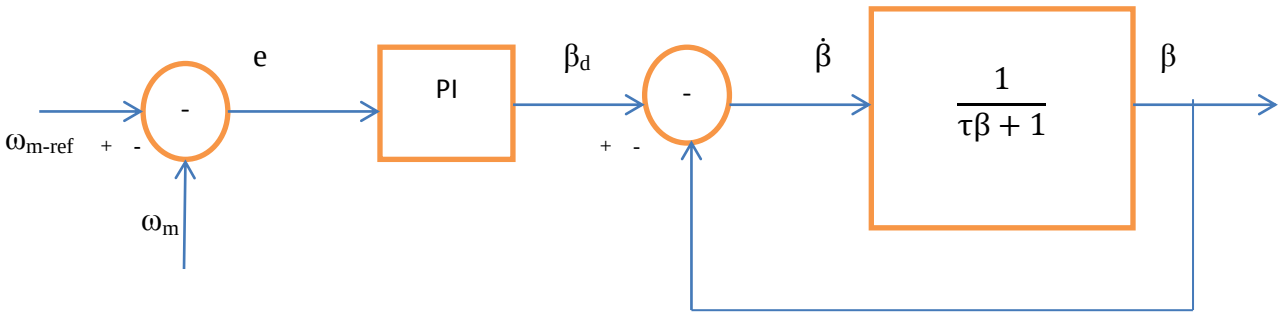

Figure 4.2 PI controller system

The output signal from PI-controller is β_d as showing in Figure. 4.2 above, which also contains the actuator's transfer function that obtained from above equation. The PI-controller and desired pitch angle can be expressed as follows:

$$\beta_d=K_pe+K_i\int edt \tag{4.17}$$

Where, $e=\omega_{m\text{-}ref}-\omega_m$, $\omega_{m\text{-}ref}$-is the rated rotor speed (reference generator speed).

To find the solution, let be x,

$$x=K_i\int edt \text{ or } \frac{dx}{dt}=K_ie \tag{4.18}$$

$\beta_d=K_pe+K_i\int edt$ and $x=K_i\int edt$ from this equation, the partial derivatives of β_d with respect to e, is expressed as follows:

$$\frac{d\beta d}{de}=\frac{d(K_Pe+K_I\int edt)}{de} \tag{4.19}$$

$$\frac{d\beta d}{dt}=K_p+\frac{dx}{dt}\Rightarrow K_p+\frac{dx/dt}{de/dt}\Rightarrow K_p+\frac{K_Ie}{de/dt} \tag{4.20}$$

For an adjustable slip asynchronous generator, the variation range of e is very small. Moreover, K_p is far greater thanK_I. Equation (4.20) can be simplified as follows:

$$K_p=\frac{d\beta d}{de}\Rightarrow d\beta_d=\beta_d(\ \beta_{d0}=0\text{- initial value}) \tag{4.21}$$

To find the direct relation between β and β_d we reduce inner closed loop for the actuator in above Figure 4.2, to the forward path and assuming τ_β=1 sec. then we obtain the transfer function:

$\frac{\beta}{\beta d}=\frac{1}{\tau\beta+1}=\frac{1}{s+2}$, in the steady state let s $\Rightarrow$ 0, $\frac{\beta}{\beta d}=\frac{1}{s+2}=\frac{1}{0+2}\Rightarrow\beta_d=2\beta$ (4.22)

The K_p and K_I are:

$$K_p=\frac{2\beta}{\omega_{m\_ref\_\omega m}} \quad (4.23)$$

$$K_i=\frac{1}{\omega_{m\_ref\_\omega m}}*(\frac{2\beta}{\omega_{m\_ref\_\omega m}}-Kp)*\frac{\partial\Delta\omega}{\partial t} \quad (4.24)$$

From equations (4.23) and (4.24), the value of the integral coefficient $K_I\approx 0$, since the middle of the equation (4.24) is equal to zero. The gain of the PI controller is obtained from the proportional gain K_p and integral gain K_I. These gains reduce the rise time, steady state error and increases overshoot and settling time.

$$G_{PI}(s)=K_p+\frac{Ki}{s} \quad (4.25)$$

For fault condition the above equations become:

$\frac{\beta}{\beta d}=\frac{1}{\tau\beta+1}=\frac{1}{s+2}$, in the fault state let s $\Rightarrow$ t, $\frac{\beta}{\beta d}=\frac{1}{s+2}=\frac{1}{t+2}\Rightarrow\beta_d=(t+2)\beta$, then K_p and K_I:

$$K_p=\frac{(t+2)\beta}{\omega_{m\_ref\_\omega m}} \quad (4.26)$$

$$K_i=\frac{1}{\omega_{m\_ref\_\omega m}}*(\frac{(t+2)\beta}{\omega_{m\_ref\_\omega m}}-Kp)*\frac{\partial\Delta\omega}{\partial t} \quad (4.27)$$

Where, t is the fault time interval.

4.4. Design of Inner Control Loop

In low wind speed below a rated value, the speed controller can continually adjust the speed of the rotor to maintain the speed at a level, which gives the maximum power coefficient, and then the efficiency of the turbine will be increased. Pitch angle regulation is required in conditions above the rated wind speed when the rotational speed is kept constant. Small changes in pitch angle can affect the power output. The inner loop is designed with outer loop variables viewed as constants.

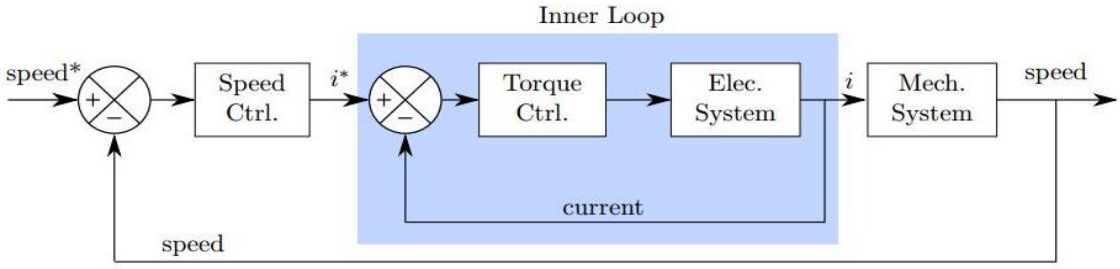

Figure 4.3 Standard cascading control structure

For the DFIG there are two of cascaded control loops, see Figure 5.3. Vector control acts on the inner loop and regulates the fastest changing electrical variables. The torque producing component i_{rq} can then be related to real power in the outer loop. The flux producing component i_{rd} is related in the outer loop to the reactive power of the machine. In this way decoupled control of active and reactive power is achieved.

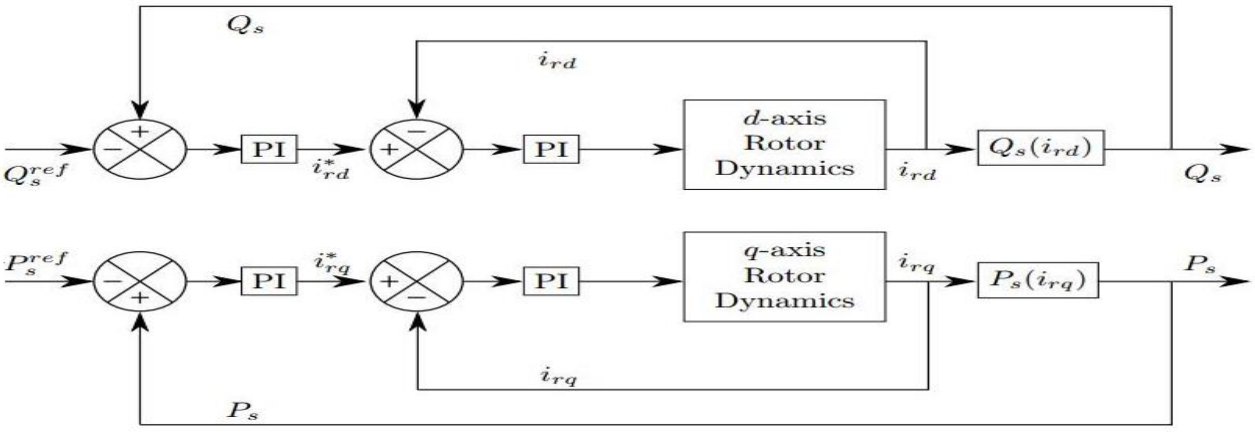

Figure 4.4 Top: the d-axis control loop regulating Q_s, Bottom: the q-axis control loop regulating P_s

A slight modification and improvement to the cascading control structure of DFIG method is provided by Tapia. et al [33] in their work with DFIGs. Instead of completely ignoring the inner loops, they approximate them by simple first order systems.

Many authors and researchers use a standard PI controller to satisfy the inner and outer loops independently according to the method of cascaded control. The proportional part is fed directly from the measured value instead of from the error signal. Figure 4.5shows the standard PI control structure and Tapia's modification. The transfer function for the inner loop is derived in Appendix C:

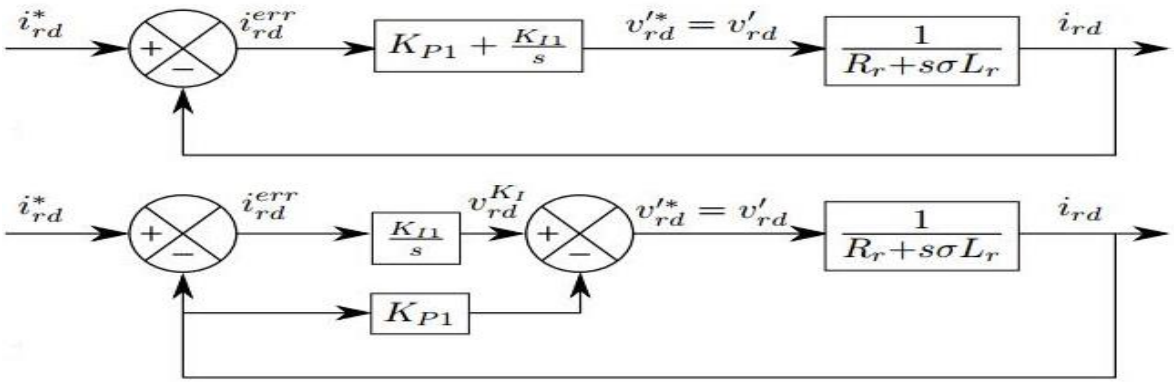

Figure 4.5 Top: standard PI configuration, Bottom: Tapia's modified configuration

The advantage to this structure is that the transfer function of the dynamics will be in standard second order form, as opposed to the standard PI structure which leads to a zero in the transfer function.

$$\text{Standard: } \frac{i_{rd(s)}}{i_{rd(s)}^*} = \frac{K_{P1}s + K_{I1}}{s^2\sigma L_r + s(R_r + K_{P1}) + K_1} \tag{4.28}$$

$$\text{Tapia: } \frac{i_{rd(s)}}{i_{rd(s)}^*} = \frac{\frac{R_r + K_{P1}}{\sigma L_r}}{s^2 + s\left(\frac{R_r + K_{P1}}{\sigma L_r}\right) + \frac{K_{I1}}{\sigma L_r}} \tag{4.29}$$

Notice that Tapia's structure results in a transfer function in the standard 2nd order form of:

$$G(s) = \frac{\omega^2{}_n}{s^2 + 2\xi\omega_n s + \omega^2{}_n} \tag{4.30}$$

Calculation of Inner Loop Controller Constants K_{P1} and K_{I1}

The first criterion that Tapia's method requires is that the system is critically damped. This sets the following condition: $\xi = 1$.

The inner loop must be critically damped so that it exhibits no overshoot and its second order dynamics can later be approximated accurately with a first order system. The second criteria that Tapia suggests are to specify the natural frequency ω_n by demanding a reasonable settling time. According to [34], the time for a standard second order system to settle with 2% of its final value is,

$$T_s = \frac{4}{\xi \omega_n} \tag{4.31}$$

Comparing coefficients in equations 4.29 and 4.30, K_{P1} and K_{P2} are determined,

$$\omega_{n1}^2 = \frac{K_{I1}}{\sigma L_r} \tag{4.32}$$

$$2\xi\omega_{n1} = \frac{R_r + K_{P1}}{\sigma L_r} \tag{4.33}$$

Imposing the criteria from equation 4.31 in Equations 4.32 and 4.33 yields,

$$K_{p1} = \frac{8}{T_{s1}} \sigma L_r - R_r \tag{4.34}$$

$$K_{I1} = \frac{8}{T_{s1}} \sigma L_r - R_r \tag{4.35}$$

Tapia suggests an inner loop settling time of T_{s1}= 40ms. Checking the bandwidth criterion in $\omega_B \approx 0.65\omega_n$, and $\omega_B < 2\pi 500$. Where, ω_B the bandwidth of the closed loops system.

$$\omega_B \approx 0.65*4/T_{s1} = 0.65*4/0.04 = 65 < 2\pi 500. \tag{4.36}$$

This settling time is more than conservative enough to be achieved with a 5kHz inverter.

The rotor voltage dynamics are derived by aligning the rotor voltage equation to the stator flux.

$$V_r = [R_r + j(\omega_g - \omega_m)]i_r + L_r \frac{d}{dt} ir + j(\omega_g - \omega_m) L_m i_s + L_m \frac{d}{dt} is \tag{4.37}$$

Next the stator current is eliminated, which at the same time will align the equation to the stator flux linkage, the derivation of σ-available on the appendix on the last page of the thesis paper.

$$V_r = [R_r + j(\omega_{\psi s} - \omega_m)\sigma L_r]i_r + \sigma L \frac{d}{dt} ir + j((\omega_{\psi s} - \omega_m)\frac{Lm}{Ls}\psi_{sd} + \frac{Lm}{Ls}\frac{d}{dt}\psi_{sd} \tag{4.38}$$

$\Rightarrow$Breaking down the expression along the d and q axes:

$$V_{rd}=R_r i_{rd}+\sigma L_r \frac{d}{dt} ird-\sigma L_r(\omega_{\psi s}-\omega_m) i_{rq}+L_m/L_s \frac{d}{dt} \psi sd \quad (4.39)$$

$$V_{rq}=R_r i_{rq}+\sigma L_r \frac{d}{dt} irq-\sigma L_r(\omega_{\psi s}-\omega_m) i_{rd}+(\omega_{\psi s}-\omega_m) L_m/L_s \frac{d}{dt} \psi sd \quad (4.40)$$

Where, $R_r i_{rd}+\sigma L_r \frac{d}{dt} ird$ —d-axis dynamics, $R_r i_{rq}+\sigma L_r \frac{d}{dt} irq$ —q-axis dynamics, $\sigma L_r(\omega_{\psi s}-\omega_m) i_{rq}$—cross coupling term (d-axis compensation terms), $\sigma L_r(\omega_{\psi s}-\omega_m) i_{rd}$—cross coupling term (q-axis compensation terms), $L_m/L_s \frac{d}{dt} \psi sd$ and $(\omega_{\psi s}-\omega_m) L_m/L_s \frac{d}{dt} \psi sd$—disturbance terms.

These expressions explicitly separate the dynamics of the rotor currents and show how they affect the rotor voltages on the same axis. The actual dynamics are simple, linear, first order systems and are the same for both axes. The compensation terms arise from the cross-coupling of the equations. They do not contain the control variables for their respective axis and thus will be seen as a disturbance for the controller.

The rotor dynamics are actually identical on both the d and q-axes, so the design is only done for one and duplicated on the other. Many authors and researchers use a standard proportional-integral (PI) controller to satisfy the inner and outer loops independently according to the method of cascaded control. In this way they completely isolate the control design for each successive loop. *Tapia et al.* [13] which uses a slightly modified version of the PI controller. The advantage to this structure is that the transfer function of the dynamics will be in standard second order form, as opposed to the standard PI structure which leads to a zero in the transfer function.

4.5. Design of Outer Control Loop

The outer control variables are selected to be the real and reactive power of the stator. These are ideal for a wind turbine as decoupled control of the power is a desired feature. It will allow the turbine to follow the MPPT curve and do so at any desired power factor.

The real and reactive power at the stator is given by Equations:

$$P_s=3/2Re\{V_s i_s=3/2(V_{sd}i_{sd}+V_{sq}i_{sq}) \quad (4.41)$$

$$Q_s=3/2Im\{V_s i_s\}=3/2(V_{sq}i_{sd}+V_{sd}i_{sq}) \quad (4.42)$$

The effect of stator flux orientation is examined on the expressions. Aligning the stator voltage,

$$V_s=R_s i_s+\frac{d}{dt}\psi sd+j\omega_s\psi_{sd} \quad (4.43)$$

To further simplify the stator voltage expression a few assumptions are made. First of all, the term $\frac{d}{dt}\psi sd$ can be considered zero. Under vector control ψ_{sd} is held constant so its derivative is zero, unless there is a change to the set point of i_{sd}. While this will happen as the reactive power reference changes, the effect is small as all authors who adopt this method ignore it [34]. Secondly, the stator resistance is considered small enough that Rs ≈ 0. Using these assumptions,

$$V_s= j\omega_s\psi_{sd} \quad (4.44)$$

This implies that, $V_{sd}=0$, and $V_{sq}= j\omega_s\psi_{sd}=|Vs]$ (4.45)

Because of those assumissions the active power and reactive powers become:

$$P_s=-\frac{3}{2}\frac{Lm}{Ls}[Vs|i_{rq} \quad (4.46)$$

$$Q_s=\frac{3}{2}[Vs](\frac{\psi sd}{Ls}-\frac{Lm}{Ls}isd)=\frac{3}{2}\frac{\psi sd}{Ls}[Vs]-\frac{3}{2}\frac{Lm}{Ls}[Vs]i_{rd} \quad (4.47)$$

Therefore after a few assumptions the approximate dynamics between the rotor current and the stator real and reactive power can be found. Note that the reactive power has a term that does not depend on rotor current. It is left to the controller to deal with this term as a disturbance [33].

Calculation of Outer Loop Controller Constants *KP* 2 and *KI*2

The design will be done for one axis (*q*-axis) and duplicated on the other axis (d-axis). The transfer function for the outer loop is derived in Appendix D:and is shown here,

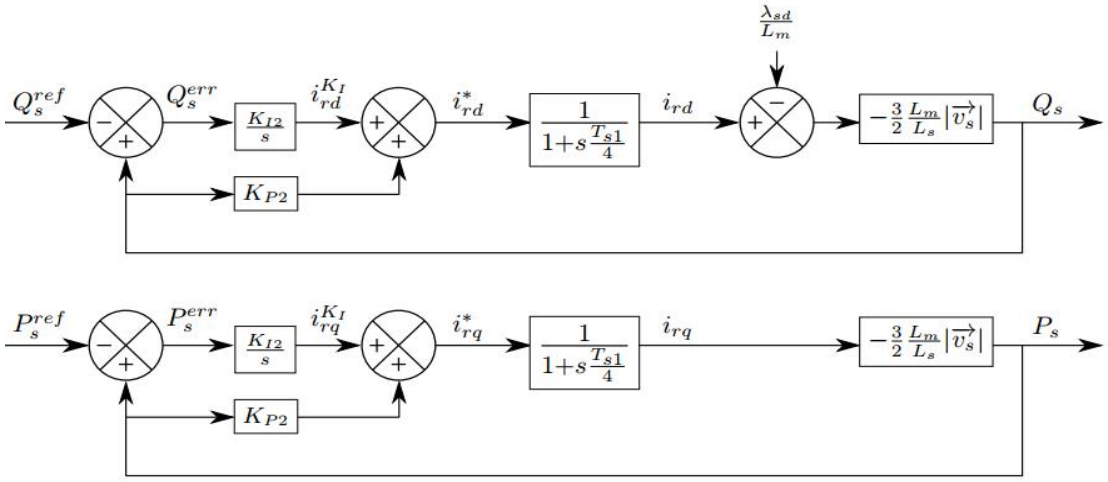

Figure 4.6 Outer control loops-Top: reactive power loop; Bottom: real power loop

$$\frac{P_s(s)}{{P_1}^{ref}{}_s(s)}=\frac{Q_s(s)}{{Q_1}^{ref}{}_s(s)}=\frac{6\frac{L_m|v_s|}{L_s T_{s1}}K_{I2}}{s^2+\left(\frac{4}{T_{s1}}+6\frac{L_m|v_s|}{L_s T_{s1}}K_{I2}\right)s+6\frac{L_m|v_s|}{L_s T_{s1}}K_{I2}} \tag{4.48}$$

Again, the transfer function is in standard form for a general second order system. The same procedure applied to the inner loop is used to calculate K_{P2} and K_{I2}. This time the settling time is selected to be longer than it was for the inner loop. It does not have to be orders of magnitude larger, because the inner loop dynamics have been accounted for in the outer loop transfer function. Tapia suggests 70ms for the outer loop settling time.

From equation 4.48 we can get:

$$\omega_{n2}{}^2 = 6\frac{L_m}{L_s}\frac{|v_s|}{T_{s1}}K_{I2} \tag{4.49}$$

$$2\xi\omega_{n1}=\frac{4}{T_{s1}}+6\frac{L_m}{L_s}\frac{|v_s|}{T_{s1}}K_{I2} \tag{4.50}$$

Imposing the criteria in Equation 4.31

$$K_{P2}=\frac{2}{3}\left(\frac{2T_{s1}-T_{s2}}{T_{s2}}\right)\frac{L_s}{L_m}\frac{1}{|v_s|} \tag{4.51}$$

$$K_{I2}=\frac{8}{3}\frac{T_{s1}L_s}{T_{s2}{}^2 L_m}\frac{1}{|v_s|} \tag{4.52}$$

5. Chapter Five: Simulation and Result Discussion

5.1. Introduction

According [27], Simulink is a block diagram environment for multi-domain simulation and Model-Based Design. It supports system level design, simulation, automatic code generation and continuous test and verification of embedded systems. Simulink provides a graphical editor, customizable block libraries and solvers for modeling and simulating dynamic systems. It is integrated with MATLAB, enabling you to incorporate MATLAB algorithms into models and export simulation results to MATLAB for further analysis.

5.2. Simulation Model Description

5.2.1. Detail Description of Simulink Model

The wind turbine and the generator which constitute the physical subsystems that are being simulated and the associated control blocks which are governing their behavior. The physical generator is simulated and then the measurable outputs are fed to the machine estimator, which computes the values of other variables which are not measurable but are necessary for the control. It is important to keep this distinction between physical system and virtual control clear. This is because every signal in the models treated as the same and looks the same whether it is a real power or reactive power signal or an estimated value that would only exist in a microcontroller in the real world.

The inverter dynamics are not studied in this work, so they appear in the model as simply a gain of one. The input to this inverter would be the desired rotor voltage waveforms. Then through PWM techniques the inverter would replicate the signals at the desired power levels, with some harmonic distortion. This reality is neglected by the simulation; the control blocks calculate the required rotor voltage and it is fed directly to the machine. At its output, the generator model calculates every variable within the machine: the torque, speed, flux and current. In reality it is only practical to measure some of these variables: the current, the rotor speed and perhaps the voltages. This is why only these variables are fed back to the estimator and the control. It would be useless to design a control system that requires all of the variables. Again, any dynamics in the sensors and any realistic concerns such as sampling and analogue to digital conversion are ignored by the models well. Therefore this model must be taken for what it is: an ideal functional

description of a DFIG wind turbine connected to a grid that treats each component in the most simple and fundamental way possible.

5.2.2. Physical System of the DFIG Wind Turbine Connected to the Grid System

The two physical components, the generator and the wind turbine, have their shafts coupled by a gearbox. Gearbox is a transmission device that transforms the incoming mechanical energy to a different characteristic (Speed and Torque) mechanical energy gearbox is the key component of the turbine drive train. Gearbox can be defined as an assembly of parts including the speed changing gears and the propeller shaft by which the power source to the output shaft [28]. Gearbox uses gears and gear trains to provide speed and torque conversions from a rotating power source to another rotating device (Generator).The relationship between speed and torque is inversely proportional: If the gearbox increases the output speed, the torque decreases and if the gearbox decreases the output speed, the torque increases. The information of its shaft speed comes from the generator model which computes the speed based on an inertial model and the balance of its own back torque and the torque input of the turbine.

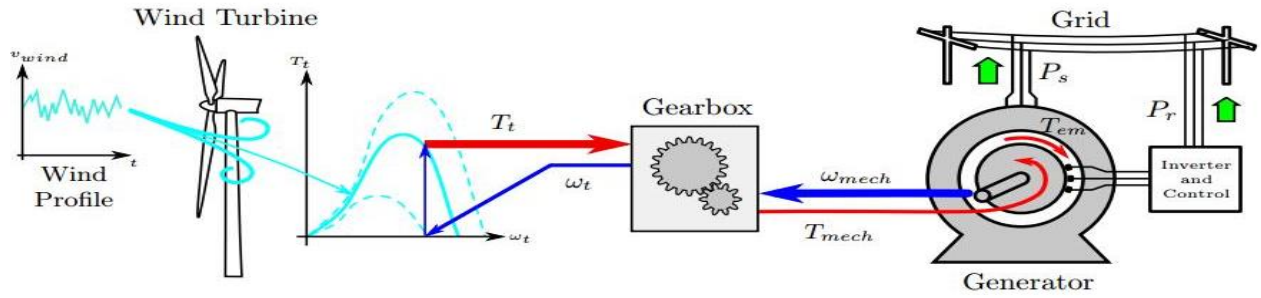

Figure 5.1 Overview of the simulation

5.2.3. Wound Rotor Induction Machine Parameters

DFIG has parameters like, stator voltage, rated rotor voltage, apparent power, speed, number of pole pairs, stator resistance, stator reactance, etc. For the simulation obtaining those required parameters from manufacturer nameplates or data sheets is not sufficient. Parameter determination experiments must be run on the machine to determine the equivalent circuit parameters. A 1.5MW generator was chosen as it will be of sufficient size to be matched to a multi-megawatt turbine. This machine is also ideally suited for doubly-fed operation. DFIGs realize their main advantage by limiting their slip about 30% around synchronous speed.

5.3. Operational Characteristics of a DFIG at Normal Condition of the Grid System

A 9MW wind farm consisting of six 1.5 MW wind turbines connected to a 25kV distribution system exports power to a 120kV grid through a 30km, 25kV feeder. 2MVA plant consisting of a motor load and of a 200kW resistive load 800kvar power factor (PF) correction capacitor is connected on the same feeder at bus B-25. Both the wind turbine and the motor load have a protection system monitoring voltage, current, machine speed and the DC-link voltage of the DFIG. Wind turbines use a DFIG consisting of Double Squirrel-Cage Induction Generators (DSCIG) and an AC/DC/AC Insulated-Gate Bipolar Transistor (IGBT)-based Pulse Width Modulation (PWM) converter and frequency converters that converts frequency from 0Hz to 12Hz. The stator winding is connected directly to the 50 Hz grid while the rotor is fed at variable frequency through the AC/DC/AC converter. The DFIG technology allows extracting maximum energy from the wind for low wind speeds by optimizing the turbine speed, while minimizing mechanical stresses on the turbine during gusts of wind. The optimum turbine speed producing maximum mechanical energy for a given wind speed is proportional to the turbine speed.

5.3.1. Converter Control System

The back to back PWM converter has two converters, one is connected to rotor side (RSC) and another is connected to grid side (GSC).

5.3.1.1. Rotor Side Converter Control System

The rotor-side converter is used to control the wind turbine power output and the voltage measured at the grid terminal. The terminal voltage controller is designed to control the terminal voltage to maintain a constant value such that the terminal of this wind turbine DFIG system can be modeled as a variable wind speed.

The power is controlled in order to follow a pre-defined power-speed characteristic, named power tracking characteristic. This characteristic is illustrated by the **ABCD** curve superimposed to the mechanical power characteristics of the turbine obtained at different wind speeds. The actual speed of the turbine ω_r is measured and the corresponding mechanical power of the tracking characteristic is used as the reference power for the power control loop. The tracking characteristic is defined by four points: **A, B, C** and **D**. From zero speed to speed of point **A** the reference power is zero. Between point **A** and point **B** the tracking

characteristic is a straight line. Between point **B** and point **C** the tracking characteristic is the locus of the maximum power of the turbine (maxima of the turbine power vs turbine speed curves). The tracking characteristic is a straight line from point **C** and point **D**. The power at point **D** is one per unit (1p.u.). Beyond point **D** the reference power is a constant equal to one per unit (1p.u.).

For wind speeds lower than 8m/s the rotor is running at sub-synchronous speed. At high wind speed it is running at hyper-synchronous speed. Open the turbine menu, select "Turbine data" and check "Display wind turbine power characteristics". The turbine mechanical power as function of turbine speed is displayed for wind speeds ranging from 5m/s to 13.4m/s. The DFIG is controlled in order to follow the red curve. Turbine speed optimization is obtained between point B and point C on this curve. Another advantage of the DFIG technology is the ability for power electronic converters to generate or absorb reactive power.

For the rotor-side controller the d-axis of the rotating reference frame used for d-q transformation is aligned with air-gap flux. The actual electrical output power, measured at the grid terminals of the wind turbine, is added to the total power losses (mechanical and electrical) and is compared with the reference power obtained from the tracking characteristic. A Proportional-Integral (PI) regulator is used to reduce the power error to zero. The output of this regulator is the reference rotor current I_{qr_ref} that must be injected in the rotor by rotor side converter. This is the current component that produces the electromagnetic torque T_{em}. The actual I_{qr} component is compared to I_{qr_ref} and the error is reduced to zero by a current regulator (PI). The output of this current controller is the voltage V_{qr} generated by rotor side controller. The current regulator is assisted by feed forward terms which predict V_{qr}. The voltage at grid terminals is controlled by the reactive power generated or absorbed by the rotor side converter.

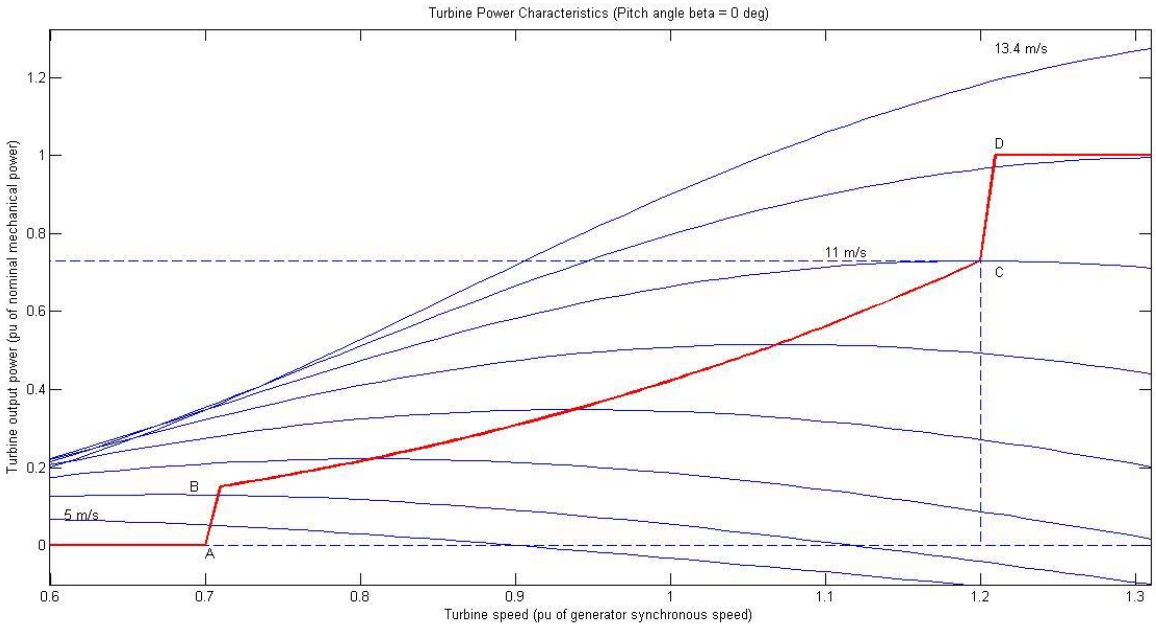

Figure 5.2 Wind turbine power characteristics curve

The reactive power is exchanged between rotor side controller and the grid side controller through the generator. In the exchange process the generator absorbs reactive power to supply its mutual and leakage inductances. The excess of reactive power is sent to the grid or to rotor side controller.

When the wind turbine is operated in var regulation mode the reactive power at grid terminals is kept constant by a var regulator. The output of the voltage regulator or the var regulator is the reference d-axis current I_{dr_ref} that must be injected in the rotor by rotor side converter. The same current regulator as for the power control is used to regulate the actual I_{dr} component of positive-sequence current to its reference value. The output of this regulator is the d-axis voltage V_{dr} generated by rotor side converter. The current regulator is assisted by feed forward terms which predict V_{dr}. V_{dr} and V_{qr} are respectively, the d-axis and q-axis of the rotor voltage V_r.

The rotor side control loop is illustrated in Figure 5.3 below. For the rotor-side controller the d-axis of the rotating reference frame used for d-q transformation is aligned with the air-gap flux.

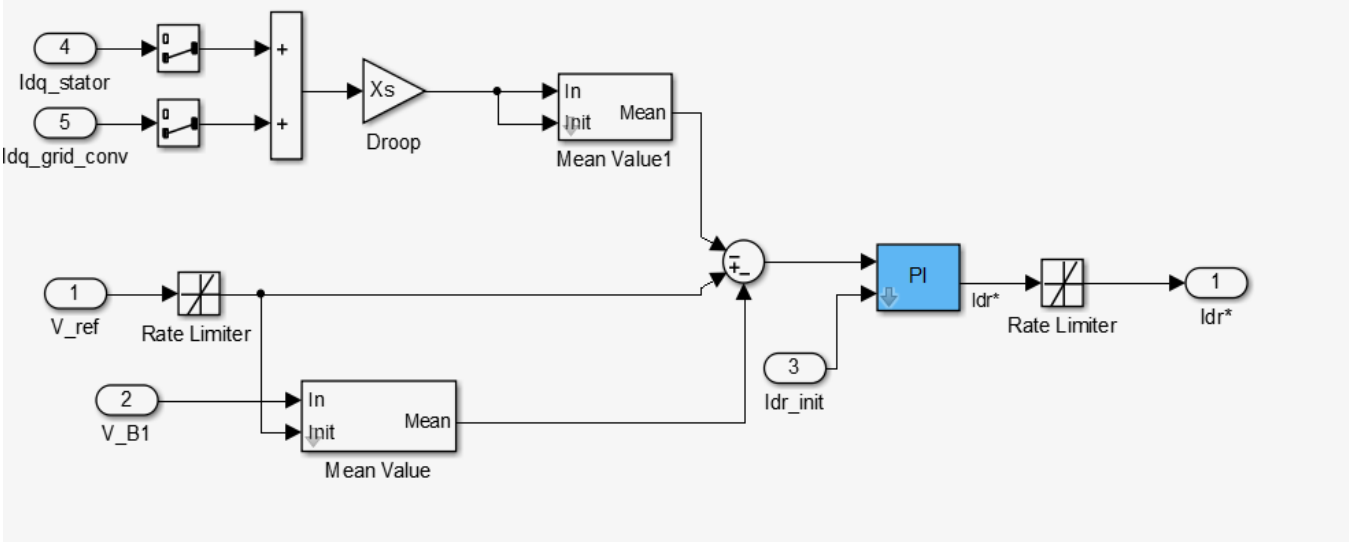

Figure 5.3 Matlab/Simulink of voltage control system in rotor side of DFIG

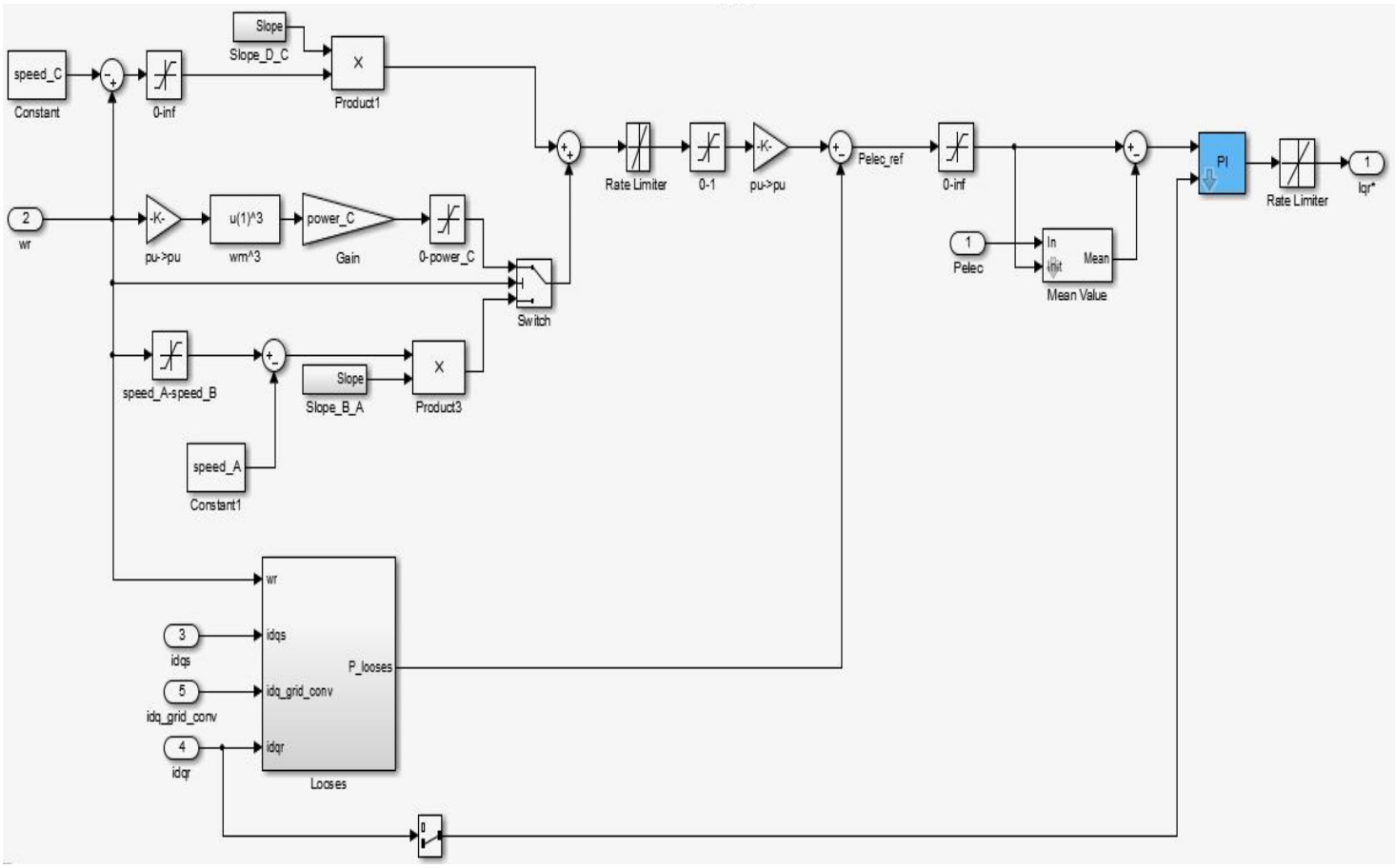

Figure 5.4 Matlab/Simulink of power control system in rotor side of DFIG

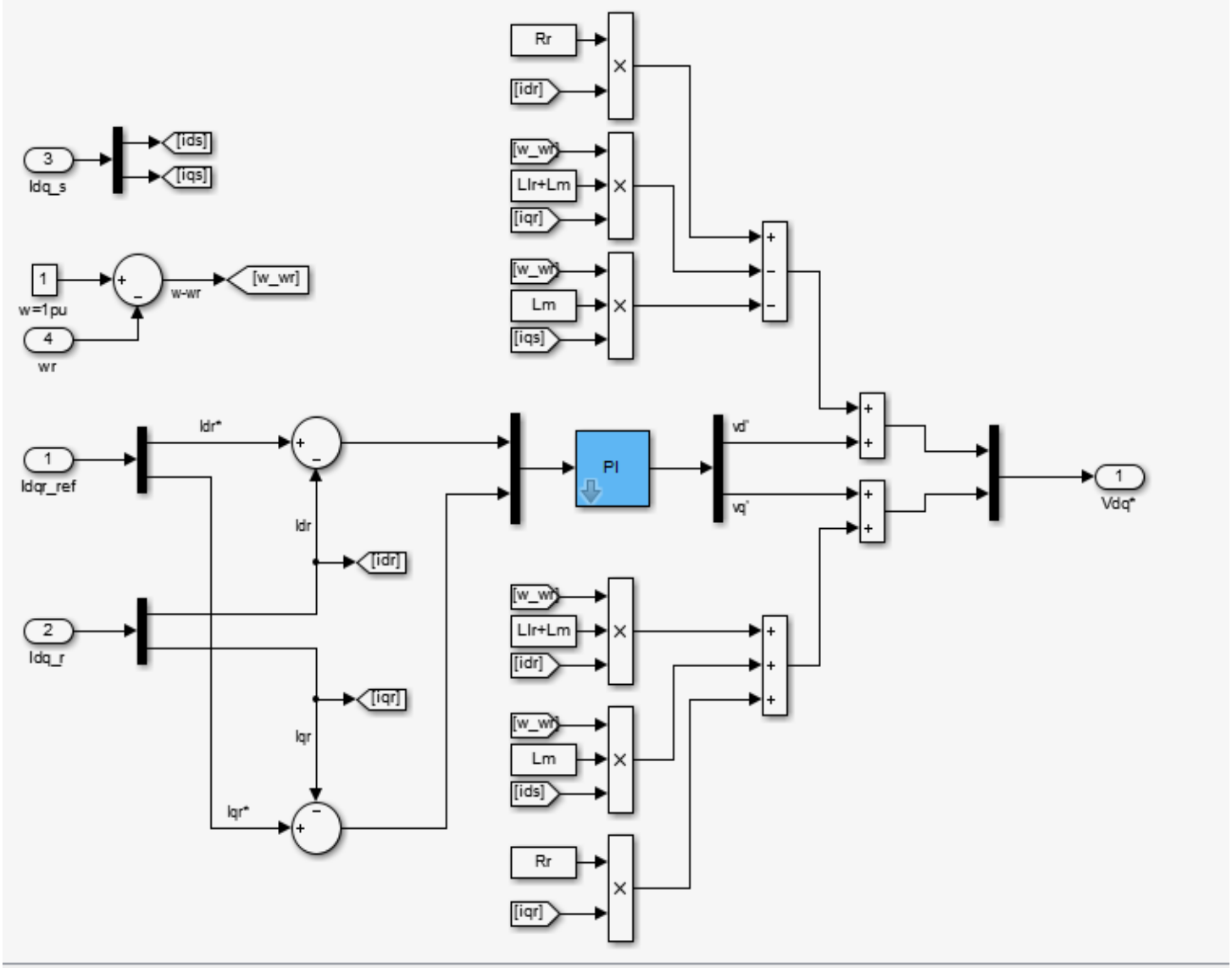

Figure 5.5 Matlab/Simulink of current control system in rotor side of DFIG

5.3.1.2. Grid Side Converter Control System

The Grid side converter is used to regulate the voltage of the DC-bus capacitor. For the grid-side controller the d-axis of the rotating reference frame used for d-q transformation is aligned with the positive sequence of grid voltage.The current regulatory controls the magnitude and phase of the voltage generated by converter grid side converter (Vgc) from the I_{dgc_ref} produced by the DC voltage regulator and specified I_{q_ref} reference. The current regulator is assisted by feed forward terms which predict the grid side converter output voltage.

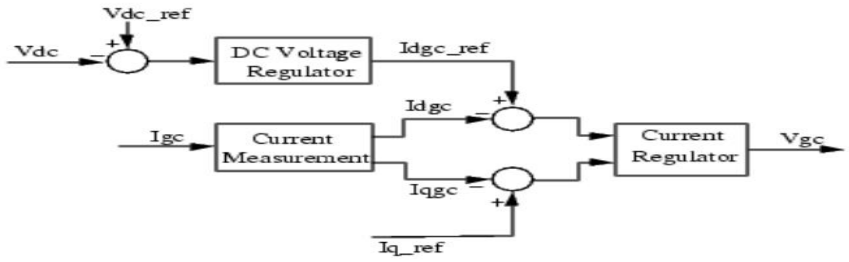

Figure 5.6 GSC control system

This controller consists of:1) A measurement system measuring the d and q components of AC currents to be controlled as well as the DC voltage V_{dc},2) An outer regulation loop consisting of a DC-voltage Regulator and 3) An inner current regulation loop consisting of a current Regulator

The grid side control system is illustrated in Figure 5.7 below. The grid side converter is used to regulate the voltage of the DC-bus capacitor. For the grid-side controller the d-axis of the rotating reference frame used for d-q transformation is aligned with the positive sequence of the grid voltage.

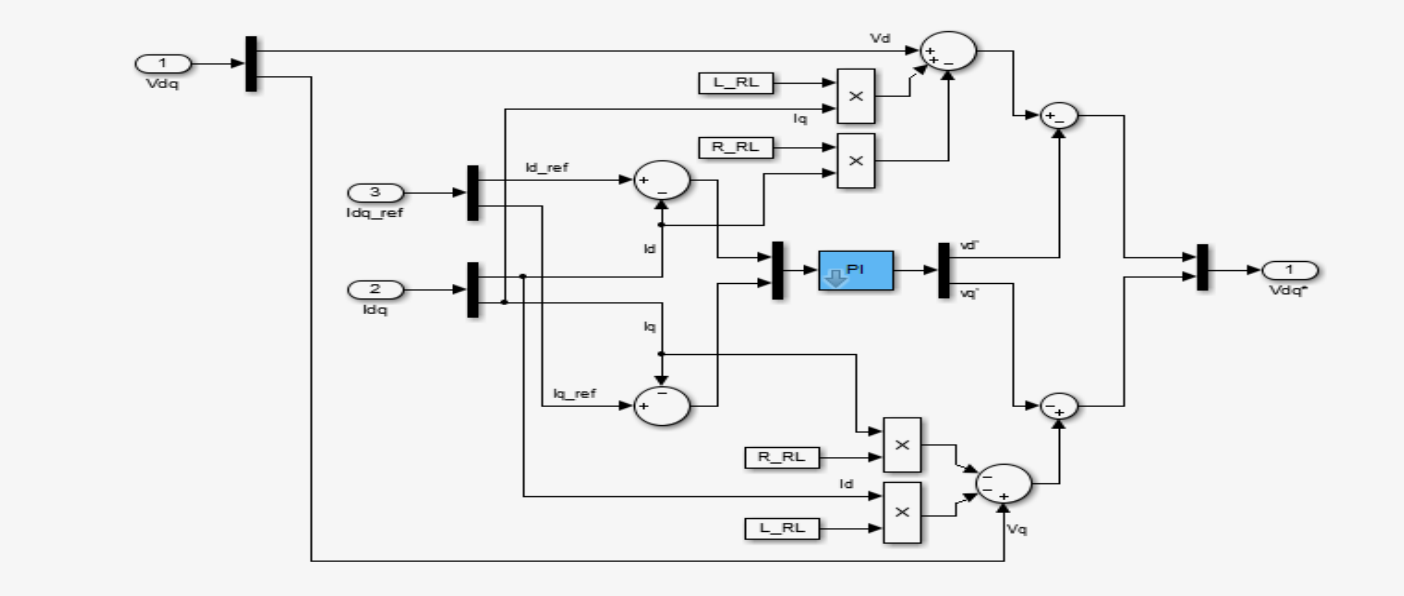

Figure 5.7 Grid side current control system Matlab/Simulink diagram

A proportional-integral (PI) controller is used to reduce the error between $V_{dc}$and V_{dc_ref}, and the output is I_{dgc_ref} for the current regulator. Here $I_{dgc}$is the current in phase with grid voltage which controls active power flow. Then, an inner current regulation loop consisting of a current regulatory controls the magnitude and phase angle of the voltage generated by the converter grid side controller i.e., V_{gc}. Here, V_{gc}has two

parts, V_{qgc} (voltage on q-axis of grid side)and V_{dgc} (voltage on d-axis of grid side)), where V_{qgc} depends on the difference between I_{qgc} and the specified reference I_{q_ref}, and V_{dgc} depends on the difference between I_{dgc} and I_{dgc_ref} which is produced by the DC voltage regulator. The current regulator is assisted by feed forward terms which predict the grid side output voltage.

5.3.1.3. Pitch Angle Control System

The pitch angle is kept constant at zero degree until the wind speed reaches aspecified value or the pitch angle controller will wait the power will reach beyond rated value. [See Figure 5.2 the power tracking characteristics curve of DFIG] [28]. Then, beyond this value, the pitch angle is proportional to the speed deviation from this specified speed. However, the rotational speed is usually chosen less than the point-D speed because it is of less interest for electromagnetic transients.

5.4. Simulation Block Diagram and Results

This is the Simulink diagram for a doubly fed induction generator connected to grid side with wind turbine protection schemes involved for protection from voltage dip,three-phase faults and ground faults. The system is connected to a 15kV, three phase source which is connected to a 9MW wind farm (6 of 1.5 MW each) via. Step down transformers, fault protection and pi- transmission line of 30km.

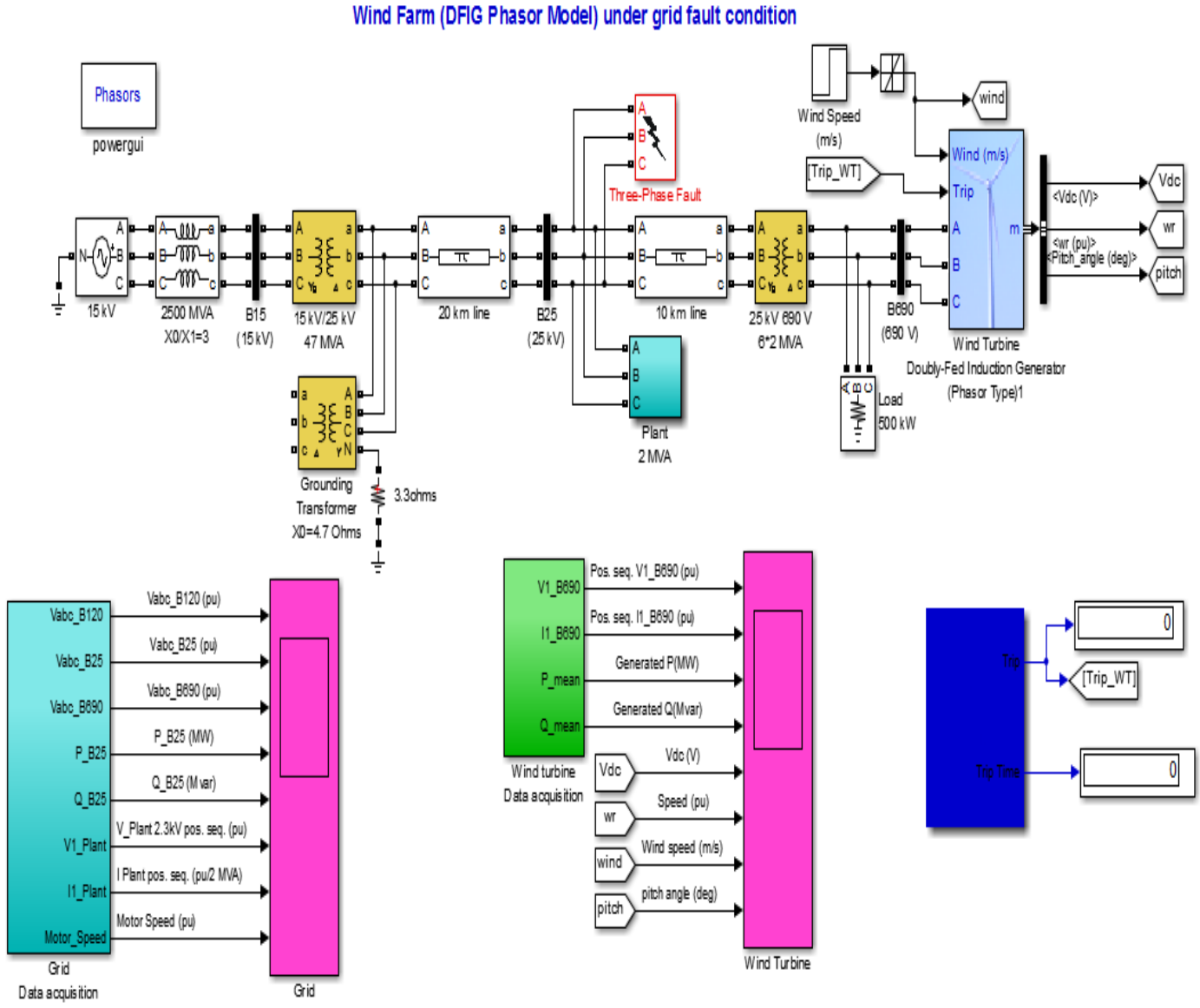

Figure 5.8 Phasor simulation of wind farm using DFIG wind turbines

5.4.1. Simulation Result of DFIG under without Grid Fault Conditions

Under this section, we will see the basic behavior of DFIG wind turbine without grid fault conditions. In this block diagram, there is no voltage sag or dip, three-phase short-circuit and ground faults. During this time, the DFIG wind turbine will operate at normal conditions because of the system is clear from any faults. The simulation shows the detail behavior of the wind turbine and grid side parameters. In this model, the pitch angle controller is constant until the active power reached to its rated value. After the active power reached its rated value the pitch angle controller try to increase the blade angle in order to protect the wind turbine from any external damage. PI- controller controls the speed of the rotor in order to get the maximum power from the wind.

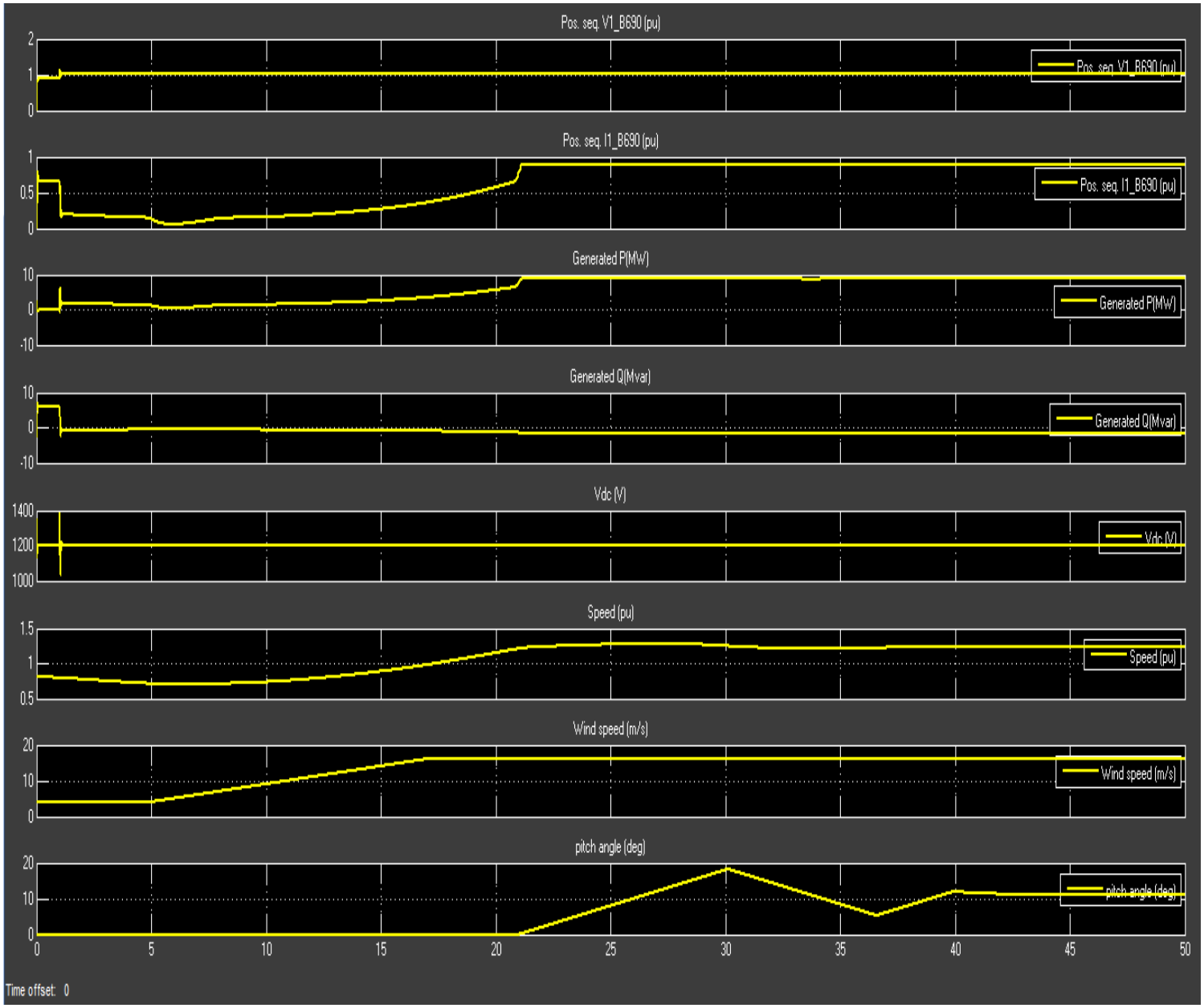

Figure 5.9 Wind turbine system simulation results without grid faults

A wind farm consisting of six 1.5MW wind turbines is connected to a 25kV distribution system and exports power to a 15kV grid through a 30km. The 9MW wind farm is simulated by three pairs of 1.5MW wind turbines. The stator winding is connected directly to the 50Hz grid and the rotor is driven by a variable-pitch wind turbine. The pitch angle is controlled in order to limit the generator output power at its nominal value for winds exceeding the nominal speed (10m/s). In order to generate power the DSCIG speed must be slightly above the synchronous speed. Speed varies approximately between 1p.u. at no load and 1.005p.u at

full load. In this thesis, speed of the rotor is controlled by a PI-controller in order to control the slip of the generator at a time of fault and normal operations.

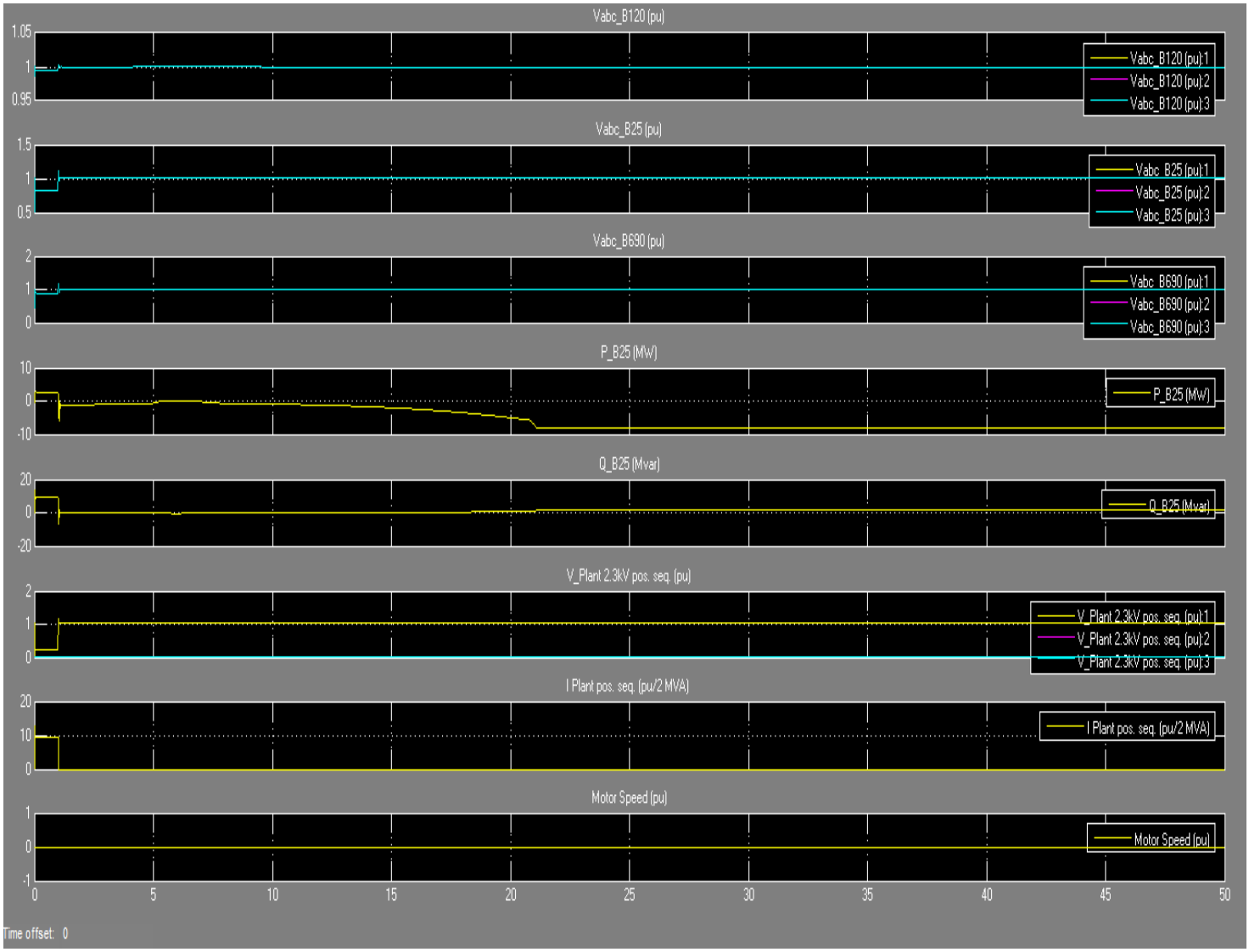

Figure 5.10 Grid system simulation results without grid faults

Reactive power absorbed by the DFIGs is partly compensated by capacitor banks connected at each wind turbine low voltage bus and the rest of reactive power required maintaining the 25kV voltage at bus B25 close to 1p.u.

Grid side blocks are:

Three-phase source with 120kv voltage source is used to generate a three-phase sinusoidal voltage with time-varying parameters. You can program the time variation forthe amplitude, phase, or frequency of the fundamental component of the source [13].

The Three-Phase Mutual Inductance Z1-Z0 block implements a three-phase balanced inductive and resistive impedance with mutual coupling between phases. This block performs the same function as the three-winding Mutual Inductance block. For three-phase balanced power systems, it provides a more convenient way of entering system parameters in terms of positive- and zero-sequence resistances and inductances than the self- and mutual resistances and inductances [13].

Three-Phase V-I Measurement: is used to measure instantaneous three-phase voltages and currents in a circuit. When connected in series with three-phase elements, it returns the three phase-to-groundor phase-to-phase peak voltages and currents [13].The block can output the voltages and currents in per unit (p.u)values or in volts and amperes.

If you choose to measure phase-to-ground voltages in per unit, the block converts the measured voltages based on peak value of nominal phase-to-ground voltage:

$$V_{abc}(pu)=\frac{V_{phase-to-ground}}{V_{base}} \quad (5.1)$$

Where, $V_{base}=0.8165*V_{nom}(V_{RMS})$

If you choose to measure phase-to-phase voltages in per unit (p.u.), the block converts the measured voltages based on peak value of nominal phase-to-phase voltage:

$$V_{abc}(pu)=\frac{V_{phase-to-phase}}{V_{base}} \quad (5.2)$$

Where, $V_{base}=\sqrt{2}*V_{nom}(V_{rms})$

If you choose to measure currents in per unit, the block converts the measured currents based on the peak value of the nominal current:

$$I_{abc}(pu)=\frac{I_{abc}}{I_{base}} \quad (5.3)$$

Where, $I_{base}=0.8165*\frac{P_{base}}{V_{nom}}$

Three-Phase Transformer: this block implements a three-phase transformer by using three single-phase transformers. This block is using to step-down the voltages from 120kv to 25kv in grid system.Theblock allowsyou to specify the resistance and inductance of the windings in perunit (pu). The values are based on the transformer rated power $P_n$in VA, nominal frequency (fn) in Hz, and nominal voltage V_n, in V_{rms},of the corresponding winding. For each winding per unit resistance and inductance are defined as:

$$R(p.u)=\frac{R(\Omega)}{R_{base}} \quad (5.4)$$

$$L(p.u)=\frac{L(H)}{L_{base}} \quad (5.5)$$

The base resistance and base inductance used for each windingare:

$$R_{base}=V^2_n/P_n \quad (5.6)$$

$$L_{base}=R_{base}/2\pi f_n \quad (5.7)$$

Three-Phase PI Section Line: [13] The Three-Phase PI Section Line blocks implements a balancedthree-phase transmission line model with parameters lumped in a PI-section. Contrary to the distributed parameter line model where the resistance,inductance, and capacitance are uniformly distributed along the line,the Three-Phase PI Section Line block lumps the line parameters ina single PI-section as shown in the figure below.The line parameters R, L, and C are specified as positive- andzero-sequence parameters that take into account the inductive andcapacitive couplings between the three phase conductors, as well asthe ground parameters. This method of specifying line parameters assumes that the three-phases are balanced.The self and mutual resistances (R_s, R_m),self and mutual inductances (L_s, L_m)of the three coupled inductors, as well as phase capacitances Cp andground capacitances Cg, are deduced from the positive-and zero-sequence RLC parameters as follows.

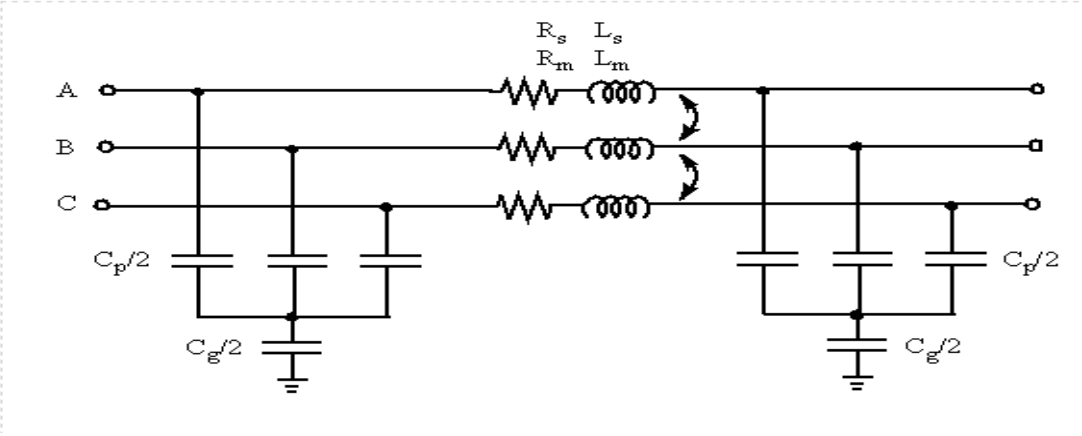

Figure 5.11 Three-phase PI-section line(transmission system) model

For a short line section (approximately line section<50 km), correction factors are negligible (close to unity).The RLC line section parameters are then computed as follows:

$R_s=(2R_1+R_0)/3$, $R_m=(R_0-R_1)/3$, $C_p=C_1$ and

$L_s=(2L_1+L_0)/3$, , $L_m=(L_0-L_1)/3$, $C_g=3C_1C_0/(C_1-C_0)$ (5.8)

Three-Phase Fault:uses three Breaker blocks that canbe individually switched on and off to program phase-to-phase faults,phase-to-ground faults, or a combination of phase-to-phase and groundfaults. Use this block to program a fault (short-circuit) between any phase and the ground and phase to phase.

5.4.2. Simulation Result of DFIG under Grid Fault Conditions with PI controller

In the fault instant, the voltage at the DFIG generator terminal drops and it leads to a corresponding decrease of the stator and rotor flux in the generator. This results in a reduction of the electromagnetic torque and active power. As the stator flux decreases, the magnetization that has been stored in the magnetic field has to be released. In the fault moment, as the stator voltage decreases significantly, high current transients appear in the stator and rotor windings. In order to compensate for the increasing rotor current, the rotor side converter increases the rotor voltage reference by controlling the rotor speed in order to follow the slip curve of DFIG wind turbine, which implies a "rush" of power from the rotor terminals through the converter.

On the other side, as the grid voltage has dropped immediately after the fault, the grid side converter is not able to transfer the whole power from the rotor through the converter furtherto the grid. The grid side

converters control of the DC-voltage reaches thus quickly its limitation. As a result, the additional energy goes into charging the DC-bus capacitor and the DC-voltage rises rapidly.

This is the Simulink diagram for a doubly fed induction generator connected to grid side with wind turbine protection schemes involved for protection from voltage sag/dip at 15kV voltage source and three- phase short-circuit faults and ground faults. The system is connected to a 15kV, three-phase source which is connected to a 9MW wind farm via Step-down transformers, fault protection and Pi (Π) transmission line. The wind-turbine model is a phasor model that allows transient stability type studies with long simulation times. In this simulation, the system is observed during 50 seconds of simulation time. The stator winding is connected directly to the 50Hz grid and the rotor is driven by a variable pitch wind turbine. The pitch angle is controlled in order to limit the generator output power at its nominal value for winds exceeding the nominal speed (12m/s). In order to generate power the DFIG speed must be slightly above the synchronous speed. Speed varies approximately between 0.8p.u at no load and 1.10p.u at full load. Each wind turbine has a protection system monitoring voltage, current and machine speed. Reactive power absorbed by the DFIGs is partly compensated by capacitor banks connected at each wind turbine low voltage bus.

5.4.2.1. Simulation of a voltage sag/dip on the 15kV system and short-circuit on grid side

During the fault, the stator voltage and rotor flux have been reduced, the injected rotor voltage has been changed and the rotor speed has been increased. This increased rotor speed is controlled by the PI controller in order to stabilize the system to the normal position. Immediately the fault is cleared the stator voltage is restored and the demagnetized stator and rotor oppose this change in flux thus leading to an increase in the rotor and stator currents.

We now observed the impact of voltage sag resulting from fault on the 15kV system. In this simulation the voltage dip will occur at the amplitude of modulation is 0.45p.u, the frequency of the voltage sag modulation is 2Hz and the voltage sag and short-circuit variation timing is between 10s and 10.5s lasting for 0.5s is programmed to occur. We neglect the harmonic generation of the source. We observed the plant voltage, current as well as active power and the reactive power.

The PI damping controller is tuned damping actively torsion oscillation observe during grid fault system in the drive-train system. PI Damping controller acting fast power converter controlled by controlling rotor speed. Damping controller provided the rotor side converter quickly damped out oscillation associate with a

generator speed. Wind speed is to be constant during grid fault simulation. Monitoring DC-link voltage and rotor current during grid disturbance a suitable optimum protection system both for rotor side converter and DFIG can be design.

5.4.2.1.1.Simulation Result Discussion for Wind Turbine Side

In the simulation of wind turbine during grid fault, we observed eight basic parameters in this simulation.

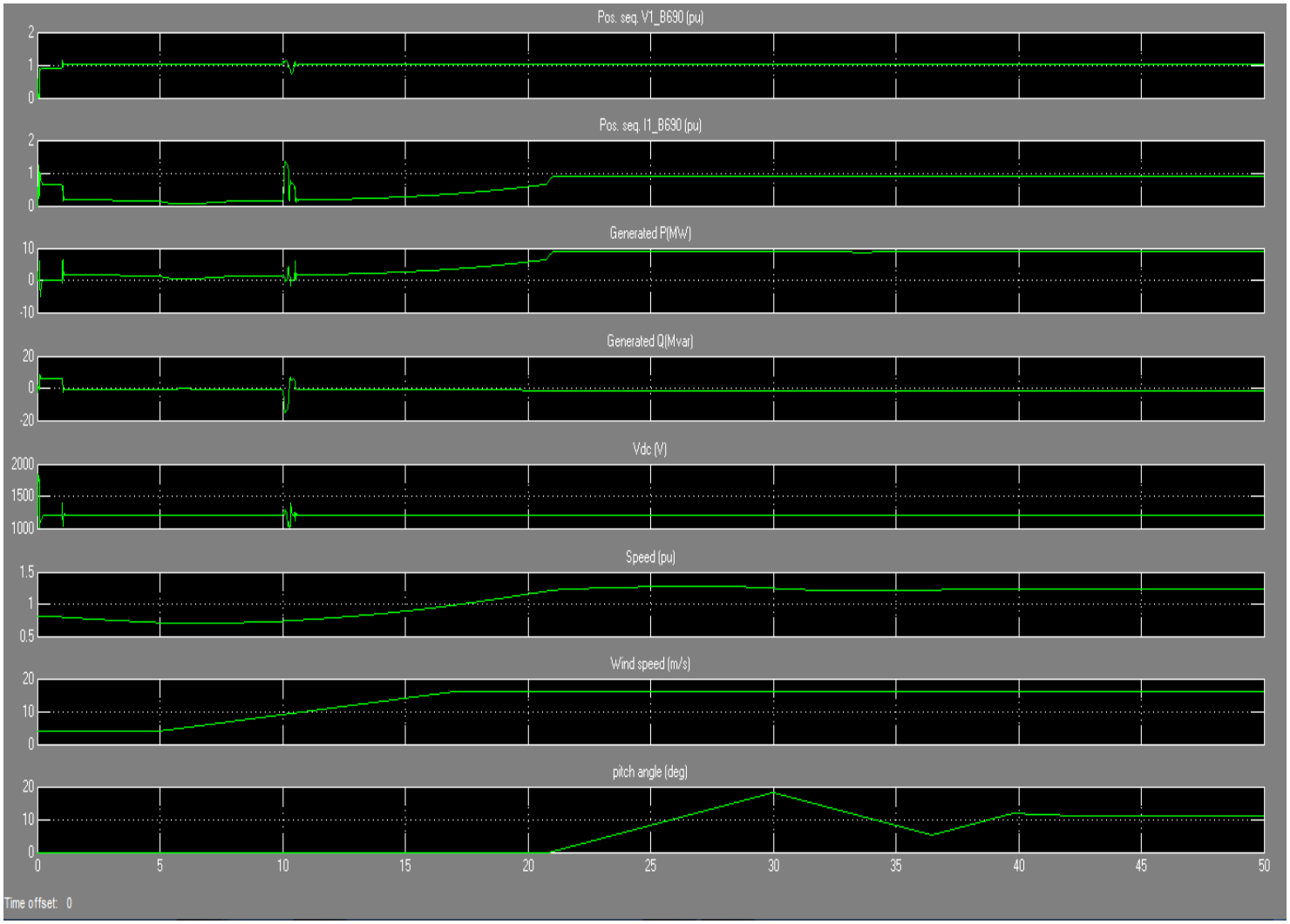

Figure 5.12 Wind turbine simulation results at a time of grid faults

Those values are; positive sequence voltage of the DFIG (B-690V (p.u)), positive sequence current of the DFIG (B-690A (p.u)), generated active power (MW), reactive power (MVAr), DC-link voltage, the speed, wind speed and the pitch angle(degree).

Table 1 Simulation results of wind turbine parameters

Wind turbine parameters	Before grid fault	During grid fault	After grid fault
Pos. seq. Voltage (V1-B-690p.u)	0 to 1	b/n 0.7 & 1.12	Constant (1)
Pos. seq. current (I1-B-690p.u)	0.2 to 1	b/n 0.2 & 1.36	Increase 0.15 to 0.89
Generated active power(MW)	0 to 5.1	b/n 0 & 6	Increase 2 to 9
Generated reactive power(Mvar)	4	b/n 0.75 &0.42	Decreased 0.65 to 1.5
DC-link Voltage(V)	Constant (1200)	b/n 1000 & 1300	Constant (1200)
Speed(p.u)	Decreased (0.8-0.72)	Increasing	Increasing
Wind speed(m/s)	Increasing	Increasing	Increasing
Pitch angle(degree)	Constant (0°)	Constant (0°)	Constant (0°)

The positive sequence of voltage (V1-B-690) before the fault happen at t=1sec the value of voltage is 0.9p.u and from t=2sec to 10sec the voltage (V1-B-690) is constant at 1p.u. During the voltage sag, three-phase short circuit and ground fault happen the voltage is fluctuated between 1.12p.u and 0.7p.u with the frequency of modulation at 2Hz. After those faults are cleared the voltage of the DFIG is constant at 1p.u.

At the starting time of the simulation the positive sequence of current (I1-B-690) is fluctuate between 0.2p.u and 1p.u for a time interval of 1sec. After simulation is simulated for 1sec the system is stabilized and the positive sequence current of wind turbine is 0.2p.u for 10sec. After 10sec simulation the fault will happen for 0.5sec. During this time, the positive sequence current is fluctuating between 0.2p.u and 1.36p.u with frequency of modulation for 2Hz. After the faults are cleared by the PI-controller controlling the speed of the rotor, the current is smoothly increased until the rated value reached. After the fault is cleared the current is smoothly increased from 0.15p.u value to 0.89p.u for 11sec. After this smoothly increasing of the value it is reached to the rated value then it is constant.

At the starting time of the simulation the active power is increase from 0MW to 5.1MW until the fault will happen at t=10sec. During the fault times the generated active power is fluctuated between 0MW and 6MW for 0.5sec until the fault is cleared by the PI-controller. After the fault is cleared by the PI-controller the generating active power will be smoothly increasing until the rated value is reached. After t=10.6sec, the

faults are cleared and the active power is 2MW and smoothly increased to the rated value of 9MW of power that generated from the DFIG wind turbines.

At the starting time of the simulation the reactive power is generating 4MVAr of reactive power to the system for 1sec in order to stabilize the system. After 1sec the DFIG is starting to consume the reactive power between -0.75MVAr and -0.42MVAr value from the system until the faults happen at t=10sec. During voltage dip and short-circuit happen at the grid side the DFIG wind turbine system of the reactive power is fluctuated between 5MVAr and -15MVAr, until the faults are cleared by the PI-controller from the system. After the faults are cleared from the system, the reactive power is -0.65MVAr after 10.6sec and smoothly decreased to the rated value of -1.5MVAr.

The pitch angle of wind turbine is directly related to the active power. When the active power is reached to the rated value, the pitch angle is tried to increase the angle of the blades in order to extract maximum power from the wind. It also follows the characteristic curve of the wind turbine. By increasing and decreasing the pitch angle of the blade the PI-controller will manage the maximum power that extracted from the wind.

5.4.2.1.2.Simulation Result Discussion for Grid Side Parameters

Before the voltage dip and faults happen on the grid side, the 15kv voltage source (bus bar B_15) has constant voltage at the value of 1p.u for 10s. At a time of faults, the voltage of the source is fluctuating between 0.6p.u and 1.4p.u with the frequency of modulation of 2Hz. After the faults are cleared by the PI-controller from the system, the voltage of 15kV voltage source is constant at its rated value of 1p.u.

The voltage at bus bar of 25kV (B_25) is constant at the value of 1p.u, before the faults happened on grid side. At the faulty time, the voltage of this bus bar is fluctuating b/n 0.61p.u and 1.21p.u for 0.5s with, the frequency of modulation of 2Hz. After the faults are cleared by PI-controller, the voltage of this bus bar is constant at the rated value of 1p.u throughout the simulation.

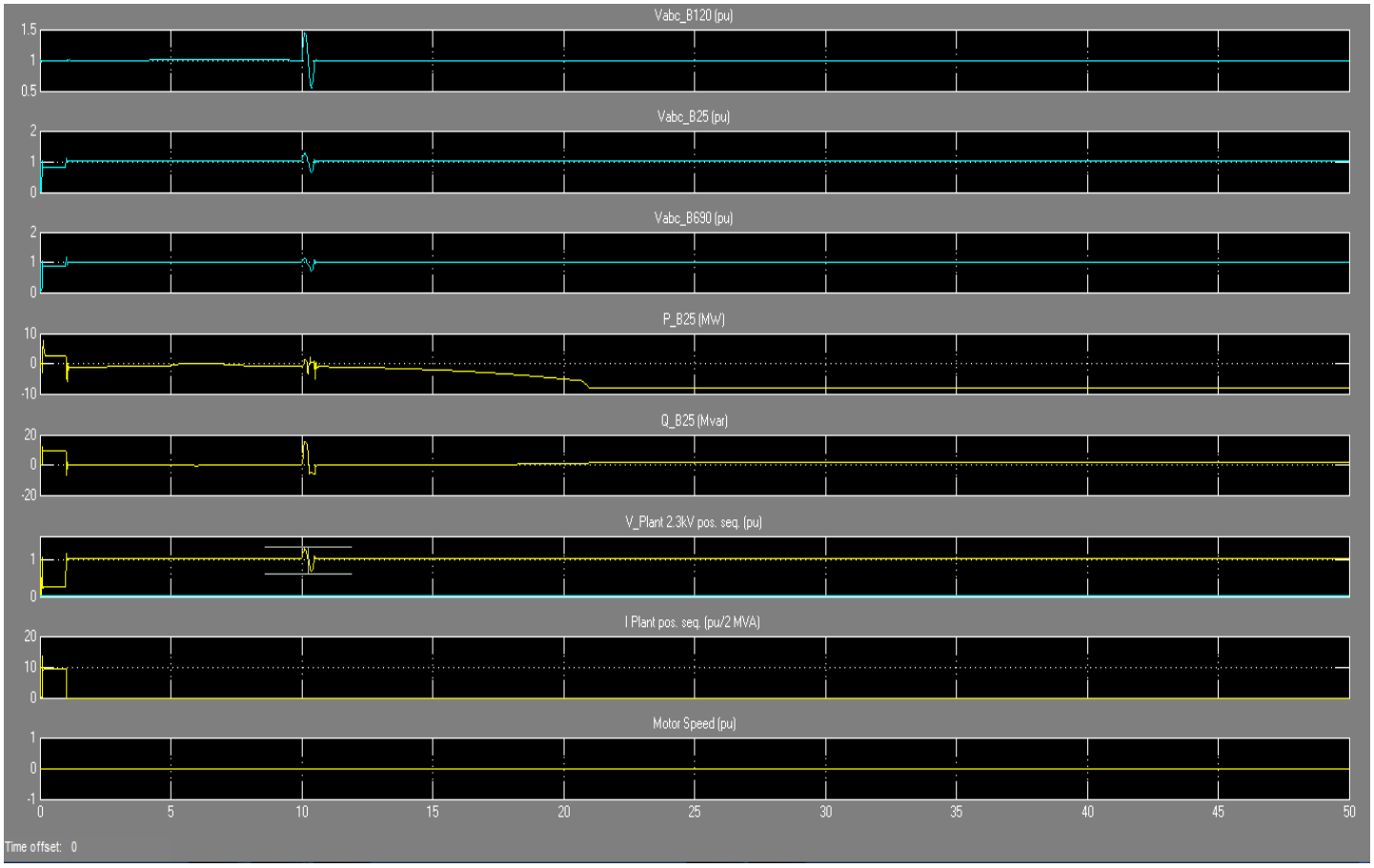

Figure 5.13 Grid system results at a time of grid faults

Table 2 Simulations results of grid side parameters

Grid side parameters	Before grid fault	During grid fault	After grid fault
Pos. seq. Voltage ($\mathbf{V_{abc\_}}$ **B-15**)	Constant(1p.u)	b/n 0.6 & 1.4 p.u	Constant (1p.u)
Pos. seq. Voltage ($\mathbf{V_{abc\_}}$ **B-25**)	Constant(1p.u)	b/n 0.61 &1.21 p.u	Constant(1p.u)
Pos. seq. Voltage ($\mathbf{V_{abc\_}}$ **B-690**)	Constant(1p.u)	b/n 0.75 & 1.19 p.u	Constant(1p.u)
Generated Active power(**P_B25**(MW))	b/n 0MW &5MW	b/n 3.9MW &2.1MW	Consume 8MW
Reactive power(**Q_B25**(MVAr))	b/n 0Mvar & 9MVAr	b/n -5MVAr & 15MVAr	Generate 1.4MVAr
Plant voltage pos. seq.(**V_plant**)	1.03p.u	b/n 0.75p.u & 1.21p.u	1.03p.u
Plant current in Pos. seq.(**I_plant**)	b/n 0.12A & 10A	0.12A	0.12A

Like, the above bus bars, the bus bar of B_690 is constant before the faults happen on grid system. But at a time of grid fault the voltage is fluctuate b/n 0.75p.u and 1.19p.u for 0.5s. After this time the voltage of this bus bar is constant a rated value of 1p.u.

The active power of the source is fluctuating b/n -5MW and 5MW for 1.2second until it synchronized with the system. After the system is stabilized, the source is consuming the active power from the wind turbine with the value of -1MW for 8.8s. During the faults happen the active power of the source is fluctuating between -3.9MW and 2.1MW for 0.5s. After this the system is cleared from the faults by PI controllers, the system is total consume the power from DFIG wind turbine system. It consume power from the DFIG wind turbine approximately -8MW of generated active power.

The reactive power of the source that generated from the source to the system is 9MVAr for 1.2s and after this time the reactive power is goes to zero for 8.8s. During the faulty time, the reactive power is fluctuating b/n 15MVAr and -5MVAr for 0.5s. After the fault is cleared from the system the reactive power is zero for 10s but after 20s total the source is generating reactive power to the system with the value b/n 1.2MVAr and 1.4MVAr.

The plant voltage has the same behavior as the bus bar we have observe in above section. The plant voltage is 1.03P.u before the faults happen on the system. During faulty time, the voltage is fluctuating b/n 0.75p.u and 1.21p.u. After the faults are cleared from the system the voltage is constant with the value of 1.03p.u. The plant current is 10A for 1.2s after that time it is constant with value of 0.12A.

5.4.3. DFIG Wind Turbine System Disconnected from Grid System

The DFIG wind turbine system is disconnected from the system because of the grid faults and voltage sag or dip on voltage source. In this simulation, we observed pos. seq. voltage, pos. seq. current, active power and reactive power, DC link voltage, the rotor speed and the pitch angle of the DFIG wind turbine.

Pos. seq. voltage (V_1_B690) of DFIG wind turbine is slowly increased from 0p.u to 1p.u before the faults happened on the grid side. During the fault times, it is fluctuating b/n 0.45p.u and 1.55p.u. In this time, the DFIG is waiting until the faults cleared by PI controller. But the voltage is reached above the rated value of the protection system. In protection system the voltage range is 0.75p.u and 1.1p.u, but on this simulation the voltage out of the range. Because of this the wind turbine is disconnected from the system.

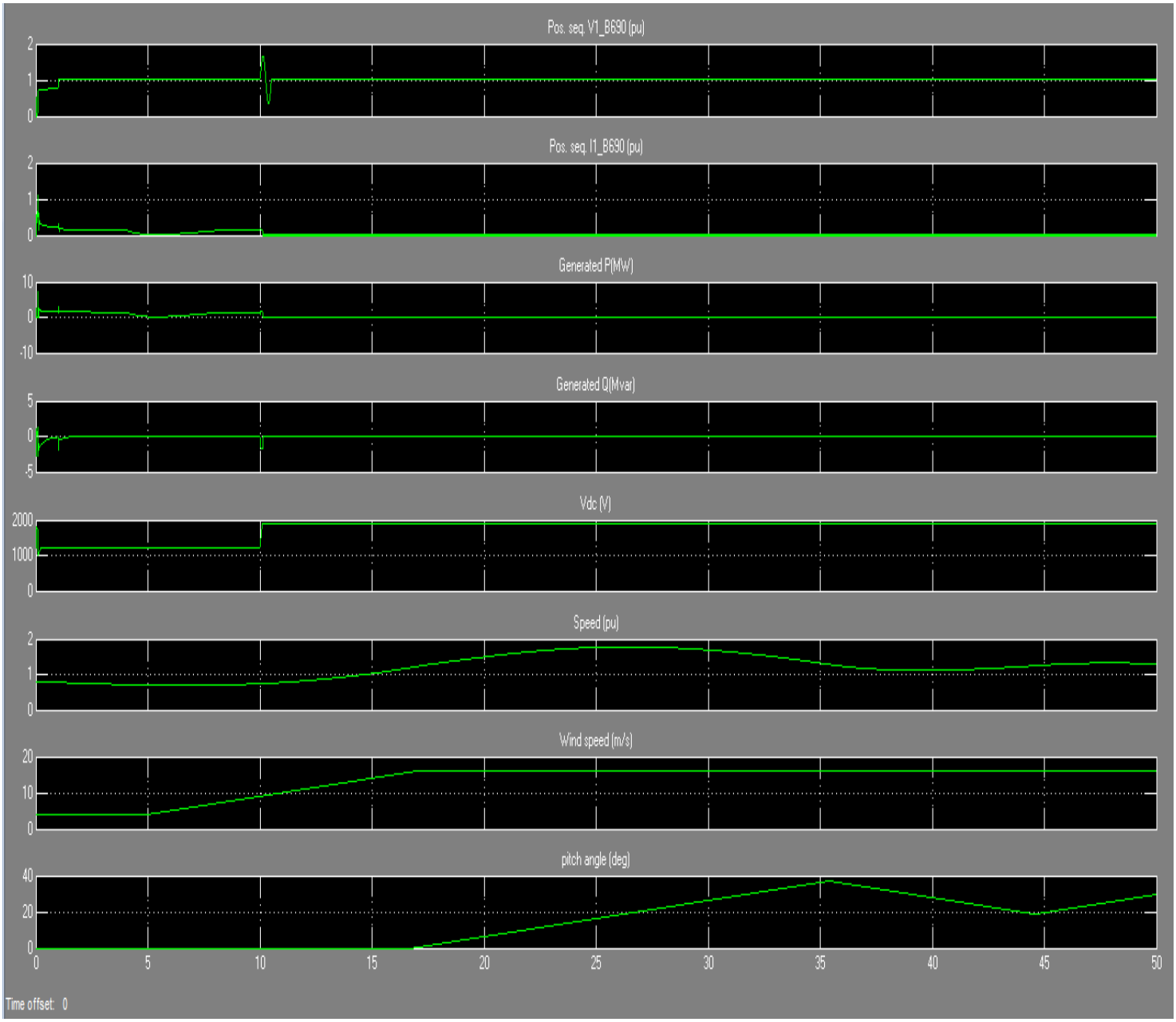

Figure 5.14 DFIG is disconnected from the system after grid faults happen

Pos. seq. current (I_1_B690) of the DFIG wind turbine has the value of decreasing from 0.8p.u to zero and the returned to 0.2p.u before the faults happened on grid side. On fault time the current is automatically goes to zero value. On protection system the maximum value of AC current and minimum AC current set at the value of 1.10p.u and 0.20p.u, respectively. But on this simulation the AC current is zero, this makes the DFIG disconnected from the grid system.

Table 3 Wind turbine parameters when wind turbine disconnected from system

Wind turbine parameters	Before grid fault	During grid fault	After grid fault
Pos. seq. Voltage (V1-B-690p.u)	0 to 1	b/n 0.45 & 1.55	Constant (1)
Pos. seq. current (I1-B-690p.u)	0.8 to 0 to 0.2	0	Constant (0)
Generated active power(MW)	0 to 2	b/n 2 to 0	Constant (0)
Generated reactive power(MVAr)	-2 to 0	-2	Constant (0)
DC-link Voltage(V)	Constant (1200)	Increased to 1900	Constant (1900)
Speed(p.u)	0.73 to 0.8	Increasing to 1.8	Increasing to 1.8
Wind speed(m/s)	Increasing	Increasing	Increasing
Pitch angle(degree)	Constant (0°)	Increasing 39°	Fluctuated b/n 20° and 40°

Active power, which generated from the DFIG wind turbine, is slowly increased from zero MW to 2MW until the faults happened on the grid side. After the faults happened, the voltages and AC currents reached its maximum values, which trip the wind turbine from the system. On this time, the PI-controller automatically disconnects the DFIG from the system. After the faults happened, the active power is goes to zero. This means, the DFIG is totally shut down or tripped. The reactive power is also shows the same behaviors as active power of the DFIG wind turbine. The reactive power is consumed from the system before the faults happened on grid system. During fault time, the reactive power is reached at a value of 2MVAr. But, after the faults the reactive power is goes to zero.

The DC-link voltage is normal at the rated value of 1200v DC, but a time of faults the DC voltage is reached to 1900v DC. But this DC voltage value is the trip value that set on the PI-controller and the protection system. This value makes the DFIG wind turbine to disconnect from the grid system. The rotor speed is on normal condition before the faults happen on the grid side. After the faults happen, the rotor speed is try to increase smoothly and reached at a value of 1.8p.u.This value is not controlled by the PI controller because it reached out of ranges. On protection system the maximum value of rotor speed is 1.5p.u.

Table 4 Grid side parameters when wind turbine disconnected from the system

Grid side parameters	Before grid fault	During grid fault	After grid fault
Pos. seq. Voltage (**$V_{abc\_}$ B-120**)	Constant(1p.u)	b/n 0.6 & 1.5 p.u	Constant (1p.u)
Pos. seq. Voltage (**$V_{abc\_}$ B-25**)	b/n 0.75 & 1p.u	b/n 0.59&1.42 p.u	Constant(1p.u)
Pos. seq. Voltage (**$V_{abc\_}$ B-690**)	b/n 0.71 & 1p.u	b/n 0.51 & 1.49 p.u	Constant(1p.u)
Generated Active power(**P_B25**(MW))	b/n 2 & 0.4MW	b/n 3.9MW &2.1MW	Consume 8MW
Reactive power(**Q_B25**(Mvar))	b/n 0Mvar & 9Mvar	b/n -5Mvar & 15Mvar	Generate 1.4Mvar
Plant voltage pos. seq.(**V_plant**)	1.03p.u	b/n 0.75p.u & 1.21p.u	1.03p.u
Plant current in Pos. seq.(**I_plant**)	b/n 0.12A & 10A	0.12A	0.12A

After this value, the rotor is running on the over-speed range. That makes the complete shutdown of the DFIG wind turbines from the system. This work is done by the PI controller, in order to protect the DFIG from damage. When the rotor speed reaches above the rated value, the pitch angle is try to expand the angle of the blade and decrease the rotor speed.

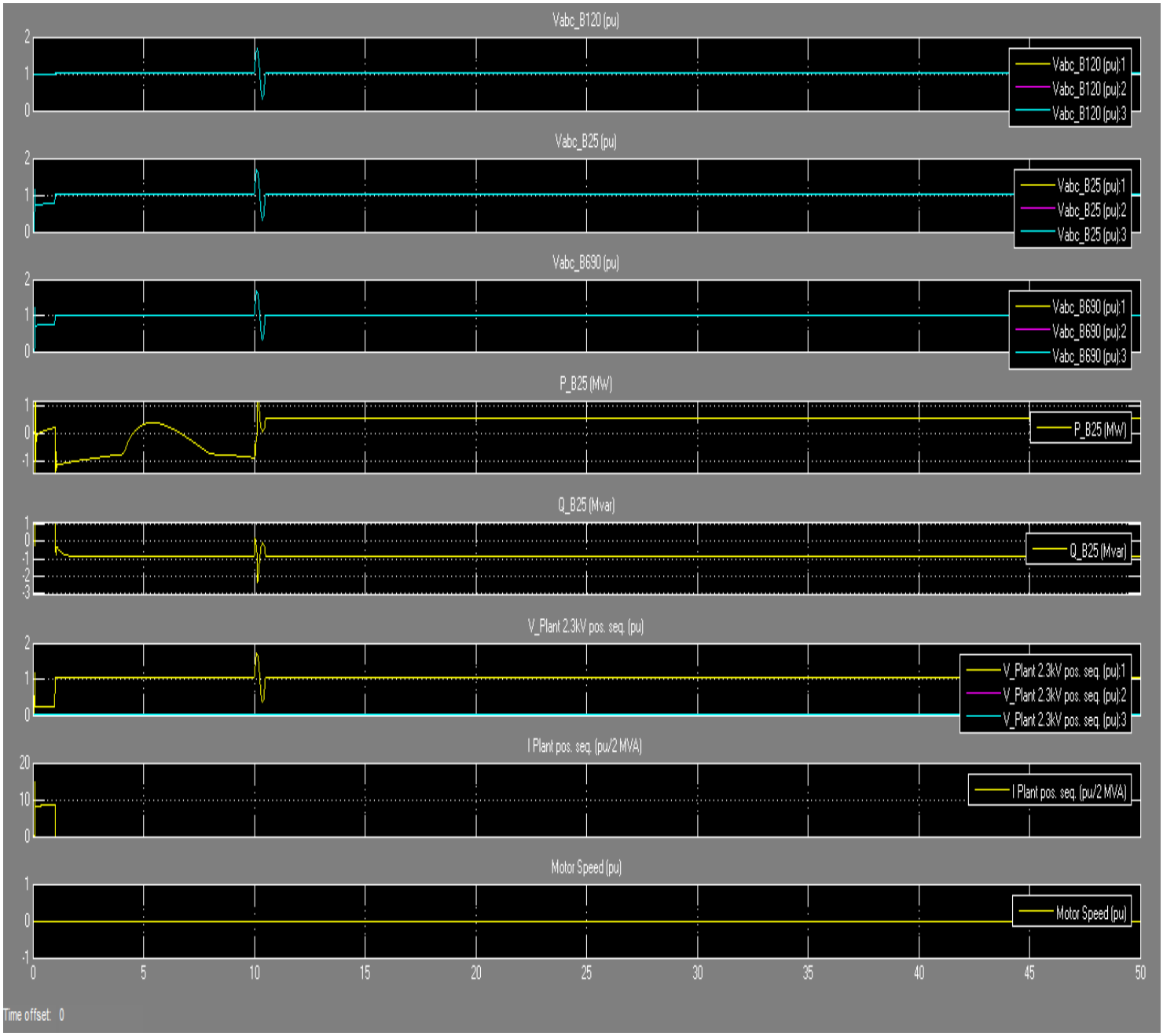

Figure 5.15 Grid system is continuous its function after the faults happen

5.4.4. Simulation of a voltage sag/dip on the 15kV system and short-circuit on grid side without controller

The DFIG wind turbine system is disconnected from the system because of the grid faults and voltage sag or dip on voltage source. In this simulation, we observed pos. seq. voltage, pos. seq. current, active power and reactive power, DC link voltage, the rotor speed and the pitch angle of the DFIG wind turbine.

Pos. seq. voltage (V_1_B690) of DFIG wind turbine is slowly increased from 0p.u to 1p.u before the faults happened on the grid side. During the fault times, it is fluctuating b/n 0.45p.u and 1.55p.u. But the voltage is reached above the rated value of the protection system. In protection system the voltage range is 0.75p.u and 1.1p.u, but on this simulation the voltage out of the range. Because of this the wind turbine is disconnected from the system.

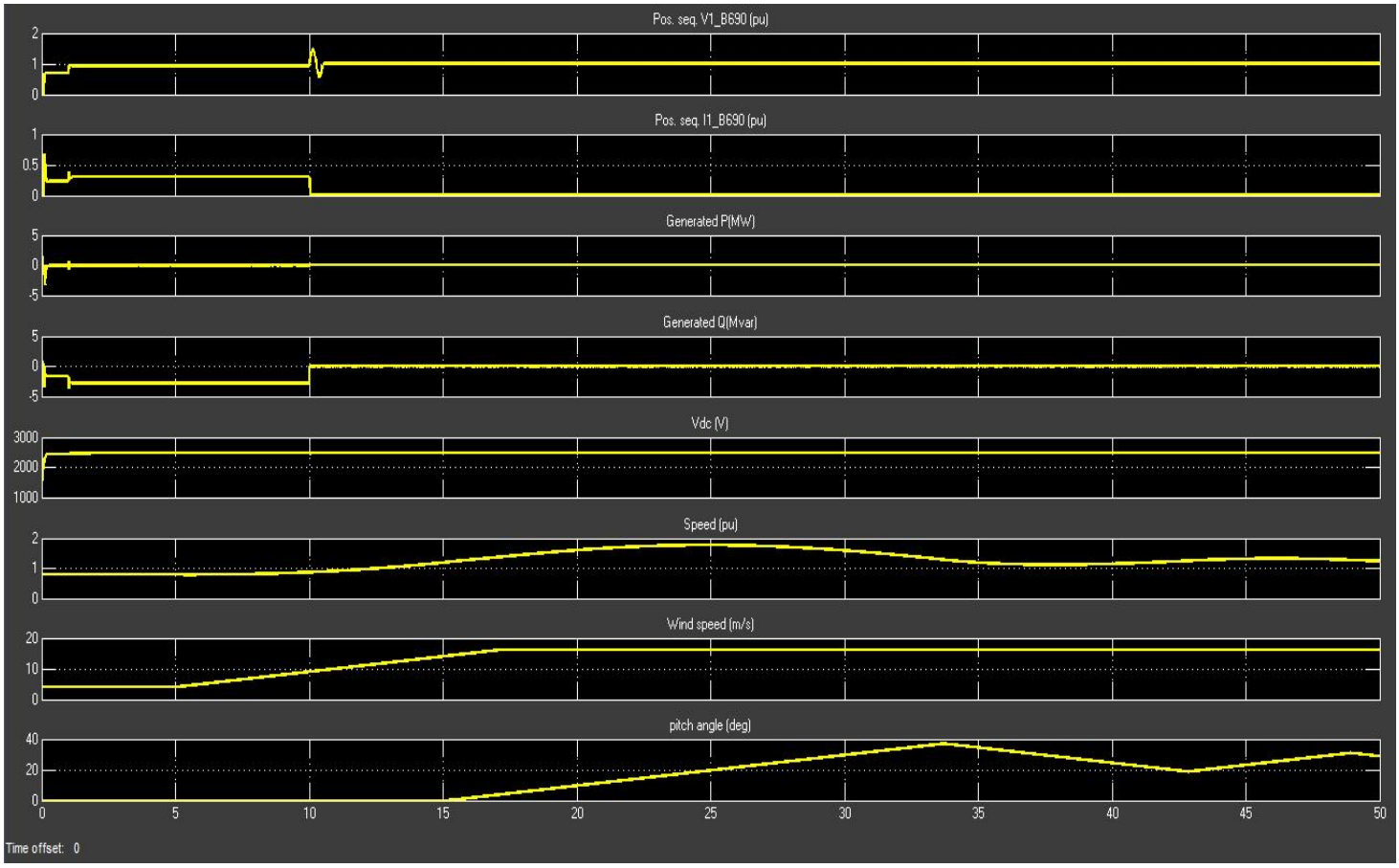

Figure 5.16 DFIG is disconnected from the system after grid faults happen

Table 5 Wind turbine parameters when wind turbine is tripped from the system

Wind turbine parameters	Before grid fault	During grid fault	After grid fault
Pos. seq. Voltage (V1-B-690p.u)	0 to 1	b/n 0.45 & 1.55	Constant (1)
Pos. seq. current (I1-B-690p.u)	0.8 to 0 to 0.2	0.4 to 0	Constant (0)
Generated active power(MW)	Constant (0)	Constant (0)	Constant (0)
Generated reactive power(Mvar)	-2 to 0	Constant (0)	Constant (0)
DC-link Voltage(V)	Constant (2200)	Increased to 2500	Constant (2500)
Speed(p.u)	0.73 to 0.8	Increasing to 1.8	Decreasing 1.8 to 1
Wind speed(m/s)	Increasing	Increasing	Increasing
Pitch angle(degree)	Constant (0°)	Increasing 39°	Fluctuated b/n 0° and 40°

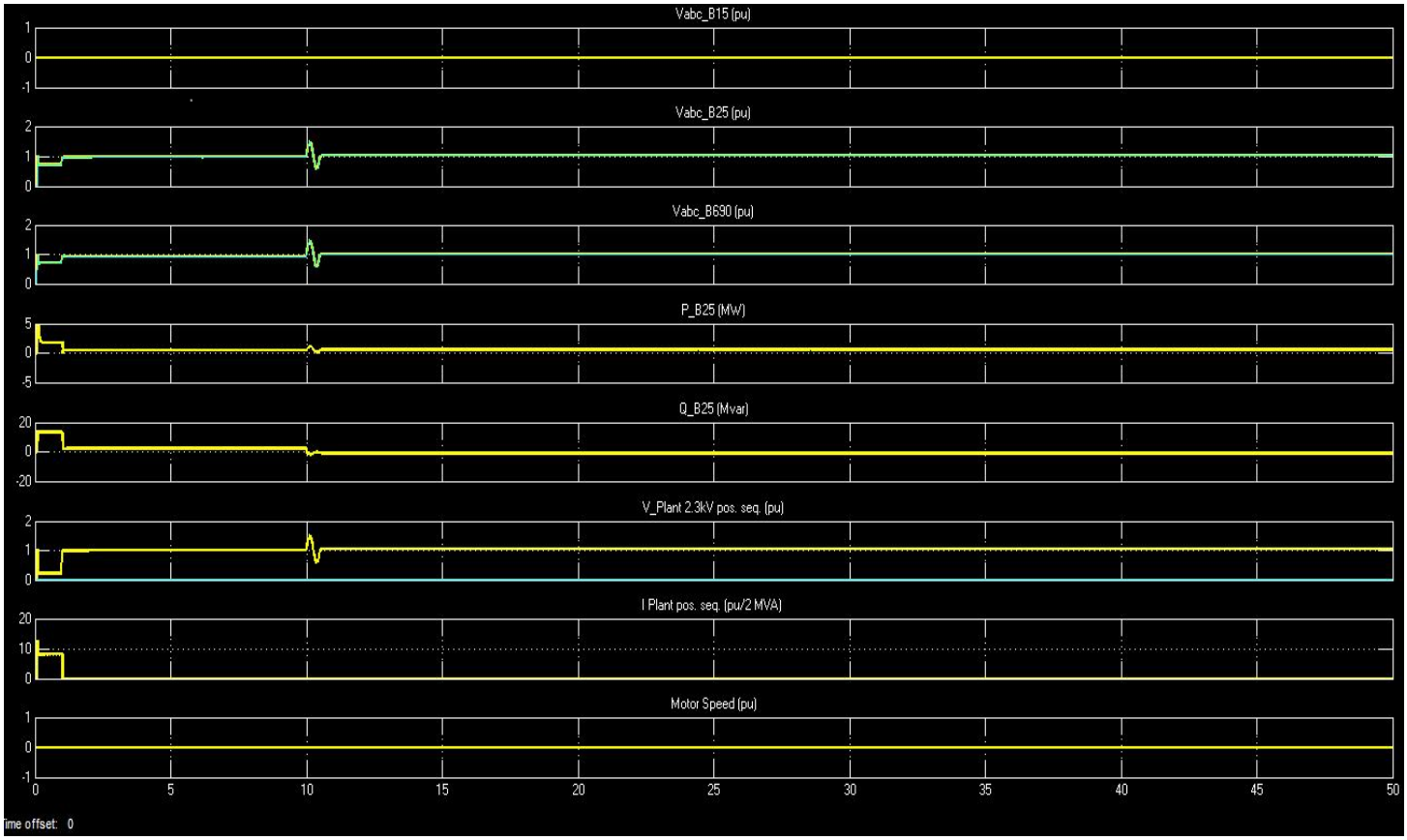

Figure 5.17 Grid system is continuous its function after the faults happen

Table 6 Grid side parameters when wind turbine is tripped from the system

Grid side parameters	Before grid fault	During grid fault	After grid fault
Pos. seq. Voltage (**$V_{abc\_}$ B-15**)	Constant(1p.u)	b/n 0.6 & 1.5 p.u	Constant (1p.u)
Pos. seq. Voltage (**$V_{abc\_}$ B-25**)	b/n 0.75 & 1p.u	b/n 0.59&1.42 p.u	Constant(1p.u)
Pos. seq. Voltage (**$V_{abc\_}$ B-690**)	b/n 0.71 & 1p.u	b/n 0.51 & 1.49 p.u	Constant(1p.u)
Generated Active power(**P_B25**(MW))	b/n 2 & 0.4MW	b/n 3.9MW &2.1MW	Consume 8MW
Reactive power(**Q_B25**(Mvar))	b/n 0Mvar & 9Mvar	b/n -5Mvar & 15Mvar	Generate 1.4Mvar
Plant voltage pos. seq.(**V_plant**)	1.03p.u	b/n 0.75p.u & 1.21p.u	1.03p.u
Plant current in Pos. seq.(**I_plant**)	b/n 0.12A & 10A	0.12A	0.12A

6. Chapter Six: Conclusions, Recommendations and Future Works

6.1. Conclusions

This thesis presents a study of the variable speed DFIG wind turbine and the grid system is subjected to disturbances; such as, voltage sag or dip, and three-phase short-circuit faults. The dynamic behavior of DFIG without disturbance of grid, after the grid system disturbance and under grid system disturbance was simulated using MATLAB/SIMULINK platform using rotor speed control in order to control the slip of the machine. Accurate transient simulations are required to investigate the influence of the wind power on the power system stability. The stator is directly connected to the grid and the rotor is interface via a back-to-back partial scale power converter. Power converter are usually controlled utilizing speed of rotor control techniques which allow the decoupled control of both active and reactive power flow to the grid. In the present investigation, the dynamic DFIG performance is presented for both normal and abnormal grid conditions. The control performance of DFIG is satisfactory in normal grid conditions and it is found that, both active and reactive power maintains a study pattern in spite of fluctuating wind speed and net electrical power supplied to grid is maintained constant. During grid disturbance; voltage, current, active power and reactive power of DFIG has been observed. The detailed results of steady state and faulty or three-phase short circuit on grid system has been noted and analyzed with proper justification. In this study observed a property of DFIG with controller and without controller.

6.2. Recommendation

From the simulation results obtained, it has been validated that the system is fully functional. However, the following recommendations have been made as work that could be done to further improve the system. Using DC bus voltage to run the generator to synchronous speed and the switching in the stator at this point to connect and synchronize it to the grid. This would enhance the automation of the system and reduce the number of components in the system. In order to increase the fault ride through capabilities of the system, crowbar protection and series dynamic resistor could be added to the system.

6.3. Future Works

In future work aims to develop a controller, which can effectively improve the dynamic stability, transient response of the system during normal condition and faulty grid conditions. To develop a protection system for power converter and DFIG for large disturbances like phase-to-phase and phase-to-ground fault of little

cycle duration as the power converter is very sensitive to grid disturbance. And also implement this work of DFIG and power flow during grid faults. Cost benefit analysis should also be investigated and verified after an external fault. Complete protection schemes such as under and over voltage, over current, speed and frequency deviation protection should be developed for the DFIG.

REFERENCES

[1] Robert Zavadil, Nicholas Miller, Abraham Ellis, and Eduard Muljadi, "Making Connections", IEEE Power & Energy, Vol. 3, No. 6, November/December 2005.

[2] S. Muller, M. Deicke, R.W. De Doncker, "Doubly Fed Induction Generator Systems for Wind Turbines", IEEE Industry Applications Magazine, Vol. 8, No. 3, pp. 26-33, May/June 2002.

[3] "Study of wind turbine driven DFIG using AC/DC/AC converter" by prof. K.B.Mohanty, dept. of Electrical Engineering., National Institute of technology Rourkela-769008.

[4] N.W Miller, W.W Price, J.J Sanchez-Gasca, "Dynamic Modeling of GE 1.5 and 3.6 Wind Turbine-Generators", Version 3.0, Technical Report, GE Power Systems Consulting, Schenectady, NY, October 27, 2003

[5] "Modeling and Simulation of Doubly Fed Induction Generator Coupled With Wind Turbine-An Overview" by AnkitGupta,S.N. Singh and Dheeraj K. Khatod.

[6] Paul C. Krause, Oleg Wasynczuk "Analysis of electrical machines & Drive system" 2nd edition, IEEE, Purdue University,ISBN 9812-53-150-2, 2007.

[7] Rubén Penaa, Roberto Cardenasb, Enrique Escobarb, Jon Clarec, Pat Wheelerc "Control strategy for a Doubly-Fed Induction Generator feeding an unbalanced grid or stand-alone load" Electric PowerSystems Research (2009) 355–364.vol.79.

[8] L. Dusonchet, F. Massaro and E. Telaretti "Transient stability simulation of a fixed speed wind turbineby Matlab/Simulink"

[9] "Decoupled Active and Reactive Power Control of a Doubly-Fed Induction Generator (DFIG)", by A.Dendouga, R.Abdessemed, M.L.Bendaas and A. Chaiba, Batna University, Algeria.

[10] "Analysis and Vector Control of a cascaded doubly-fed induction generator in wind energy applications", by ZoheirTir, HammoudRajeai and RachidAbdessemed, University of Setif, Algeria.

[11] "Control design and analysis of Doubly-Fed Induction Generator (DFIG) in wind power application", by ShukulMazari, The University of Alabama, Alabama, 2009.

[12] B. K. Bose "Modern power electronics and ac drives" forth impression 2007 Pearson Prentice Hall,ISBN: 81-7758-876-1, 2007.

[13] Ned Mohan, Ted K. A. Brekken "Control of a Doubly Fed Induction Wind Generator under Unbalanced Grid Voltage Conditions" IEEE Transaction Energy conversion,vol.no22.1,Mar 2007.

[14] "Renewable Energy Focus Handbook," Linacre House, Jordan Hill, Oxford OX28DP, UK, 1st edition, eBook available at http://www.elsevierdirect.com/

[15] G.L Johnson, "*Wind Energy Systems*," Prentice-Hall, Englewood Cliff, New Jersey, 1985.

[16] L.L. Freris, "*Wind Energy Conversion System"*, Prentice-Hall, Upper Saddle, New Jersey,1990.

[17] The MathWorks, "SimPowerSystems for Use with Simulink", User's Guide Version 4.

[18] M. Singh, E. Muljiadi, J. Jonkman, and V. Gevorgian, "Simulation for Wind Turbine Generators—With FAST and MATLAB-Simulink," National Renewable Energy Laboratory, Nanyang Technological University, April 2014.

[19] Sun, T."Power Quality of Grid-Connected Wind Turbines with DFIG and Their interaction with the Grid" Aalborg: Institute for Energiteknik, Aalborg University in 2004.

[20] S. Engelhardt, I. Erlich, C. Feltes, J. Kretschmann, F. Shewarega, "Reactive power capability of wind turbines based on doubly fed induction generators", IEEE Trans. Energy Convers.26(1) (2011).

[21] T. Lund, P. Sorensen, J. Eek, "Reactive power capability of a wind turbine with doubly fed induction generator, Wind Energy"10(4) (2007),

[22] "Alstom wind turbine concept and general operation for operation and maintenance", Module 3, by ALSTOM wind turbine manufacturer, 2010.

[23] Johan Morren, Sjoerd W.H. de Haan, "Ride through of Wind Turbines with Doubly-Fed Induction Generator during a Voltage Dip" IEEE transaction on energy conversion June, 2005, vol.20.

[24] A. Fitzgerald, C. Kingsley, and S. Umans, '*Electric Machinery",6/E*, ser. McGraw-Hill series in electrical and computer engineering, McGraw-Hill, 2002.

[25] G. Abad, L. Marroyo, G. Iwanski*et al.*,"*Doubly Fed Induction Machine: Modeling and Controlfor Wind Energy Generation*." Wiley-IEEE Press, 2011, vol. 86.

[26] "HANDBOOK OF RENEWABLE ENERGY TECHNOLOGY", edited by Ahmed F. Zobaa and Ramesh C. Bansal, World Scientific Publishing Co. Pte. Ltd, 2011.

[27] I. Boldea, "*Variable speed generators"*. CRC, 2005, vol. 2.

[28] R. Krishnan, "*Electric Motor Drives: Modeling, Analysis, and Control"*. Prentice Hall UpperSaddle River, NJ, 2001, vol. 626.

[29] Transformers and Electrical Machines; Ion Boldea; EdituraPolitehnica Timisoara 2002ISBN 973-9389-97-X.

[30] T. Miller, "Theory of the doubly-fed induction machine in the steady state," in Electrical Machines (ICEM), 2010 XIX International Conference on, 2010,

[31] G. Tapia, A. Tapia, and J. Ostolaza, "Two alternative modeling approaches for the evaluation of wind farm active and reactive power performances," *Energy Conversion, IEEE Transactions on*, vol. 21, no. 4, pp. 909–920, 2006.

[32] R. C. Dorf, *Modern control systems*. Addison-Wesley Longman Publishing Co., Inc., 1991.

[33] G. Abad, L. Marroyo, G. Iwanski*et al.*, *Doubly Fed Induction Machine: Modeling and Control for Wind Energy Generation*. Wiley-IEEE Press, 2011, vol. 86.

APPENDIX

Appendix A:1.5MW DFIG Parameters

DFIG Parameters	Values
Rated stator voltage (volt)	690V
Rated rotor voltage(volt)	1863V
Rated apparent power(KVA)	1667KVA
Rated speed(rpm)	1800rpm
No pole pairs	2
Stator resistance	0.00706p.u
Stator reactance	0.0171p.u
Rotor resistance	0.005 p.u
Rotor reactance	0.156 p.u
Magnetizing reactance	2.9 p.u
Generator inertia	5.04kgm^2

Power coefficient (C_p) calculation

$P_m=C_p(\lambda,\beta)A\rho V^3_{wind}$ $C_p(\lambda,\beta)=C_1(C_2/\lambda_i-C_3\beta-C_4)e^{-C5/\lambda i}+C_6\lambda$. Where, $C_1=0.5$, $C_2=116$, $C_3=0.4$, $C_4=5$, $C_5=21$ and $C_6=0.0068$.

$\frac{1}{\lambda i}=\frac{1}{\lambda+0.08\beta}-\frac{0.035}{\beta3+1}$, Assume $\beta=0°$ and $\lambda=8.1$, then calculate Cpmax

$\frac{1}{\lambda i}=\frac{1}{\lambda+0.08\beta}-\frac{0.035}{\beta3+1}=\frac{1}{8.1+0.08(0)}-\frac{0.035}{(0)3+1}\Rightarrow\frac{1}{\lambda i}=\frac{1}{8.1}$-0.035=0.12346-0.035=0.0884

λ_i=11.3049, then C_{max} is $C_p(\lambda,\beta)=C_1(C_2/\lambda_i-C_3\beta-C_4)e^{-C5/\lambda i}+C_6\lambda$

$C_p(8.1,0)=0.5176(\frac{116}{11.3049}-0.4(0)-5)e^{-21/11.3049}+0.0068(8.1)=0.5176(10.2609-5)e^{-1.8576}+0.05508$

$=(0.5176*5.2609)e^{-1.8576}+0.05508=2.72304e^{-1.8576}+0.05508=0.4800$

Appendix B: Doubly fed induction generator modeling

In d-q synchronously rotating reference frame:

$V_{sd}=R_sI_{sd}+\frac{d}{dt}\psi sd-\omega_s\psi_{sq}$……(i) $V_{sq}=R_sI_{sq}+\frac{d}{dt}\psi sq-\omega_s\psi_{sd}$……(ii)

$V_{rd}=R_rI_{rd}+\frac{d}{dt}\psi rd-\omega_r\psi_{rq}$……..(iii) $V_{rq}=R_rI_{rq}+\frac{d}{dt}\psi rq-\omega_r\psi_{rd}$……(iv)

$\Psi_{sd}=L_sI_{sd}+L_mI_{rd}$……(v) $\psi_{sq}=L_sI_{sq}+L_mI_{rq}$……(vi)

$\Psi_{rd}=L_rI_{rd}+L_mI_{sd}$ ……(vii) $\Psi_{rq}=L_rI_{rq}+L_mI_{sq}$ ……(viii)

Where ψ—is a flux linkage, ω_s—is stator electrical angular frequency and $\omega_r=s\omega_s$—is rotor slip angular frequency. Since the stator is connected to the grid, and the influence of the stator resistance is small, the stator flux can be considered constant. By stator flux orientation concept, i.e, with the d-axis of the d-q coordinate system oriented along the stator flux vector position ($\psi_{sdq}=\psi_{sd}$ and $\psi_{sq}=0$) and assuming the stator voltage vector to be constant and neglecting stator resistance R_s. Then the above equations can be reduced to:

$|\mathbf{V}sdq|=|Vsd+jVsq|=\left|RsIsd+\frac{d}{dt}\psi sd-\omega s\psi sq+jVsq\right|=V_{sq}$…….(ix)

$|\psi sdq|=|\psi sd+j\psi sq|=\psi_{sd}$. Substituting equation (v-viii) into equation (iii &iv), it yields:

$V_{rd}=R_rI_{rd}+\frac{d}{dt}[LrIrd+LmIsd]-\omega_r[L_rI_{rq}+L_mI_{sq}]\Rightarrow V_{rd}=R_rI_{rd}+L_r\frac{d}{dt}Ird+L_m\frac{dIsd}{dt}-\omega_r[L_rI_{rq}+L_mI_{sq}]$……(x)

$V_{rq}=R_rI_{rq}+\frac{d}{dt}[L_rI_{rq}+L_mI_{sq}]+\omega_r[L_rI_{rd}+L_mI_{sd}]\Rightarrow V_{rq}=R_rI_{rq}+L_r\frac{d}{dt}I_{rq}+L_m\frac{d}{dt}I_{sq}]+\omega_r[L_rI_{rd}+L_mI_{sd}]$……..(xi)

But from equation (v-viii), we have; $\psi_{sd}=L_sI_{sd}+L_mI_{rd}$ and $\psi_{sq}=L_sI_{sq}+L_mI_{rq}=0\Rightarrow I_{sq}=\frac{-Lm}{Ls}I_{rq}$……(xii)

From equations (i & ii), we can solve for:

$V_{sq}=R_sI_{sq}+\frac{d}{dt}\psi sq+\omega_s\psi_{sd}\Rightarrow V_{sq}=\omega_s\psi_{sd}=V_s$……(xiii) $\psi_{sd}=L_sI_{sd}+L_mI_{rq}\Rightarrow I_{sd}=\frac{\psi sd-LmIrq}{Ls}$…….(xiv)

Therefore, $I_{sd}=\frac{Vs-LmIrq}{Ls}$. Substituting equation (xii) and (xiv) into equation (x) & (xi), we get:

$V_{rd}=R_rI_{rd}+L_r\frac{d}{dt}Ird + Lm\frac{d}{dt}[\frac{\psi sd-LmIrd}{Ls}-\omega_r[L_rI_{rq}+L_m(\frac{-LmIrq}{Ls})]$

$V_{rd}=R_rI_{rd}+L_r[1-L^2_m/L_rL_s]\frac{d}{dt}Ird-\omega_rL_r[1-\frac{L2m}{LrLs}]I_{rq}\Rightarrow V_{rd}=R_rI_{rd}+\sigma L_r\frac{d}{dt}Ird-\omega_r\sigma L_rI_{rq}$……..(xv)

Similarly: $V_{rq}=R_rI_{rq}+L_r\frac{dIrq}{dt}+L_m\frac{dIsq}{dt}+\omega_r[L_rI_{rd}+L_mI_{sd}]$ &

$V_{rq}=R_rI_{rq}+L_r\frac{dIrq}{dt}+L_m\frac{d}{dt}[-\frac{LmIrq}{Ls}]+\omega_r\{L_rI_{rd}+L_m(\frac{Vs-LmIrd}{Ls})\}$, those two equations simplified to:

$V_{rq}=R_rI_{rq}+L_r[1-L^2_m/L_rL_s]\frac{d}{dt}Irq+\omega_rL_r[1-L^2_m/L_rL_s]I_{rd}+\omega_rV_s\,Lm/Ls\Rightarrow V_{rq}=R_rI_{rq}+$

$+\sigma L_r\frac{d}{dt}Irq+\omega_r+\sigma L_rI_{rd}+\omega_rV_sLm/Ls$

Where: $\sigma=1-L^2_m/L_rL_s$ ……..is a leakage coefficient, $Vs=V_{sq}=\omega_s\psi_{sd}$, $\omega_r=s\omega_s=\omega_s-\omega_r\Rightarrow s=\frac{\omega s-\omega r}{\omega s}$.....is slip.

Appendix C: Transfer Functions the Modified Inner Loop Control Structure

Referring to Figure 4.5, three equations can be readily determined:

$$i_{rd}^{err}(s) = i_{rd}^{*}(s) - i_{rd}(s)$$
$$v'_{rd}(s) = i_{rd}^{err}(s)\frac{K_{I1}}{s} - i_{rd}(s)K_{P1}$$
$$i_{rd}(s) = v'_{rd}(s)\frac{1}{R_r + \sigma L_s s}$$

Substituting the first two expressions into the third one yield:

$$i_{rd}(s) = \left[i_{rd}^{err}(s)\frac{K_{I1}}{s} - i_{rd}K_{P1}\right]\frac{1}{R_r + \sigma L_r s}$$
$$= \left[(i_{rd}^{*}(s) - i_{rd}(s))\frac{K_{I1}}{s} - i_{rd}K_{P1}\right]\frac{1}{R_r + \sigma L_r s}$$

Grouping like terms:

$$i_{rd}(s)\left[1 + \left(\frac{K_{I1}}{s} + K_{P1}\right)\frac{1}{R_r + \sigma L_r s}\right] = i_{rd}^{*}(s)\frac{K_{I1}}{s(R_r + \sigma L_r s)}$$

Dividing output by input:

$$\frac{i_{rd}(s)}{i_{rd}^*(s)} = \frac{K_{I1}}{s(R_r+\sigma L_r s)} \frac{1}{1+\frac{K_{P1}s+K_{I1}}{s(R_r+\sigma L_r s)}}$$
$$= \frac{K_{I1}}{s^2\sigma L_r + s(R_r+K_{P1})+K_{I1}}$$
$$= \frac{\frac{K_{I1}}{\sigma L_r}}{s^2 + s\frac{(R_r+K_{P1})}{\sigma L_r} + \frac{K_{I1}}{\sigma L_r}}$$

Appendix D: The Outer Loop Transfer Function

From Figure 5.8, the following equations are written:

$$i_{rq}(s) = i_{rq}^*(s)\frac{1}{1+\frac{T_{s1}}{4}s}$$
$$i_{rq}^*(s) = P_s^{err}(s)\frac{K_{I2}}{s} + K_{P2}P_s(s)$$
$$P_s^{err}(s) = P_s(s) - P_s^*(s)$$
$$P_s(s) = -\frac{3}{2}\frac{L_m}{L_s}|\overrightarrow{v_s}|i_{rq}(s)$$

Substituting the third equation into the second:

$$i_{rq}^*(s) = [P_s(s) - P_s^*(s)]\frac{K_{I2}}{s} + K_{P2}P_s(s)$$

Substituting in the first equation:

$$i_{rq}(s)\frac{1}{1+\frac{T_{s1}}{4}s} = P_s(s)\left(K_{P2}+\frac{K_{I2}}{s}\right) - P_s^*(s)\frac{K_{I2}}{s}$$

Substituting in the fourth equation:

$$\frac{P_s(s)}{-\frac{3}{2}\frac{L_m}{L_s}|\overrightarrow{v_s}|}\cdot\frac{1}{1+\frac{T_{s1}}{4}s}=P_s(s)\left(K_{P2}+\frac{K_{I2}}{s}\right)-P_s^*(s)\frac{K_{I2}}{s}$$

Collecting terms:

$$P_s(s)\left(K_{P2}+\frac{K_{I2}}{s}+\frac{\frac{1}{1+\frac{T_{s1}}{4}s}}{\frac{3}{2}\frac{L_m}{L_s}|\overrightarrow{v_s}|}\right)=P_s^*(s)\frac{K_{I2}}{s}$$

Dividing output by input:

$$\begin{aligned}\frac{P_s(s)}{P_s^*(s)}&=\frac{\frac{K_{I2}}{s}}{\left(K_{P2}+\frac{K_{I2}}{s}+\frac{\frac{1}{1+\frac{T_{s1}}{4}s}}{\frac{3}{2}\frac{L_m}{L_s}|\overrightarrow{v_s}|}\right)}\\&=\frac{6\frac{L_m}{L_s}\frac{|\overrightarrow{v_s}|}{T_{s1}}K_{I2}}{s^2+\left(\frac{4}{T_{s1}}+6\frac{L_m}{L_s}\frac{|\overrightarrow{v_s}|}{T_{s1}}K_{P2}\right)s+6\frac{L_m}{L_s}\frac{|\overrightarrow{v_s}|}{T_{s1}}K_{I2}}\end{aligned}$$

Appendix E: Initialization Script

This M-file gives in hard copy form, the Matlab code necessary to run the model. All code is alsoprovided on the accompanying in the file *InitSystem.m.*

```
% Initialize DFIG and Wind Turbine Simulation
% Author: TESHALE TADESSE
% Last Modified: Apr 18, 2016
closeall
clear
clc
%% Turbine Model Initialization
% Load Turbine Characteristic into the model
% Turbine Parameters
GR = 103.2; % gear-box ratio(dimensionless)
R = 34; % turbine radius [m]
```

```
rho = 1.21; % air density [kg/m^3]
A = pi*R^2; % swept area in [m^2]
% tip speed ratio from manufacturer datasheet
TSR_vector=xlsread('CpVsTSR_D49.xlsx',1,'A2:A67');
Cp_vector =xlsread('CpVsTSR_D49.xlsx',1,'B2:B67');
% Turbine Performance Curves (used in lookup tables)
vwind_vector = linspace(4,9,18); % vector of wind speeds [m/s]
wt_vector = linspace(0.1234,3.6192,1000);% vector of turbine shaft speeds
% [mech rad/sec]
[X,Y]=meshgrid('vwind_vector, wt_vector'); % X stores v, Y stores w
% v increases RIGHT, w increases DOWN
L= R*Y./X; % tip speed ratio [dimensionless]
Cp= interp1(TSR_vector,Cp_vector,L); % performance factor [dimensionless]
Pt=(1/2)*rho*A*X.^3.*Cp; % Turbine power [W]
Tt_matrix = Pt./Y; % Turbine torque [Nm]
Tt_matrix(isnan(Tt_matrix)) = 0; % remove NANs
Tmech = Tt_matrix/GR; % Torque available at shaft of generator [Nm]
% Maximum Power Point Tracking[MPPT]
MPPT1=zeros(1,length(vwind_vector)); % vector of maximum power points [W]
MPPT_w = zeros(1,length(vwind_vector)); % vector of turbine shaft speeds
% that correspond to the maximum power point [mech rad/sec]
for i = 1:1:length(vwind_vector);
[MPPT1(i),IND, MAX] = max(Pt(:,i)); % find maximum power points
MPPT_w(i) = wt_vector(IND_MAX);
end
% fitting the function MPPT = Kopt*(wt)^3 yields:
% Curve fitting done offline using Matlab Curve Fit Toolbox
Kopt = 3.364e5;
% Initialization Starts Here %
vw_0 = 4; % initial wind speed [m/s]
%%Initial Turbine Parameters calculated from initial wind speed
L_0 = R*wtvector/vw_0; % initial tip speed ratio
Cp_0 = interp1(TSR_vector,Cp_vector,L_0); % initial performance factor
Pt_0 = (1/2)*rho*A*vw_0^3.*Cp_0; % initial turbine power curve
%Initial values of MPPT
[MPPT_0,INDMAX] = max(Pt_0);
MPPT_w_0 = wt_vector(IND_MAX);
% Initialization of turbine for a particular wind speed
Pt_init = MPPT_0;
wt_init = MPPT_w_0;
% Plot Wind Turbine Data
figure(1)
holdon
gridon
for i = 1:1:length(vwind_vector)
```

```
plot(wt_vector*60/(2*pi)*GR,Pt(:,i),'b-','Linewidth',1)
end
plot(wt_vector*60/(2*pi)*GR,Pt_0,'b-','Linewidth',3)
plot(MPPT_w*60/(2*pi)*GR,MPPT,'r-','Linewidth',1)
holdoff
%% Initialize Double squirrel cage Rotor Machine
% Load Parameters of Generator
VLLrms = 690; % line to line, rms, stator voltage [V]
fs = 50; % line frequency [Hz]
Pp = 2; % number of poles pairs [dimensionless]
J = 5.04 ;% system inertia (reduced for short simulation) [kg m^2]
TR = 0.34; % equivalent turns ratio [dimensionless]
Rs = 7.06e-3*1; % stator resistance [ohms]
Rr = 5e-3*1; % referred rotor resistance [ohms]
Lls = 1.7e-2; % stator leakage inductance [H]
Llr = 15.6e-2; % referred rotor leakage inductance [H]
Lm = 2.9e-1; % magnetizing inductance [H]
Ls = Lm+Lls; % stator inductance [H]
Lr = Lm+Llr; % rotor inductance [H]
sig = 1-Lm^2/(Ls*Lr); % leakage factor [dimensionless]
% Conversion Multipliers
D2R = pi/180; % degrees to radians [rad/deg]
R2D = 180/pi; % radians to degrees [deg/rad]
%% Starting Point
% Starting Speeds
ws = 2*pi*fs; % synchronous angular frequency in [electrical rad/sec]
w_mech = wt_init*GR; % rotor shaft angular frequency in [mechanical rad/sec]
wm_0 = Pp*w_mech; % rotor shaft angular frequency in [electrical rad/sec]
s = (ws - wm_0)/ws; % slip [dimensionless]
wr = s*ws; % rotor angular frequency in [electrical rad/sec]
% P and Q references
Ps_ref =-Pt_init; % real stator power reference, three phase, [MW]
Qs_ref = 0; % reactive stator power reference, three phase, [VAR]
%% Solve for rotor voltage accounting for Rs, and Rr, aiming for P and Q_ref
% Step 1: solve for stator current from P and Q power reference
% line to neutral rms stator voltage magnitude [V]
Vs_mag = VLLrms/sqrt(3);% stator voltage taken as reference [rad]
Vs_ang = 0;
Vs_phasor = Vs_mag*exp(1i*Vs_ang);% stator voltage phasor, rms [V]
% stator current phasor, rms [A]
Is_phasor = (Ps_ref/3-1i*Qs_ref/3)/Vs_phasor;
Is_mag = abs(Is_phasor);
Is_ang = angle(Is_phasor);
% Step 2: solve for all other phasors
% stator flux linkage phasor, rms [wb-turns]
```

```
Fs_phasor = (Vs_phasor- Rs*Is_phasor)/(1i*ws);
Fs_mag = abs(Fs_phasor);
Fs_ang = angle(Fs_phasor);
% rotor current phasor, rms [A]
Ir_phasor = (Fs_phasor-Ls*Is_phasor)/Lm;
Ir_mag = abs(Ir_phasor);
Ir_ang = angle(Ir_phasor);
% rotor flux linkage phasor, rms [wb-turns]
Fr_phasor = Lm*Is_phasor + Lr*Ir_phasor;
Fr_mag = abs(Fr_phasor);
Fr_ang = angle(Fr_phasor);
% rotor voltage phasor, rms [V]
Vr_phasor = 1i*wr*Fr_phasor + Rr*Ir-phasor;
Vr_mag = abs(Vr_phasor);
Vr_ang = angle(Vr_phasor);
% Power (positive consuming)
Ps1=3*real(Vs_phasor.*conj(Is_phasor)); % real stator power [W]
Pr=3*real(Vr_phasor*conj(Ir_phasor)); % real rotor power [W]
Qs1=3*imag(Vs_phasor*conj(Is_phasor)); % reactive stator power [Var]
Qr=3*imag(Vr_phasor*conj(Ir_phasor)); % reactive rotor power [Var]
Ps_cu = 3*Is_mag^2*Rs; % stator copper loss [W]
Pr_cu = 3*Ir_mag^2*Rr; % rotor copper loss [W]
% electromagnetic torque [Nm]
Tem = 3*Lm/(sig*Lr*Ls)*Pp*imag(conj(Fr_phasor)*Fs_phasor);
nm = w_mech*30/pi; % rotor speed [rpm]
P_mech = Tem*w_mech; % mechanical power [W]
disp('_____Initial Steady State Operating Point_____')
disp('_____Phasor Solution _____')
disp([' Vs | ',num2str(Vs_mag),' /- ',num2str(Vs_ang*R2D),' V'])
disp([' Vr | ',num2str(Vr_mag),' /-',num2str(Vr_ang*R2D),' V'])
disp([' Is | ',num2str(Is_mag),' /-',num2str(Is_ang*R2D),' A'])
disp([' Ir | ',num2str(Ir_mag),' /-',num2str(Ir_ang*R2D),' A'])
disp([' Fs | ',num2str(Fs_mag),' /-',num2str(Fs_ang*R2D),' wb-turns'])
disp([' Fr | ',num2str(Fr_mag),' /-',num2str(Fr_ang*R2D),' wb-turns'])
disp('_____')
disp([' Ps | ',num2str(Ps),' W'])
disp([' Pr | ',num2str(Pr),' W'])
disp([' Qs | ',num2str(Qs),' VAR'])
disp([' Qr | ',num2str(Qr),' VAR'])
disp([' Ps_cu | ',num2str(Ps_cu),' W'])
disp([' Pr_cu | ',num2str(Pr_cu),' W'])
disp('_____POWER BALANCE_____')
disp([' Ps + Pr | ',num2str(Ps+Pr),' W'])
disp([' Pmech + Pcu | ',num2str(Ps_cu + Pr_cu + P_mech),' W'])
disp('_____')
```

```
disp([' Tem | ',num2str(Tem),' Nm'])
disp([' nm | ',num2str(nm),' rpm'])
disp([' P_mech | ',num2str(P_mech),' W'])
disp('_____________________________________________________________')
%% Initialize Dynamic model from Phasor Solution (align to stator flux)
% Phasor of Stator and Rotor Voltages are related to their space vectors at
% t=0 using Equation Va=V/sqrt(2)*angle of phase
%Stator Voltage
vas_0 = sqrt(2)*Vs_mag*cos(Vs_ang); % a-phase stator voltage at t=0
vbs_0 = sqrt(2)*Vs_mag*cos(Vs_ang-2*pi/3); % b-phase stator voltage at t=0
vcs_0 = sqrt(2)*Vs-mag*cos(Vs_ang-4*pi/3); % c-phase stator voltage at t=0
vsD_0 = (2/3)*(vas_0-0.5*vbs_0- 0.5*vcs_0); % D-axis stator voltage
vsQ_0 = (2/3)*(sqrt(3)/2*vbs_0-sqrt(3)/2*vcs_0); % Q-axis stator voltage
Vs_s_0 = vsD_0 + 1i*vsQ_0; % stator voltage space vector (stator frame)
%Rotor Voltage
var_0 = sqrt(2)*Vr_mag*cos(Vr_ang); % a-phase rotor voltage at t=0
vbr_0 = sqrt(2)*Vr_mag*cos(Vr_ang-2*pi/3); % b-phase rotor voltage at t=0
vcr_0 = sqrt(2)*Vr_mag*cos(Vr_ang-4*pi/3); % c-phase rotor voltage at t=0
vD_0 = (2/3)*(var_0-0.5*vbr_0 -0.5*vcr_0); % d-axis rotor voltage
vQ_0 = (2/3)*(sqrt(3)/2*vbr_0-sqrt(3)/2*vcr_0);% q-axis rotor voltage
Vr_r_0 = vd_0 + 1i*vq_0; % rotor voltage space vector (rotor frame)
%Initial rotor angle taken as 0(zero degree)
Vr_s_0 = Vr_r_0*exp(-1i*(0)); % rotor voltage space vector (stator frame)
vrD_0 = real(Vr_s_0); % D-axis rotor voltage
vrQ_0 = imag(Vr_s_0); % Q-axis stator voltage
% Using the voltage space vector aligned to the stator frame, the flux is
% calculated using the state equations for the electrical subsystem are,
%with the derivative vector set to zero
FM = [-Rs/(sig*Ls), ws, Lm*Rs/(Ls*Lr*sig), 0; ...
    -ws, -Rs/(sig*Ls), 0, Lm*Rs/(Ls*Lr*sig); ...
     Lm*Rr/(Ls*Lr*sig), 0, -Rr/(sig*Lr), wr; ...
     0, Lm*Rr/(Ls*Lr*sig) ,-wr, -Rr/(sig*Lr)];
Flux_0 =-inv(FM)*[vsD_0,vsQ_0,vrD_0,vrQ_0]';
fsD_0 = Flux_0(1);
fsQ_0 = Flux_0(2);
frD_0 = Flux_0(3);
frQ_0 = Flux_0(4);
Fs_s_0 = fsD_0 + fsQ_0*1i; % stator flux space vector at (stator frame)
Fr_s_0 = frD_0 + frQ_0*1i; % rotor flux space vector at (stator frame)
% Currents are calculated with in the general synchronously
%rotating reference frame
Is_s_0 = Fs_s_0/(sig*Ls)-Fr_s_0*Lm/(Ls*Lr*sig);
Ir_s_0 = Fr_s_0/(sig*Lr)-Fs_s_0*Lm/(Ls*Lr*sig);
isD_0 = real(Is_s_0);
isQ_0 = imag(Ir_s_0);
```

```
irD_0 = real(Ir_s_0);
irQ_0 = imag(Ir_s_0);
% Stator Flux Alignment
th_fs_0 = angle(fsD_0+ 1i*fsQ_0); % stator flux angle
% voltage, flux and current in the stator flux oriented reference frame
Vs_fs_0 = Vs_s_0*exp(-1i*(th_fs_0));
vsd_0 = real(Vs_fs_0);
vsq_0 = imag(Vs_fs_0);
Vr_fs_0 = Vr_s_0*exp(-1i*th_fs_0);
vrd_0 = real(Vr_fs_0);
vrq_0 = imag(Vr_fs_0);
Fs_fs_0 =Fs_s_0*exp(-1i*th_fs_0);
fsd_0 = real(Fs_fs_0);
fsq_0 = imag(Fs_fs_0);
Fr_fs_0 = Fr_s_0*exp(-1i*th_fs_0);
frd_0 = real(Fr_fs_0);
frq_0 = imag(Fr_fs_0);
Is_fs_0 = Is_s_0*exp(-1i*th_fs_0);
isd_0 = real(Is_fs_0);
isq_0 = imag(Is_fs_0);
Ir_fs_0 = Ir_s_0*exp(-1i*th_fs_0);
ird_0 = real(Ir_fs_0);
irq_0 = imag(Ir_fs_0);
%% Controller Initialization
% controller gains
% using Tapia's Method
% critically damped with Tset = 40ms
T1 = 40e-3; % settling time for inner loop
KI1 =(4/T1)^2*sig*Lr;
KP1 = 2*(4/T1)*sig*Lr-Rr;
% initialize the PI controller integrators
w_fs_0 = vsq_0/fsd_0+Rs*Lm/Ls*irq_0/fsd_0;
Dfsd_0 =-Rs/Ls*fsd_0 +Lm*Rs/Ls*ird_0+vsd_0;
% Inner loop PI controller initial conditions
vrd_tapia = vrd_0+sig*Lr*(w_fs_0-wm_0)*irq_0-Lm/Ls*Dfsd_0 + KP1*ird_0;
vrq_tapia = vrq_0-sig*Lr*(w_fs_0-wm_0)*ird_0...
-(w_fs_0-wm_0)*Lm/Ls*fsd_0+KP1*irq_0;
% Tapia's outer loop
T2 = 70e-3; % settling time for outer loop
KI2 = 8/3*T1/(T2^2)*Ls/Lm/(VLLrms*sqrt(3/2));
KP2 = 2/3*(2*T1-T2)/T2*Ls/Lm/(VLLrms*sqrt(3/2));
% Outer loop PI controller initial conditions
ird_tapia_IC = ird_0*(1+KP2*3/2*Lm/Ls*VLLrms*sqrt(3/2))...
-KP2*3/2/Ls*VLLrms*sqrt(3/2)*fsd_0;
irq_tapia_IC = irq_0*(1 + KP2*3/2*Lm/Ls*VLLrms*sqrt(3/2));
```